



저작자표시-비영리-변경금지 2.0 대한민국

이용자는 아래의 조건을 따르는 경우에 한하여 자유롭게

- 이 저작물을 복제, 배포, 전송, 전시, 공연 및 방송할 수 있습니다.

다음과 같은 조건을 따라야 합니다:



저작자표시. 귀하는 원저작자를 표시하여야 합니다.



비영리. 귀하는 이 저작물을 영리 목적으로 이용할 수 없습니다.



변경금지. 귀하는 이 저작물을 개작, 변형 또는 가공할 수 없습니다.

- 귀하는, 이 저작물의 재이용이나 배포의 경우, 이 저작물에 적용된 이용허락조건을 명확하게 나타내어야 합니다.
- 저작권자로부터 별도의 허가를 받으면 이러한 조건들은 적용되지 않습니다.

저작권법에 따른 이용자의 권리는 위의 내용에 의하여 영향을 받지 않습니다.

이것은 [이용허락규약\(Legal Code\)](#)을 이해하기 쉽게 요약한 것입니다.

[Disclaimer](#)

이학박사학위논문

**Ecological and molecular biological
responses of *Aristolochia contorta* to
herbivory stress**

초식 스트레스에 대한 쥐방울덩굴의
생태학적·분자생물학적 반응

2021년 2월

서울대학교 대학원
과학교육과 생물전공
남 보 은

Ecological and molecular biological responses of *Aristolochia contorta* to herbivory stress

초식 스트레스에 대한 쥐방울덩굴의
생태학적·분자생물학적 반응


지도 교수 김 재 근

이 논문을 이학박사 학위논문으로 제출함
2020년 10월

서울대학교 대학원
과학교육과 생물전공
남 보 은

남보은의 이학박사 학위논문을 인준함
2020년 12월

위원장	이 은 주	(인)
부위원장	김 재 근	(인)
위원	박 충 모	(인)
위원	김 상 규	(인)
위원	주 용 성	(인)



Abstract

Aristolochia contorta (Aristolochiaceae) is herbal vine species, which has the distinctive secondary metabolites of family Aristolochiaceae and the specialist herbivore *Seriginus montela* (swallowtail butterfly). To enhance the sustainability of co-existence of *A. contorta* and *S. montela*, interaction between the two species should be studied. To assess the response of *A. contorta* to the herbivory, I studied the ecological and molecular-biological aspects of *A. contorta* under the herbivory stress.

First, I assessed genetic diversity of *A. contorta* populations to understand the long-term sustainability of *A. contorta* population. Genomic DNA samples of *A. contorta* leaf were used for analysis from four populations (CJ, GP, PT, and YJ) where the vigorous growth was observed in the South Korea. Intra-population genetic diversity and inter-population genetic distance were assessed using randomly amplified polymorphic DNA (RAPD). Overall intra-population genetic diversity was lower, compared to the other riparian plant species (h : 0.0607 ~ 0.1401; I : 0.0819 ~ 0.1759). Despite of the geographical distance, population GP showed the larger genetic distance from other populations. This result seemed to be caused by the fragmented habitat and lower sexual reproduction of *A. contorta*.

Secondly, I performed the mesocosm experiment to assess the phenotypic plasticity of *A. contorta* under the herbivory stress. Physical damage on the young leaf or mature leaf was applied to one-year-old *A. contorta* seedlings under two light availability conditions (daylight and shade condition). Light availability significantly affected the most of the morphological characteristics. Leaf damage seemed to induce the emergence of branch and new leaf. Biomass production also increased under leaf damage treatment. Compensatory growth effect of leaf, shoot,

and biomass production seemed to be stronger when young leaves were damaged rather than mature leaves. The higher phenotypic plasticity to leaf damage was observed under the daylight treatment. These results indicate that *A. contorta* could show the vigorous growth under the moderate leaf damage stress with sufficient light.

Subsequently, I tried to assess the transcriptomic response of the *A. contorta* under herbivory stress by *de novo* transcriptome assembly. Transcriptome of the *A. contorta* leaves under control, simple wounding (W+DW), and simulated herbivory with oral secretion of *S. montela* (W+OS) treatment were compared. In addition, systemic response was also assessed from the upper leaves (systemic leaf). Total 92,323 contigs were filtered, and 28,231 contigs could be annotated under Gene Ontology (GO) database. Over half of the total DEGs (1,875 of 3,177 contigs) differentially expressed only by W+OS treatment. Secondary cell wall seemed to be reinforced under both W+DW and W+OS treatments from the cell wall related terms and lignin biosynthesis pathway. Both W+DW and W+OS treatments seemed to trigger the reactive oxygen species (ROS), ethylene, and jasmonic acid related signaling pathway. Contigs which are predicted to be involved in general herbivory response such as polyphenol oxidase, chitinase, MYB transcription factors, and jasmonate O-methyltransferase were up-regulated under W+OS treatment. Biosynthesis of some secondary metabolites including alkaloids were predicted to be induced by herbivory, which could affect the generalist herbivores rather than the specialist herbivores. However, specific secondary metabolite biosynthesis of *Aristolochia* such as aristolochic acids seemed to be not induced by herbivory. This results suggest the major defense mechanism against specialist herbivore of basal angiosperms could be similar to the previously studied eudicots.

From my study, *A. contorta* seemed to be able to co-exist with the specialist

herbivore *S. montela* even under the herbivory stress with the compensatory growth and defense mechanism. On the other hand, genetic diversity of *A. contorta* population was relatively low. To enhance the sustainability of the co-existence of *S. montela* and *A. contorta*, proper environmental condition should be provided. Results from this study could contribute to the integrative understanding of plant response to herbivory as well as the conservation of plant-herbivore interaction.

Keyword: *Aristolochia contorta*, compensatory growth, genetic diversity, secondary metabolites, *Sericanus montela*, specialist herbivore, transcriptome

Student Number: 2013-23382

This research was supported by the National Research Foundation of Korea (NRF) grant funded by the Korea government (MSIT) (NRF-2018R1A2B2002267; PI: Jae Geun Kim) and the Next-Generation BioGreen 21 Program (PJ013134; PI: Chung-Mo Park) provided by the Rural Development Administration of Korea.

Table of Contents

Abstract	i
LIST OF FIGURES	vii
LIST OF TABLES	x
Chapter 1. Introduction	1
1.1. Study Background	1
1.1.1. Plant-herbivore interaction and herbivory	1
1.1.2. Plant population under herbivory stress	1
1.1.3. Plant defense to herbivory	2
1.1.4. Secondary metabolites of basal angiosperms	3
1.1.5. <i>Aristolochia contorta</i> and its specialist herbivore <i>Seriginus montela</i> ..	3
1.2. Purpose of Research	4
Chapter 2. An analysis of the genetic diversity of a riparian marginal species, <i>Aristolochia contorta</i>	5
2.1. Introduction	5
2.2. Methods	7
2.2.1. Study site	7
2.2.2. Analysis of genetic diversity	7
2.3. Results and Discussion	9
2.3.1. Intraspecific genetic diversity	9
2.3.2. Genetic distance among populations	11
2.3.3. Genetic diversity of <i>A. contorta</i> and implications to the conservation	12
2.4. Conclusion	14
Chapter 3. Different growth response to the leaf damage under different relative light intensity in herbal vine <i>Aristolochia contorta</i>	15
3.1. Introduction	15
3.2. Methods	17

3.2.1. Growth condition and treatment	17
3.2.2. Measurement of growth characteristics	19
3.2.3. Phenotypic plasticity	19
3.2.4. Statistical analysis	20
3.3. Results	20
3.3.1. Growth characteristics under different light condition and herbivory	20
3.3.2. Phenotypic plasticity against leaf damage under different light condition	26
3.4. Discussion	30
3.4.1. Shade tolerance of <i>Aristolochia contorta</i>	30
3.4.2. Daylight enhance the phenotypic plasticity against leaf damage	30
3.4.3. Possible response of <i>Aristolochia contorta</i> against herbivory	32
3.5. Conclusion	33
Chapter 4. <i>De novo</i> transcriptome assembly of <i>Aristolochia contorta</i> reveals the defense strategy against its specific herbivore, <i>Sericanus montela</i>	34
4.1. Introduction	34
4.2. Methods	37
4.2.1. Plant materials and treatment	37
4.2.2. mRNA library construction	39
4.2.3. <i>De novo</i> assembly and functional annotation	39
4.2.4. Differentially expressed gene analysis	40
4.2.5. Ordination of differentially expressed genes	40
4.2.6. Validation of gene expression	41
4.3. Results	43
4.3.1. Overview of the <i>A. contorta</i> transcriptome	43
4.3.2. Gene expression among experimental conditions	44

4.3.3. Gene Ontology enrichment analysis	48
4.3.4. Kyoto Encyclopedia of Genes and Genomes (KEGG) pathway enrichment analysis	56
4.3.5. Difference in the expression profile on the herbivory defense	61
4.3.6. Validation of gene expression by qRT-PCR	77
4.4. Discussion	83
4.4.1. Response to the special herbivory in the wounded leaf	83
4.4.2. Systemic response against special herbivory	86
4.4.3. Defense of the <i>Aristolochia contorta</i> against its specific herbivore ..	87
Chapter 5. General conclusion	93
Reference	95
Abstract in Korean	104
Appendix A. Detailed methods for RNA extraction of <i>Aristolochia</i> <i>contorta</i>	106
Appendix B. GO (gene ontology) barplot of enriched contigs under wounding or artificial herbivory treatment in <i>A. contorta</i>	108

LIST OF FIGURES

Fig. 2-1. (a, b) Location of study sites; (c) Location of <i>Aristolochia contorta</i> population in each sites.	8
Fig. 2-2. Genetic diversity (<i>h</i> : Nei's genetic diversity; <i>I</i> : Shannon's diversity index) within each of four studied populations and whole individuals.	10
Fig. 2-3. UPGMA dendrogram based on Nei's genetic diversity among four studied populations.	11
Fig. 2-4. 2-D plot of principal component analysis (PCA) of 54 <i>A. contorta</i> individuals with the presence and absence of 14 polymorphic loci from RAPD.	12
Fig. 3-1. Summary of experimental treatments on <i>A. contorta</i> . Young and mature leaf damaged treatments were made by hole punch to 25% of the uppermost leaves and the lowermost leaves, respectively.	18
Fig. 3-2. Variations in morphological traits among treatments in the mesocosm experiment. (a) Stem length; (b) Internode length; (c) Number of primary branches; (d) Number of secondary branches; (e) Total leaf area; (f) Number of leaves; (g) Single leaf area; (h) petiole length; (i) Specific leaf area (SLA); (j) Chlorophyll content.	22
Fig. 3-3. Variations in biomass allocation among treatments in the mesocosm experiment.	23
Fig. 3-4. Relative distance plasticity index (RDPI) of morphological traits under different light availability treatments. (a) RDPI of stem length; (b) RDPI of internode length; (c) RDPI of number of primary branch; (d) RDPI of number of secondary branch; (e) RDPI of total leaf area; (f) RDPI of leaf number; (g) RDPI of single leaf area; (h) RDPI of petiole length; (i) RDPI of specific leaf area (SLA); (j) RDPI of chlorophyll content (SPAD).	27
Fig. 3-5. Relative distance plasticity index (RDPI) of biomass allocation under different light availability treatments. (a) RDPI of root dry weight; (b) RDPI of shoot dry weight; (c) RDPI of leaf dry weight; (d) RDPI of total dry weight	28

Fig. 3-6. Carbon: nitrogen ratio (C/N ratio) of leaf under experimental conditions. (a) 1 st treatment (August); (b) 2 nd treatment (September).	29
Fig. 3-7. Summary of the leaf damage experiment under different light availability on <i>A. contorta</i> individual.	33
Fig. 4-1. Schematic diagram of artificial herbivory treatment.	38
Fig. 4-2. Principal component analysis (PCA) on the expression level (FPKM values) of each contigs.	44
Fig. 4-3. The number of DEGs in three comparison groups. (a) Venn diagram of all DEGs (all up- and down-); (b) the number of up- and downregulated DEGs (compared to the control) of local and systemic leaf.	47
Fig. 4-4. The result of Gene Ontology (GO) analysis by REVIGO (biological process). (a) Control versus W+DW local leaf; (b) Control versus W+OS local leaf; (c) Control versus W+DW systemic leaf; (d) Control versus W+OS systemic leaf.	49
Fig. 4-5. GO circle plot displaying gene annotation enrichment analysis. (a) most-enriched DEGs in W+DW (versus control), local leaf; (b) most-enriched DEGs in W+OS (versus control), local leaf; (c) most-enriched DEGs in W+DW (versus control), systemic leaf; (d) most-enriched DEGs in W+OS (versus control), systemic leaf.	54
Fig. 4-6. Top 20 enriched KEGG pathways among the annotated DEGs across four comparisons. (a) Control versus W+DW local leaf; (b) Control versus W+OS local leaf; (c) Control versus W+DW systemic leaf; (d) Control versus W+OS systemic leaf.	57
Fig. 4-7. Expression profile heatmap and clustering in some herbivory and specific secondary metabolite related GO annotations under various treatments. Color represents the Z-score of the average expression level. (a) GO:0006952 (defense response); (b) GO:0009611 (response to wounding); (c) GO:0044550 (secondary metabolite biosynthesis process); (d) GO:0009821 (alkaloid biosynthetic process); (e) GO:0004837 (tyrosine decarboxylase activity).	62
Fig. 4-8. The result of qRT-PCR for selected genes in GO term “defense response” (GO:0006952). (a) c48813_g2_i1 (<i>AcCht6</i>); (b) c44532_g1_i1	

(<i>AcMYB34</i>); (c) c91572_g1_i1 (<i>AcNCSI</i>); (d) c63371_g1_i1 (<i>AcNCS2</i>); (e) c73635_g1_i1 (<i>AcYLS9</i>).	78
Fig. 4-9. The result of qRT-PCR for selected genes in GO term “response to wounding” (GO:0009611). (a) c51887_g1_i1 (<i>Ac4CL2</i>); (b) c36845_g1_i1 (<i>AcACS</i>); (c) c64728_g1_i3 (<i>AcCNMT</i>); (d) c51752_g2_i1 (<i>AcJMT</i>); (e) c60393_g2_i1 (<i>AcPAL</i>).	79
Fig. 4-10. The result of qRT-PCR for selected genes in GO term “secondary metabolite biosynthesis process” (GO:0044550). (a) c106305_g1_i1 (<i>AcCYP73A5</i>); (b) c67503_g1_i1 (<i>AcCYP76B1</i>); (c) c67391_g1_i1 (<i>AcCYP76B6</i>); (d) c50583_g1_i1 (<i>AcCYP80B2</i>); (e) c55025_g1_i2 (<i>AcCYP82C4</i>); (f) c64750_g2_i1 (<i>AcNES</i>); (g) c61823_g1_i3 (<i>AcSCPL8</i>).	81
Fig. 4-11. The result of qRT-PCR for selected genes in GO term “alkaloid biosynthetic process” (a, b; GO:0009821), GO term “tyrosine decarboxylase activity” (c, d; GO:0004837), DOPA monooxygenase activity (e; GO:0036263), and DOPA dioxygenase activity (f; GO:0046556). (a) c62822_g1_i2 (<i>AcSSL10</i>); (b) c64106_g1_i1 (<i>Ac6OMT</i>); (c) c66826_g5_i1 (<i>AcTyrDC2</i>); (d) c74598_g1_i1 (<i>AcTyrDC3</i>); (e) c8034_g1_i1 (<i>AcDODA</i>); (f) c64496_g1_i4 (<i>AcPPO</i>). ...	82
Fig. 4-12. Secondary metabolite content in control (undamaged) and induced (wounded and rubbed with the oral secretion of <i>S. montela</i> and sampled after 48 hours) in greenhouse experiment.	89
Fig. 4-13. Summary of the transcriptomic change of <i>A. contorta</i> under artificial herbivory of <i>S. montela</i>	92
Fig. 5-1. Summary of the response of <i>A. contorta</i> to the herbivory stress.	94
Fig. B-1. GO barplot displaying gene annotation enrichment analysis of DEGs in W+DW versus control, local leaf of <i>A. contorta</i>	108
Fig. B-2. GO barplot displaying gene annotation enrichment analysis of DEGs in W+OS versus control, local leaf of <i>A. contorta</i>	112
Fig. B-3. GO barplot displaying gene annotation enrichment analysis of DEGs in W+DW versus control, systemic leaf of <i>A. contorta</i>	116
Fig. B-4. GO barplot displaying gene annotation enrichment analysis of DEGs in W+OS versus control, systemic leaf of <i>A. contorta</i>	118

LIST OF TABLES

Table 2-1. Used random primer sequences and number of amplified RAPD fragments (*: number of polymorphic loci).	8
Table 3-1. Two-way analysis of variance results for traits of <i>A. contorta</i> in the mesocosm experiment; <i>F</i> statistics are shown.	25
Table 4-1. Used primers in qRT-PCR.	42
Table 4-2. Summary of annotations of the <i>Aristolochia contorta</i> transcriptome.	43
Table 4-3. Contigs which showed the higher eigenvalues on principal component analysis of FPKM values. PC = principal component.	46
Table 4-4. Differentially expressed genes (DEGs) in the cluster of upregulated genes under artificial herbivory of local leaf in defense response (GO:0006952).	67
Table 4-5. Upregulated genes ($\log_2fc > 0.5$) in the cluster of upregulated group under artificial herbivory of systemic leaf in defense response (GO:0006952).	69
Table 4-6. Differentially expressed genes (DEGs) in the cluster of upregulated genes under artificial herbivory of local leaf in response to wounding (GO:0009611).	71
Table 4-7. Differentially expressed genes (DEGs) in the cluster of upregulated genes under artificial herbivory (W+OS) of local leaf in secondary metabolite biosynthesis process (GO:0044550).	73
Table 4-8. Upregulated genes ($\log_2fc > 0.5$) in the cluster of upregulated group under artificial herbivory of systemic leaf in secondary metabolite biosynthesis process (GO:0044550).	75
Table 4-9. Fold changes of contigs which are involved in (a) alkaloid biosynthetic process (GO:0009821) and (b) tyrosine decarboxylase activity (GO:0004837).	76
Table A-1. Average (\pm SD) quantity and quality of extracted RNA of <i>A. contorta</i> by modified TRIzol method.	107
Table B-1. List and enrichment score of enriched GO terms in the GO barplot (Fig. B-1) of in W+DW versus control, local leaf of <i>A. contorta</i>	109

Table B-2. List and enrichment score of enriched GO terms in the GO barplot (Fig. B-2) of in W+OS versus control, local leaf of <i>A. contorta</i>	113
Table B-3. List and enrichment score of enriched GO terms in the GO barplot (Fig. B-1) of in W+DW versus control, systemic leaf of <i>A. contorta</i>	117
Table B-4. List and enrichment score of enriched GO terms in the GO barplot (Fig. B-4) of in W+OS versus control, systemic leaf of <i>A. contorta</i>	119

Chapter 1. Introduction

1.1. Study Background

1.1.1. Plant-herbivore interaction and herbivory

Land plants are always exposed to the risk of herbivory. Interaction between plant and herbivore has been regarded as the driver of the biodiversity of both plant and herbivore (Jander, 2014). Plant has been developed its own defense mechanism such as secondary metabolites, whereas many of phytophagous insects develop physiological mechanisms to cope with the plant defense simultaneously (Wu and Baldwin, 2010; de Castro et al., 2018). Therefore, specific “arms-race” between plant and herbivore could accelerate the adaptive co-evolution to each other (Jander, 2014; Kergoat, 2016; Endara et al., 2017). Survivorship of both plant and herbivore population has high dependence on the defense of the plant and adaptation of the herbivore to the plant defense (Endara et al., 2017).

1.1.2. Plant population under herbivory stress

Herbivory could affect the plant population both positively and negatively (McNaughton, 1979; Züst and Agrawal, 2017). Excessive herbivory by herbivore outbreak could even exploit the plant tissue, which cause the risk of extinction (Crawley, 1989). However, plant could compensate the moderate loss of plant tissue for rapid re-occupation of environmental resource (McNaughton, 1979). Some over-compensatory growth by herbivory make the more vigorous growth of plant rather than in the undamaged individuals (Jämeiro et al., 1996). While compensatory growth also differs among species and environment (Ballina-Gómez et al., 2010), understanding the phenotypic plasticity of the plant species against herbivory is necessary for the conservation of plant population and its herbivore.

1.1.3. Plant defense to herbivory

Plant primes the further herbivory by development of defense mechanism as well as the compensatory growth (Gatehouse, 2002). For example, inhibition of the herbivore metabolism by gene expression of inhibitory enzyme encoding genes is an example of defense mechanism (Gatehouse, 2002). Reinforcement of plant structure could be accompanied such as biosynthesis of secondary cell wall (e.g. lignin), which also could lead to decrease of food quality (Xie et al., 2018). In addition, biosynthesis of secondary metabolites could role as diverse way to prevent the further herbivory. They could cope with herbivore directly or indirectly. Some toxic compounds could directly inhibit the metabolism of herbivore, whereas the other compounds attract predator or parasite of the herbivore in indirect way (Wu and Baldwin, 2010).

Plant recognize the herbivory with diverse signal, such as physical damage, herbivore elicitor, and reactive oxygen species (Gatehouse, 2002; Schuman and Baldwin, 2016). Plant defense mechanism is a product of the complex signaling cascades and enzyme reaction, thus the plant defense is affected by the complex regulation of gene expression (Schuman and Baldwin, 2016). Therefore, assessment of the differentially gene expression under herbivory from transcriptome analysis could enhance the understanding on the defense of plant species (Reymond et al., 2004). Even in the same species, genetically heterogeneous group such as ecotype could show the different response to herbivory (Ogran et al., 2019). In addition, genetic diversity of plant population could contribute the defense and resilience to the herbivory stress (Kotowska et al., 2010; Gloss et al., 2013).

1.1.4. Secondary metabolites of basal angiosperms

As a result of the diversification of plant defense mechanism and herbivores' response, many phytophagous insects are classified as “special” herbivore with the narrow host plant range (Ali and Agrawal, 2012). Larvae of butterfly species (order Lepidoptera) also has its own host range (Enrlich and Raven, 1964; Edger et al., 2015). Swallowtail butterflies (Papilionidae) are one of the diverse butterfly group which species have the narrow host plant range (Enrlich and Raven, 1964; Miller, 1987). Many of swallowtail butterfly species use basal angiosperm species as host plant, which has the ancestral property of angiosperms (Miller, 1987). Basal angiosperm showed some distinct secondary metabolites, which are different from the products of major monocots or eudicots (Bliss et al., 2013).

1.1.5. *Aristolochia contorta* and its specialist herbivore *Seriginus montela*

Family Aristolochiaceae (Piperales) is a member of Magnoliids and basal angiosperms. There are many host plant species of the swallowtail butterfly larvae (Miller, 1987). Species of this family produces distinctive secondary metabolites such as aristolochic acids and aristololactams, which have the mortality to the generalist phytophagous insects (Bliss et al., 2013). Some specific swallow butterfly species could sequester or detoxify the aristolochic acid (Nishida, 1994; Priestap et al., 2012). *Aristolochia contorta* Bunge is herbal vine species as the member of family Aristolochiaceae. In addition, dragon swallowtail butterfly *Seriginus montela* (Papilionidae) exclusively consume only *A. contorta* (Hong et al., 2014). These two species inhabit in narrow geographical range (Russian Far East, Korea, China, and Japan; GBIF Secretariat, 2020).

1.2. Purpose of Research

From the exclusively specific herbivore and narrow distribution range, *A. contorta* seems to have distinct responses to herbivory stress as Aristolochiaceae and basal angiosperms. However, both the ecological and physiological characteristics of *A. contorta* has been poorly understood yet (Park et al., 2019). I tried to understand the response of *A. contorta* to herbivory in ecological and molecular biological perspective. Research question of this study are followed:

- 1) What about the genetic diversity of *A. contorta* population?
- 2) How growth response of *A. contorta* differ under herbivory stress?
- 3) How gene expression pattern differs in *A. contorta* under herbivory stress?
- 4) Which mechanism could maintain the co-existence of *A. contorta* and its specific herbivore *S. montela*?

To figure out the above research questions, I conducted field experiment and laboratory experiment of *A. contorta* about herbivory stress. In **Chapter 2**, genetic diversity of *A. contorta* population was examined. In **Chapter 3**, a field experiment was applied to compare the growth under leaf damage treatment. Difference in phenotypic plasticity to leaf damage among different light availability was also assessed. In **Chapter 4**, transcriptome of *A. contorta* under simulated herbivory was compared to undamaged or simply wounded individuals. I tried to assess the effect of herbivore-elicitor of *S. montela* on the additional defense response of *A. contorta*. In addition, systemic response to prime the herbivory in undamaged tissue was assessed. From these results, I tried to understand and summarize the multi-layer response of *A. contorta* to herbivory of its specialist herbivore *S. montela*.

Chapter 2. An analysis of the genetic diversity of a riparian marginal species, *Aristolochia contorta*¹

2.1. Introduction

Vegetation structure of riparian ecosystem is determined by the ecological gradient as the transition zone between aquatic ecosystem and terrestrial ecosystem (Naiman et al., 2005; Park and Kim, 2020). Upper riparian zone is affected by relative weaker impact of flooding from river or stream and increased canopy of the terrestrial plants (Vidon and Hill, 2004; Soykan et al., 2012). Therefore, vegetation of upper riparian zone seems to have specific ecological niche, while it also affects the biodiversity of neighbored aquatic and terrestrial ecosystem. For the conservation of biodiversity of the riparian vegetation, biodiversity of the upper riparian zone should be also considered.

Vine species at upper riparian zone could contribute the plant biodiversity and nutrient cycle (Hegarty et al., 1989). Vine species could enhance the biodiversity with its unique ecological niche, unless it shows invasiveness. *Aristolochia contorta* Bunge (Aristolochiaceae) is one of the perennial herbal vine species which inhabits near the river and valley. Its distribution range is known as Eastern China, Eastern Russia, Japan and Republic of Korea (Global Biodiversity Information Facility, 2020). *Aristolochia contorta* could twine up the diverse host plant such as tree, shrub, and herb, it could even twine up the artificial structure such as fence (Park et al., 2019). Also, *A. contorta* is a species-level specific host of the larvae of *Sericinus*

¹ Published in *Journal of Wetlands Research*, Vol. 22, No. 2, pp. 100-105 (May 2020; in Korean with English abstract)

montela Gray (swallowtail butterfly), which is designated as the vulnerable species (VU) in Red List of Republic of Korea. Construction of the artificial habitat for *S. montela* and *A. contorta* has been tried in Republic of Korea, which. However, there are difficulties in amplification of *A. contorta* individuals, since the seed dormancy period is long and the dormancy-breaking method is unknown (Voronkova et al., 2018).

For conservation of plant population in long-term perspective, enhancement of the genetic diversity should be also considered as well as the amplification of the individuals (Wimp et al., 2004; Gamfeldt and Källström, 2007). For conservation of the genetic diversity, genetic diversity of the natural population should be assessed in advance. Former study of Nakonechnaya et al. (2012) revealed that *A. contorta* population in Eastern Russia had the low genetic diversity from allozyme analysis (Nakonechnaya et al., 2012). Chloroplast genome of *A. contorta* had been sequenced (Zhou et al., 2017). However, nuclear genome of *A. contorta* is still unknown. Therefore, universal marker should be applied for assessment of the genetic diversity of *A. contorta*.

This study aims to assess the genetic diversity of *A. contorta* population in Republic of Korea using randomly amplified polymorphic DNA method, which could be applied without the genomic information with high intra-population resolution (Williams et al., 1990). I assessed the genetic diversity of *A. contorta* populations, which showed the vigorous growth in Republic of Korea. Also I tried to discuss about the implication for conservation of genetic diversity in *A. contorta* population.

2.2. Methods

2.2.1. Study site

Four study sites were selected among the *A. contorta* population, which have showed the vigorous growth and population density in Republic of Korea (Park et al., 2019). Population GP ($n = 11$) has been located at the neighbor of the valley in Gapyeong, Gyeonggi Province. Population PT ($n = 16$) in Pyeongtaek, Gyeonggi Province and population CJ ($n = 13$) in Cheongju, Chungbuk Province have been located at the upper riparian zone neighbor of the stream. Population YJ ($n = 14$) has been located in the upper side of the river island (Fig. 2-1). Individuals of *A. contorta* in population GP and YJ twined up diverse plant species including herbal species, shrub, and tree. Host types of population CJ were herbs, trees, and fence, whereas of population PT were herbs and fence (Park et al., 2019). Leaf samples were collected from the individuals with 2 m interval to prevent the sampling from clone. Collected leaf samples were frozen and stored at -80°C before DNA extraction.

2.2.2. Analysis of genetic diversity

Total genomic DNA were extracted from frozen samples using DNeasy Plant Mini Kit (Qiagen, Hilden, Germany) after grinding. Concentration and purity of extracted DNA samples were quantified using Nanodrop One^C (Thermo Fischer Scientific, Waltham, MA) and diluted to 50 ng/ μl with deionized water. Polymerase chain reaction of RAPD were conducted with the mixture of 1 μl of template DNA (50 ng/ μl), 2 μl of dNTP mix (2.5 mM each), 2 μl of 10x PCR buffer, 1 μl of random primer (10 pmol/ μl), 13.8 μl of DNase-free deionized water, and 0.2 μl of *Taq* DNA polymerase (5 U/ μl of BS eTaq DNA polymerase; Biosesang, Seongnam, the Republic of Korea). Polymerase chain reaction was conducted with 95°C , 5 min of

initial denaturation, 28 cycles of [95°C, 45 sec of denaturation]-[T_m (Table 2-1), 45 sec of annealing]-[72°C, 95 sec of elongation], and 72°C, 2 min of final extension. Total five random oligomers were used from eleven primers which showed the polymorphic loci (Table 2-1).

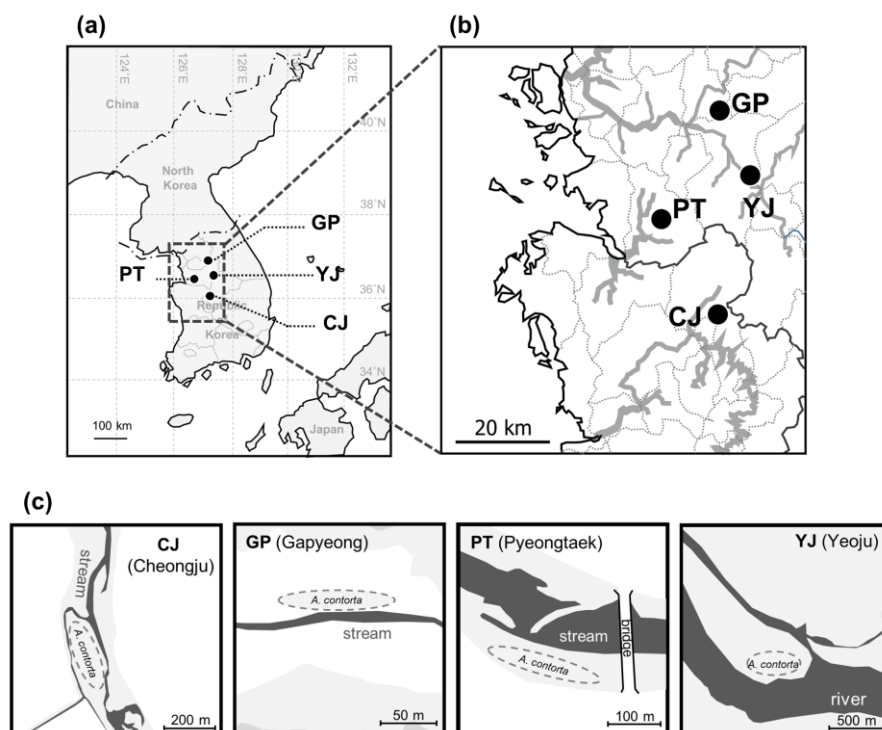


Fig. 2-1. (a, b) Location of study sites; (c) Location of *Aristolochia contorta* population in each sites.

Table 2-1. Used random primer sequences and number of amplified RAPD fragments (*: number of polymorphic loci).

Primer name	Sequence (5'→3')	T_m (°C)	No. of observed bands
N-8002	CAATCGCCGT	32	4 (2*)
N-8005	GAAACGGGTG	32	3 (2*)
N-8041	ATCGGGTCCG	34	7 (5*)
N-8045	CAAACGTCGG	32	6 (3*)
N-8072	CTTAGGGCAC	32	5 (2*)

Amplified DNA fragments were observed by electrophoresis of 1% agarose gel stained with GelRed™ (Biotium, Hayward, CA). Presence and/or absence of amplified band at polymorphic loci were scored within binary matrix (0=absence; 1=presence) under gel documentation system.

From the binary matrix, intra-population genetic diversity (h : Nei's genetic diversity; I : Shannon's diversity index) and inter-population genetic diversity (Nei's genetic distance and UPGMA dendrogram) were calculated using the software Popgen32 (Nei, 1973; Yeh and Boyle, 1997). Principal component analysis from the band presence/absence of polymorphic loci were conducted using package “vegan” (Oksanen et al., 2013) in R version 3.6.1 (R core team, 2020).

2.3. Results and Discussion

2.3.1. Intraspecific genetic diversity

Total 25 band loci were observed from the RAPD-PCR of five primers, while 14 loci (56%) showed polymorphism. Total genetic diversity was 0.1552 in Nei's genetic diversity (h) and 0.2370 in Shannon's diversity index (I). Intraspecific genetic diversity was ranged in 0.0607 ~ 0.1491 (h) and 0.0819 ~ 0.1759 (I) (Fig. 2-2). Population GP showed the highest intraspecific genetic diversity ($h = 0.1491$; $I = 0.1759$), while CJ showed the lowest intraspecific genetic diversity.

Intraspecific genetic diversity of *A. contorta* population was relatively lower than the intraspecific genetic diversity of the other wetland plants which had used RAPD marker. Genetic diversity of *A. contorta* population was relatively lower than the annual plant *Polygonum thunbergii* (h : 0.2381 ~ 0.2761; I : 0.3592 ~ 0.4100; Nam et al., 2016), which could propagate only by seed dispersal. Also, it was in the

lower range of the genetic diversity of *Typha angustifolia* (h : 0.0962 ~ 0.2392; I : 0.1419 ~ 0.3512), which could propagate both by seed dispersal and rhizome propagation (Min et al., 2012). Therefore, low genetic diversity of *A. contorta* seemed to be caused by contribution of the clonal propagation of *A. contorta*. Former study of Nakonechnaya et al. (2012) pointed the clonal growth of root sprout and apomixis, which refer the clonal seed formation without fertilization, as the cause of the lower genetic diversity of *A. contorta* population (Nakonechnaya et al., 2012). Therefore, intra-population genetic diversity of *A. contorta* population is predicted to decrease in long-term perspective.

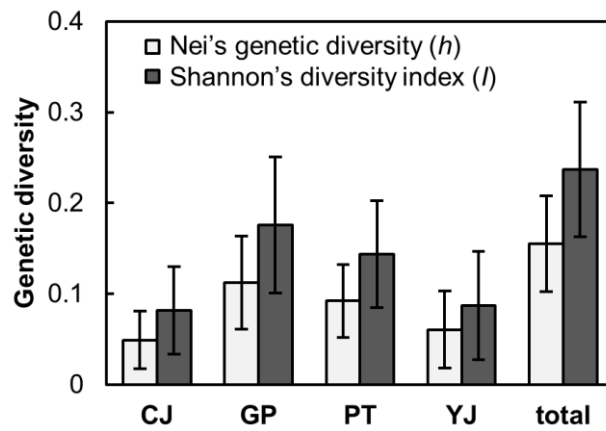


Fig. 2-2. Genetic diversity (h : Nei's genetic diversity; I : Shannon's diversity index) within each of four studied populations and whole individuals. CJ (Cheongju; $n = 13$); GP (Gapyeong; $n = 11$); PT (Pyeongtaek; $n = 16$); YJ (Yeoju; $n = 14$).

2.3.2. Genetic distance among populations

Inter-population genetic distance (Nei's genetic distance) was ranged from 0.0495 to 0.1699. Population YJ and CJ showed the shortest genetic distance (0.0495). Population GP showed the highest genetic distance between the other populations (e.g. PT ~ GP: 0.1699; Fig. 2-3). Principal component analysis by polymorphic bands also showed the relatively separated population structure of population GP from the other three populations (Fig. 2-4).

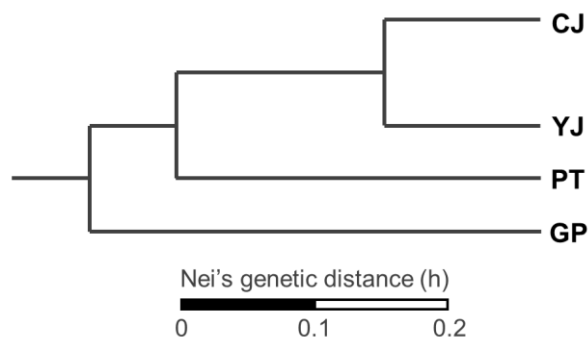


Fig. 2-3. UPGMA dendrogram based on Nei's genetic diversity among four studied populations. CJ (Cheongju; $n = 13$); GP (Gapyeong; $n = 11$); PT (Pyeongtaek; $n = 16$); YJ (Yeoju; $n = 14$).

2.3.3. Genetic diversity of *A. contorta* and implications to the conservation

Populations of *A. contorta* showed the overall low genetic diversity rather than the other riparian plant species. This could be considered as the result of the clonal propagation rather than the seed dispersal (Nakonechnaya et al., 2012). To increase the intra-population genetic diversity, optimal growth condition such as physical support could be provided at artificial habitat for inflorescence (Park et al., 2019). Lower total genetic diversity could be caused by the limited study sites. Total genetic diversity could be compensated by the further survey on the other sites.

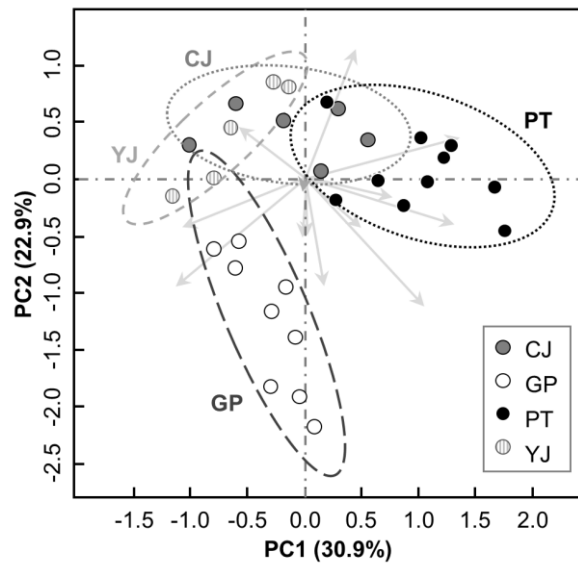


Fig. 2-4. 2-D plot of principal component analysis (PCA) of 54 *A. contorta* individuals with the presence and absence of 14 polymorphic loci from RAPD. Values in parenthesis indicate the relative eigenvalue of each axis. Dotted ellipses indicate the 95% range of standard deviation of each population. CJ (Cheongju; $n = 13$); GP (Gapyeong; $n = 11$); PT (Pyeongtaek; $n = 16$); YJ (Yeoju; $n = 14$).

Individuals of population GP, which showed the highest intra-specific genetic diversity, were distributed at diverse host types such as herbs, shrubs, and trees (Park et al., 2019). Proper host diameter varies by the age or status of the vine species, thus vine species could not twine up the relatively thick host than vine shoot (DeWalt et al., 2000). Juvenile *A. contorta* could twine up the herbal species and transfer to the neighbored shrubs and trees as increase of the age and shoot diameter. Diverse host types could provide the environment to *A. contorta* for settlement, which could enhance the intra-population genetic diversity. Therefore, diverse host plant and/or artificial physical support should be provided to *A. contorta* for transfer of the host within the growth stage.

Genetic distance among populations was independent from the geological distance (Fig. 2-3). In particular, population GP was relatively separated from the other populations. These result could be caused by habitat fragmentation from narrow ecological niche and high proportion of the clonal propagation. For *ex-situ* species conservation, plantation of mixed individuals from various source population could enhance the genetic diversity (Lesica and Allendorf, 1999). In addition, proper growth condition should be also provided for vegetative growth of *A. contorta* for providing food and habitat to vulnerable butterfly *S. montela* as well as the enhancement of genetic diversity.

2.4. Conclusion

Intra-population genetic diversity of *A. contorta* was lower than other riparian plant species. This result should be considered for conservation of *A. contorta*. Various shape and diameter of physical supports should be provided for enhance vegetative growth and genetic diversity, as well as abiotic growth condition. Also, some population was seemed to be separated from the other populations, regardless of the geological distance. From this result, mixed planting from various populations could be applied for *ex-situ* conservation with various genetic distance. Successful settlement of *A. contorta* would contribute the conservation of the vulnerable butterfly *S. montela*, as well as the connectivity of the riparian vegetation between the aquatic and terrestrial ecosystem.

Chapter 3. Different growth response to the leaf damage under different relative light intensity in herbal vine *Aristolochia contorta*

3.1. Introduction

Herbivory is one of the major plant-herbivore interaction, which could contribute the biodiversity as a result of co-evolutionary adaptation of each other (Jander, 2014). Plants are exposed to the herbivore stress in their life cycle. Herbivory stress is commonly known to affect the plant growth negatively (Züst and Agrawal, 2017). Defense mechanism of plant against herbivory which make plant able to prime the further herbivory commonly accompanies the trade-off between vegetative growth (Xie et al., 2018).

Leaf damage is one of the main phenomenon caused by herbivory, which leads to the loss of the plant tissue. Plant has its own phenotypic plasticity in response to changes in biotic and abiotic environmental change including leaf damage (Schlichting, 1986). Phenotypic plasticity under the herbivory stress could be assessed to understand the compensatory growth response (Barton, 2008). Moderate leaf damage by herbivory stress could stimulate the compensatory growth, which could enhance the vigorous growth of plant individual rather than the undamaged individual (McNaughton, 1979). Compensatory growth could be affected by the resource availability, yet the relationship between resource availability and compensatory growth response is unclear (Ballina-Gómez et al., 2010).

Light is one of a major limiting factor to plant resource acquisition and allocation (Ågren, 1985). In addition, herbivory stress is commonly known to suppress the photosynthesis (Nabity et al., 2009). Response to herbivory stress of plant is also affected by light availability (Lentz and Cipollini Jr., 1998; Hough-Goldstein and LaCross, 2012). Therefore, effect of the herbivory on the plant growth also might vary under different light availability environment.

Family Aristolochiaceae is one of the group which have distinct secondary metabolites, which allows only a few specialist herbivore species (Miller, 1987). *Aristolochia contorta* is one of the angiosperm species which have the species-level specialist herbivore butterfly species, *Sericanus montela* (dragon swallowtail; Hong et al., 2014). Because of species-level dependence of *S. montela*, population and individuals of *A. contorta* should be maintained for co-existence with *S. montela*. However, the growth response of the *A. contorta* under leaf damage stress has been poorly understood.

In this study, a mesocosm experiment of different light availability and leaf damage was conducted. I tried to reveal the difference in phenotypic plasticity to the leaf damage stress among light availability to understand the growth response of *A. contorta* under leaf damage stress. In addition, for assessment of the effect of herbivore preference on the young leaf, leaf damage treatment was subdivided into two treatments: mature leaf damaged and young leaf damaged. Phenotypic plasticity indices were calculated for each growth parameters to compare the compensatory growth among different light availability. Result of this study could enhance the fundamental understanding of the response to the leaf damage stress of *A. contorta*.

3.2. Methods

3.2.1. Growth condition and treatment

Aristolochia contorta seeds were collected from a population which located in Gapyeong, Gyeonggi Province, Republic of Korea at December 2017. Seeds were delivered to laboratory and germinated in greenhouse located at Seoul National University at May 2018. At June 2018, total 120 seedlings with about 5 cm of shoot height were individually transplanted in the pots (15 cm diameter \times 20 cm depth) filled with mix of sand and topsoil (2:1 in v/v). Physical support of plastic stake (0.3 cm diameter \times 1.3 m height) was added in each pot.

One week after transplanting (early July), two relative light availability treatments (relative light intensity, RLI; daylight = 100% of RLI to outside; shade = 50% of RLI) were applied to 60 individuals for each. Half level of RLI (shade treatment) was provided by layered black mesh 2.5 m above the steel structure, which have shown as the half level of the light intensity at outside (Park et al., 2019). Average light intensity under daylight and shade treatments were 1303.3 $\mu\text{mol m}^{-2} \text{s}^{-1}$ and 653.8 $\mu\text{mol m}^{-2} \text{s}^{-1}$ at noon, respectively. Individuals of *A. contorta* were acclimated under each light intensity treatment in one month and used to leaf damage treatment.

In each light availability treatment, leaf damage treatments were applied two times (15th August and 15th September) to mimic the temporal emergence of the larvae of *Seriginus montela* (Kim and Kwon, 2010). Three treatments were applied for each light availability treatment as follow: control (undamaged), mature leaves damaged, and young leaves damaged. In treatment “mature leaves damaged”, loss of 50% in leaf area by damage using hole puncher was applied to the 25% of the lowermost leaves in each individual. The treatment “young leaves damaged” was applied as same

as "mature leaves damaged" to the uppermost leaves (25% of total leaves; Fig. 3-1).

Individuals were additionally grown for four weeks after the second treatment.

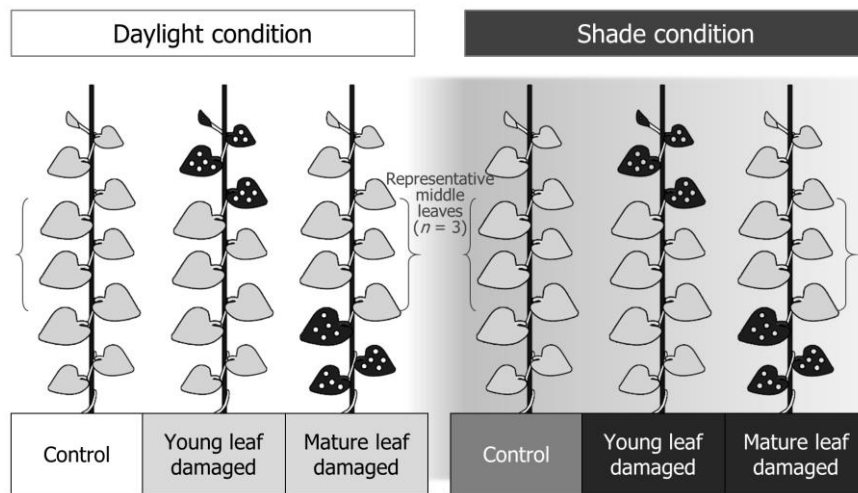


Fig. 3-1. Summary of experimental treatments on *A. contorta*. Young and mature leaf damaged treatments were made by hole punch to 25% of the uppermost leaves and the lowermost leaves, respectively.

3.2.2. Measurement of growth characteristics

Plants were harvested at four weeks after the second leaf damage treatment (October). Following characteristics were measured: number of primary and secondary branches, number of leaves, total leaf area, internode and petiole lengths, stem length, and dry weight of stem, leaf, and root. Total leaf area of each individual was measured using portable leaf area meter (LI-3000C, LI-COR Bioscience, Lincoln, NE). Internode and petiole lengths were measured as the average of three replicates at the midshoot using digital vernier caliper (Mitutoyo, Kanagawa, Japan). Chlorophyll contents were quantified from the average of the three leaf replicates at the midshoot in each individual using chlorophyll meter (SPAD-502, Konica Minolta, Tokyo, Japan). Total dry weight was calculated as the sum of the dry weight of stem, leaves, and root. Specific leaf area (SLA) was calculated from the ratio of average single leaf area (total leaf area / number of leaves) and average single leaf dry weight (leaf dry weight / number of leaves).

Punched plant leaf tissues were collected and dried. In control treatment, two leaves were collected near the midshoot and dried. Carbon: nitrogen ratio (C/N ratio) of dried plant leaf tissue samples was analyzed from total carbon and total nitrogen contents using elemental analyzer (Flash EA 1112, Thermo Fisher Scientific, Waltham, MA).

3.2.3. Phenotypic plasticity

For comparison of phenotypic plasticity to the leaf damage between two light availability treatments, a relative distance plasticity indices (RDPI) of each growth parameter were calculated (Valladares et al., 2006). Because of the discontinuity of the leaf damage treatment, relative distances under two treatments

of each light availability treatments (mature leaves damaged and young leaves damaged) from control treatment were calculated as below:

$$RDPI = \left(\sum \frac{d_{ctrl,i \rightarrow treatment,j}}{x_{ctrl,i} + x_{treatment,j}} \right) / n$$

Where n is the total number of distances.

3.2.4. Statistical analysis

Significances of light availability, leaf damage, and interaction between the light availability and leaf damage were examined by two-way analysis of variance (ANOVA) using R version 4.0.2 (R core team, 2020). Significance of the differences between group means was determined by Duncan's post-hoc test using R package "agricolae" (Mendiburu, 2020).

3.3. Results

3.3.1. Growth characteristics under different light condition and herbivory

Both stem and internode length were higher under the shade treatment, rather than the daylight treatment (Fig. 3-2a, b). Number of branches and leaves were higher under the daylight treatment rather than the shade (Fig. 3-2c, d, f). On the other hand, total leaf area and average single leaf area were higher under the shade treatment rather than the daylight (Fig. 3-2e, g). Petiole length and specific leaf area were also higher under the shade rather than the daylight (Fig. 3-2h, i). Chlorophyll content did not show the significant difference under two light availability treatments (Fig. 3-2j). Dry weight of aboveground parts (leaf and shoot) was higher under the shade treatment rather than the daylight treatment, whereas the root dry weight did not show the difference under two light availability treatments (Fig. 3-3).

Some of the growth characteristics were affected by the leaf damage treatment. Number of branches and leaves seemed to increase under the leaf damage treatment, young leaf damaged treatment in particular (Fig. 3-2c, d, f). Dry weight of root, shoot, and leaf were also higher under the leaf damage treatment (Fig. 3-3).

Morphological traits significantly differed by the light availability and leaf damage treatment, mainly by light availability (Table 3-1). Light availability treatment significantly affected the overall growth traits, such as stem and internode length, number of primary and secondary branches, total leaf area, number of leaves, average single leaf area, petiole length, SLA, shoot dry weight, and leaf dry weight ($p < 0.05$). Leaf damage treatment affected number of primary and secondary branches, number of leaves, SLA, root dry weight, shoot dry weight, and total dry weight ($p < 0.05$).

There were some significant interactions between light availability and leaf damage treatment in number of secondary branches, total leaf area, chlorophyll content, and leaf dry weight. Under the daylight treatment, number of secondary branches was the highest with young leaf damaged rather than the mature leaf damaged (Daylight/Control = 1.4 ± 0.4 ; Daylight/Young = 3.7 ± 0.4 ; Daylight/Mature = 2.4 ± 0.4). On the other hand, leaf damaged treatment showed the increase of the secondary branches under the shade treatment, yet damaged leaf part did not affect (Shade/Control = 0.3 ± 0.2 ; Shade/Young = 1.0 ± 0.2 ; Shade/Mature = 0.8 ± 0.3).

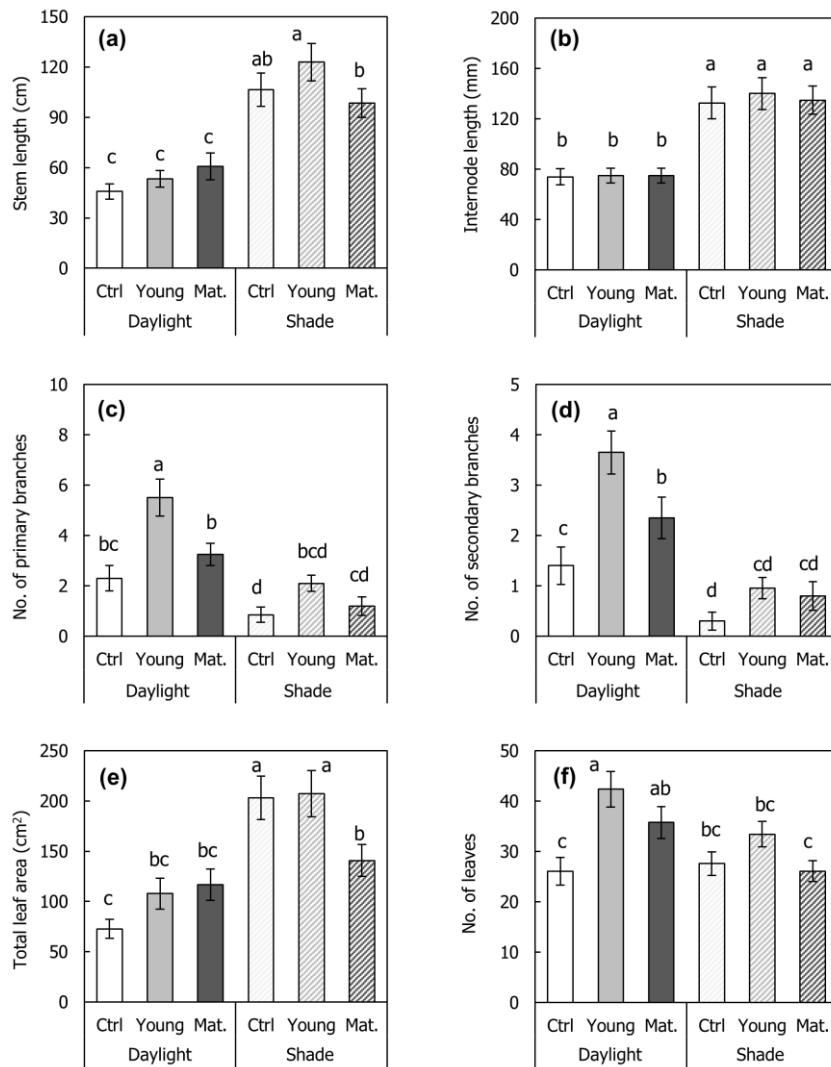


Fig. 3-2. Variations in morphological traits among treatments in the mesocosm experiment. **(a)** Stem length; **(b)** Internode length; **(c)** Number of primary branches; **(d)** Number of secondary branches; **(e)** Total leaf area; **(f)** Number of leaves; **(g)** Single leaf area; **(h)** petiole length; **(i)** Specific leaf area (SLA); **(j)** Chlorophyll content. Lower case alphabets on graph represent statistically different groups by Duncan post-hoc test (< 0.05 level). Daylight = 100% of relative light intensity (RLI); Shade = 50% of RLI; Ctrl. = control; Young = young leaf damaged; Mat. = mature leaf damaged.

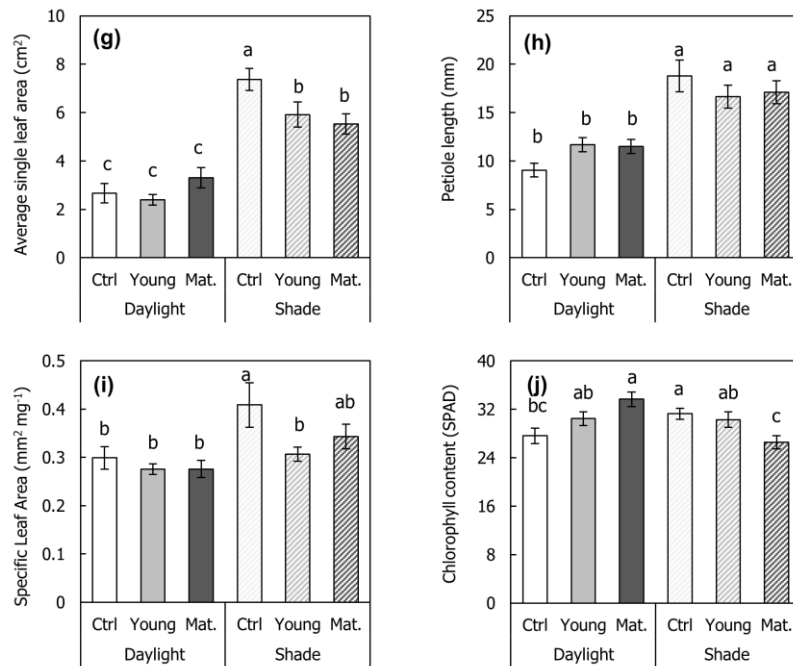


Fig. 3-2. (continued)

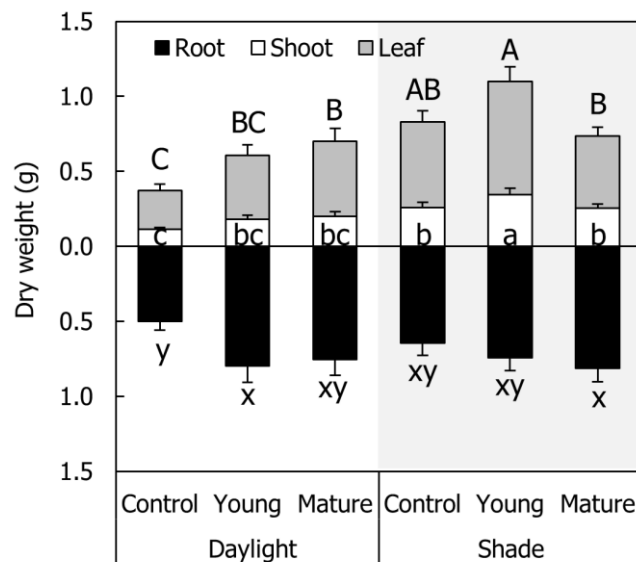


Fig. 3-3. Variations in biomass allocation among treatments in the mesocosm experiment. Alphabets on graph represent statistically different groups by Duncan post-hoc test (< 0.05 level). Daylight = 100% of relative light intensity (RLI); Shade = 50% of RLI; Ctrl. = control; Young = young leaf damaged; Mature = mature leaf damaged.

Total leaf area was increased under leaf damage treatment in the daylight. On the other hand, damage of mature leaves lead to decrease of the total leaf area under the shade (Shade/Control = $203.1 \pm 21.7 \text{ cm}^2$; Shade/Young.= $207.1 \pm 23.0 \text{ cm}^2$; Shade/Mature. = $140.8 \pm 15.9 \text{ cm}^2$). Chlorophyll content under the daylight showed the increase by the leaf damage (Daylight/Control = 27.6 ± 1.3 in SPAD; Daylight/Young.= 30.5 ± 1.1 ; Daylight/Mature. = 33.7 ± 1.2), yet leaf damage lead to the decrease of chlorophyll content under the shade (Shade/Control = 31.3 ± 0.9 ; Shade/Young.= 30.3 ± 1.3 ; Shade/Mature. = 26.6 ± 1.1). Root dry weight with young leaf damaged treatment was higher rather than mature leaf damaged treatment under the daylight (Daylight/Control = $0.50 \pm 0.06 \text{ g}$; Daylight/Young.= $0.80 \pm 0.11 \text{ g}$; Daylight/Mature. = $0.75 \pm 0.10 \text{ g}$). Meanwhile, root dry weight with mature leaf damaged treatment was slightly higher rather than young leaf damaged treatment under the shade (Shade/Control = $0.64 \pm 0.08 \text{ g}$; Shade/Young.= $0.74 \pm 0.09 \text{ g}$; Shade/Mature. = $0.81 \pm 0.09 \text{ g}$).

Table 3-1. Two-way analysis of variance results for traits of *A. contorta* in the mesocosm experiment; *F* statistics are shown. The two treatments were light availability (daylight and shade) and leaf damage (control, mature leaf damaged, and young leaf damaged). *df* = 1, 2, 114 for traits. Significant effects are shown in boldface (* *p* < 0.05, ** *p* < 0.01, *** *p* < 0.001).

	Light	Damage	Light × Damage
Stem length (cm)	69.521***	1.111	1.985
Internode length (cm)	61.478***	0.102	0.061
No. of primary branches	36.147***	11.926***	2.272
No. of secondary branches	44.169***	9.733***	3.152*
Total leaf area (cm ²)	35.476***	1.422	4.948**
No. of leaves	6.274*	8.168***	2.553
Single leaf area (cm ²)	104.625***	2.233	4.374*
Petiole length (mm)	58.085***	0.063	2.836
Specific leaf area (SLA)	10.996**	3.151*	1.163
Chlorophyll content (SPAD)	1.637	0.358	11.175***
Root dry weight (g)	0.451	3.387*	0.606
Shoot dry weight (g)	23.991***	3.329*	1.834
Leaf dry weight (g)	11.876***	2.792	3.521*
Total dry weight (g)	6.546*	3.299*	1.014

3.3.2. Phenotypic plasticity against leaf damage under different light condition

Relative distance plasticity index (RDPI) showed the difference in phenotypic plasticity to the leaf damage among two light availability treatments (Figs. 3-4 and 3-5). Total leaf area, leaf number, single leaf area, petiole length and chlorophyll content showed the higher plasticity under the daylight treatment rather than the shade treatment (Fig. 3-4e, f, g, h, j). Internode length, number of primary and secondary branch, SLA showed the higher plasticity under the shade treatment rather than the shade treatment (Fig 3-4. b, c, d, i).

Total leaf area and chlorophyll content showed the higher plasticity with mature leaf damaged treatment rather than young leaf damaged treatment (Fig. 3-4e, j). Leaf number showed the higher phenotypic plasticity to young leaf damaged treatment rather than mature leaf damaged treatment (Fig. 3-4f). The higher light availability induced the higher RDPI of stem length and single leaf area with mature leaf damaged treatment, yet not with young leaf damaged treatment (Fig. 3-4a, g). Phenotypic plasticity of biomass allocation was higher under the daylight treatment rather than the shade treatment, especially with mature leaf damaged treatment rather than young leaf damaged treatment (Fig. 3-5).

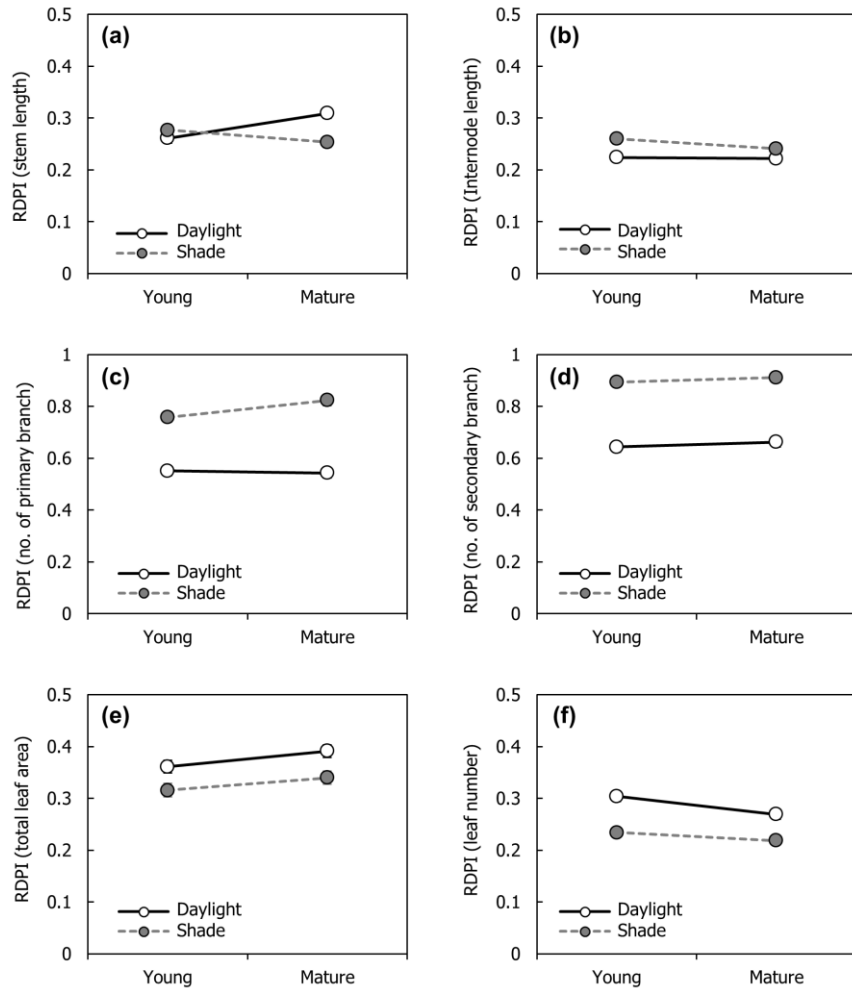


Fig. 3-4. Relative distance plasticity index (RDPI) of morphological traits under different light availability treatments. **(a)** RDPI of stem length; **(b)** RDPI of internode length; **(c)** RDPI of number of primary branch; **(d)** RDPI of number of secondary branch; **(e)** RDPI of total leaf area; **(f)** RDPI of leaf number; **(g)** RDPI of single leaf area; **(h)** RDPI of petiole length; **(i)** RDPI of specific leaf area (SLA); **(j)** RDPI of chlorophyll content (SPAD). Daylight = 100% of relative light intensity (RLI); Shade = 50% of RLI; Young = young leaf damaged; Mature = mature leaf damaged.

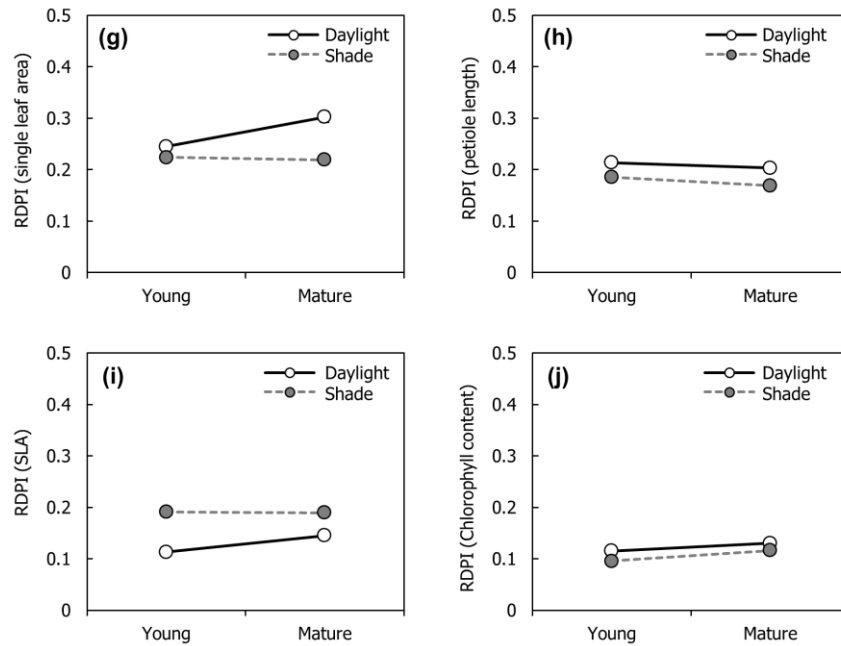


Fig. 3-4. (continued)

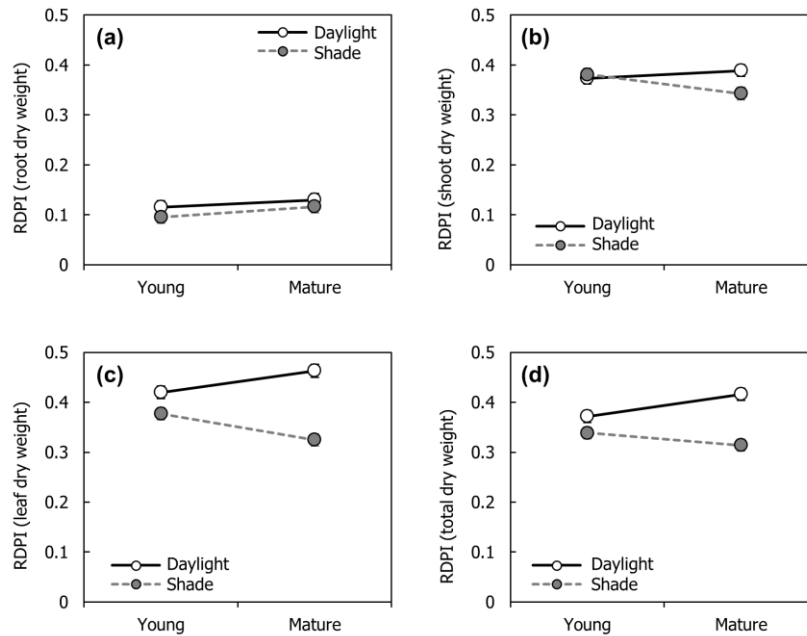


Fig. 3-5. Relative distance plasticity index (RDPI) of biomass allocation under different light availability treatments. **(a)** RDPI of root dry weight; **(b)** RDPI of shoot dry weight; **(c)** RDPI of leaf dry weight; **(d)** RDPI of total dry weight; Daylight = 100% of relative light intensity (RLI); Shade = 50% of RLI; Young = young leaf damaged; Mature = mature leaf damaged.

Carbon: nitrogen ratio (C/N ratio) at initial treatment showed that the significantly lower C/N ratio in the young leaves rather than the mature lower leaves and middle leaves (control treatment; Fig. 3-6a). Damage on the mature leaf lead to the decrease of C/N ratio under the daylight condition, while it did not show the statistical significance (Fig. 3-6b). Overall C/N ratio increased at the secondary treatment of September (17.00 ~20.63) rather than the first treatment of August (8.66 ~ 10.79).

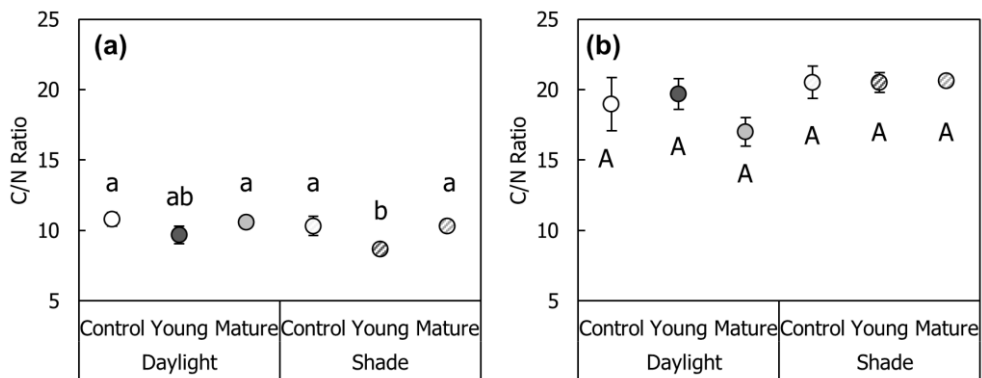


Fig. 3-6. Carbon: nitrogen ratio (C/N ratio) of leaf under experimental conditions. **(a)** 1st treatment (August); **(b)** 2nd treatment (September). Alphabets on graph represent statistically different groups by Duncan post-hoc test (< 0.05 level). Daylight = 100% of relative light intensity (RLI); Shade = 50% of RLI; Young = young leaf damaged; Mature = mature leaf damaged.

3.4. Discussion

3.4.1. Shade tolerance of *Aristolochia contorta*

In the former mesocosm experiment study, 3-year-old *Aristolochia contorta* individuals showed the relatively vigorous growth under shade with the larger leaf and the longer stem rather than full sunlight (Park et al., 2019). Similar to the 3-year-old *A. contorta* individuals, 1-year-old *A. contorta* individuals in the present study also showed the longer stem, larger leaf area, and larger biomass production under the shade treatment. On the other hand, number of leaf and branch were higher under the daylight treatment. Although light is a necessary and limiting resource for photosynthesis, excessive solar radiation could cause heat, dehydration and UV irradiation, which could inhibit the plant growth (Valladares and Niinemets, 2008). In case of vine species, light availability is mainly determined by host plant species. *Aristolochia contorta* showed the higher shoot growth and the larger leaf area under the tree host, rather than the shrub and herb host plant (Park et al., 2019). From the result of the present study, shade tolerance of one-year-old *A. contorta* individual seemed to be similar to the three-year-old individual or other individuals in the natural populations.

3.4.2. Daylight enhance the phenotypic plasticity against leaf damage

Many of growth characteristics showed the increase under the leaf damage treatment. Damage of young leaf further affected the growth characteristic parameters rather than the damage of mature leaf. Newly emerging leaves are considered to have the higher food quality the higher photosynthesis rate and nitrogen concentrations (Field and Mooney, 1983). Therefore, phytophagous insects

commonly prefer the new leaves rather than the mature leaves (Cranshaw and Radcliffe, 1980; Bazzaz et al., 1987). Damage of newly emerging leaves could make the apical dominance weaker, which trigger the emergence of new leaf or shoot (Aarssen, 1995). In the present study, damage of young leaves more induced the emergence of new leaves and branches, therefore more new leaves could re-emerge.

Compensatory response to herbivory stress in plants has been studied in diverse plant species (Trumble et al., 1993; Strauss and Agrawal, 1999). Vine plant species with climbing life-form also have compensatory response to herbivory (Rausher et al., 1993; Schierenbeck et al., 1994; Gianoli et al., 2007). In the present study, *A. contorta* showed the higher primary production under the leaf damage treatment rather than the un-damaged treatment. In some cases, plant could “overcompensate” the damage to cope with the competition for resource availability (Jämeiro et al., 1996). *Aristolochia contorta* also showed the some overcompensatory traits under moderate level of leaf damage, which could be inferred as the rapid recovery and occupation of resource.

Herbivory is known to suppress the photosynthesis indirectly (Nabity et al., 2009). Therefore, light could role as a limiting factor for compensatory growth (Lentz and Cipollini Jr., 1998; Hough-Goldstein and LaCross, 2012). Vine species could respond to the leaf damage differently by the light availability (Gianoli et al., 2007). Despite of that *A. contorta* showed the higher growth under the shade treatment, not all of the phenotypic plasticity under leaf damage stress were higher in the shade treatment rather than the daylight treatment (Figs. 3-4 and 3-5). Especially, some phenotypic plasticity indices on the biomass were higher under the daylight treatment rather than the shade treatment. Thus, compensatory growth of each parameter seemed to be affected from the environmental condition differentially.

3.4.3. Possible response of *Aristolochia contorta* against herbivory

From the result of the present study, moderate level leaf damage (25% of total leaves) seemed to induce the further growth of *A. contorta*. Therefore, proper density of herbivore could enhance the growth and maintenance of the *A. contorta* population. In addition, some alkaloids including aristolochic acids are known to be accumulated in Aristolochiaceae species, which contains the nitrogen bond (Shamma and Guinaudeau, 1985). Regardless of the statistical significance, leaf tissue of individuals with mature leaf damaged treatment under the daylight showed the lower C/N ratio rather than the other experimental treatment at September (Fig. 3-6b). Biosynthesis and accumulation of secondary metabolites is one of the core defense mechanism against herbivory both in “constitutive” and “induced” perspective (Wu and Baldwin, 2010). This result could be inferred as the induced accumulation of the secondary metabolites to prime the further herbivory when mature leaves were damaged. Accumulation of secondary metabolite involves the trade-off with the vegetative growth, thus it could be affected by both light intensity and leaf damage (Gianoli et al., 2007). This perspective could be assessed by the quantification on the secondary metabolites of *A. contorta* in future studies.

3.5. Conclusion

Most of the growth characteristics of *A. contorta* showed that leaf damage induced the compensatory growth. Phenotypic plasticity under leaf damage differed by light availability (Fig. 3-7). This results indicate that proper environmental condition could make growth and maintenance of *A. contorta* population under the herbivory stress. Furthermore, leaf C/N ratio after leaf damage treatment implied the possibility of induced secondary metabolite biosynthesis to prime the further herbivory under sufficient daylight. To understand the response of *A. contorta* to herbivore stress deeply, further research about the defense mechanism of *A. contorta* against herbivory should be studied.

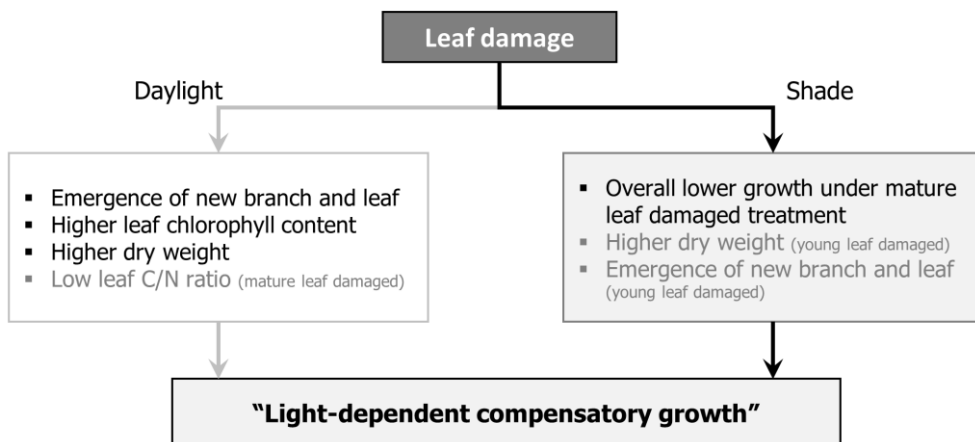


Fig. 3-7. Summary of the leaf damage experiment under different light availability on *A. contorta* individual.

Chapter 4. *De novo* transcriptome assembly of *Aristolochia contorta* reveals the defense strategy against its specific herbivore, *Seriginus montela*

4.1. Introduction

Interactions between plant and insect have been affected the biodiversity of each other (Jander, 2014). In particular, herbivory has been affected both plant and insect as “arms-race” perspective, which refers the development of the defense mechanism against each other (Jander, 2014; Kergoat, 2016; Endara et al., 2017). Plants respond and prime the herbivore attack in diverse ways. Biosynthesis of various secondary metabolites is one of the core mechanism in plant to prevent and resist to the herbivory (Wu and Baldwin, 2010). On the other hand, herbivores also adapt to the defense mechanism. For example, herbivore can sequester and/or detoxify the plant secondary metabolites (Petschenka and Agrawal, 2016). Specific herbivore could have additional specific detoxification of specific secondary metabolites (de Castro et al., 2018). As a consequence of the diversity of plant secondary metabolites and the other defense mechanisms, many herbivorous species have the narrow range of the host plant species (Bernays, 1989).

Biosynthesis of the secondary metabolites should consume and convert the primary metabolites, therefore there have been trade-off between plant growth and defense (Gatehouse, 2002). Thus, plant primes the herbivory with both “constitutive” defense and “induced” defense (Gatehouse, 2002; Wu and Baldwin, 2010). Induced defense refers the defense mechanism which are triggered by the wounding and

elicitors by the herbivores (Wu and Baldwin, 2010). Plant could recognize the herbivore specificity by herbivore elicitor during herbivory, which make the plant respond different from the other physical damage (Wu and Baldwin, 2010; Schuman and Baldwin, 2016). It is efficient for resource allocation, yet it is effective only to the later herbivory because of the delayed manner.

Plant primes the further herbivory at diverse part as well as damaged tissue (Gatehouse, 2002). Signal of herbivory damage could be propagated to other tissue or organ, by reactive oxygen species (ROS), jasmonic acid (JA), systemin, other phytohormones, and some signaling volatiles (Gatehouse, 2002; Frost et al., 2007; Koo and Howe, 2009). Undamaged tissues in damaged individuals are also induced by herbivory and accumulate the secondary metabolites (Wu and Baldwin, 2010; Schuman and Baldwin, 2016). Such “systemic response” is known as somewhat similar and different from the “local response” of the damaged tissue itself (Gatehouse, 2002). Therefore, systemic response should be also assessed to understand the response of the plant to herbivory as well as the damaged tissue.

Most of butterfly species (order Lepidoptera) has its own host range based on the similarity of the defense mechanism (Ehrlich and Raven, 1964; Edger et al., 2015). In speciation of the butterfly species, some major host shifts had been occurred and these altered host plant group have specific defense mechanism (Nallu et al., 2018; Sikkink et al., 2020). However, most of research on the specific herbivory of butterfly larvae-plant species have been conducted on the pierid butterflies-Brassicaceae plants, heliconiine butterflies-*Passiflora* plant and some pest insect species-crop monocots (de Castro et al., 2018; Nallu et al., 2018). Swallowtail butterflies (Papilionidae) are also one of the diverse butterfly group which have the narrow host range of each species (Ehrlich and Raven, 1964; Miller, 1987). Many of

the known host plant species of swallowtail butterfly larvae are classified as the basal angiosperms, which are not classified into monocots nor eudicots (Miller, 1987). This group has been diverged from the ancestral angiosperm and developed distinct defense mechanisms such as secondary metabolites, which has difference from major monocots or eudicots. Family Aristolochiaceae (Piperales) is a member of Magnoliids and basal angiosperms, which have many species as the host plant of the swallowtail butterfly larvae (Miller, 1987). Some Aristolochiaceae-specific swallow butterfly species could sequester or detoxify the specific secondary metabolite (aristolochic acid) by O-glucosylation, which have the lethality to the generalist phytophagous insects (Nishida, 1994; Priestap et al., 2012). However, mechanisms of the specific defense of plant or specific herbivory of butterfly on Aristolochiaceae and basal angiosperms is poorly understood.

Aristolochia contorta Bunge (Aristolochiaceae) is one of the Piperales species which has its exclusively dependent herbivore, *Seriginus montela* (Papilionidae; dragon swallowtail butterfly; Hong et al., 2014). These two species inhabit in narrow geographical range (Russian Far East, Korea, China, and Japan; GBIF Secretariat, 2020). Based on the exclusively specific herbivory and narrow distribution range, *A. contorta* seems to have distinct constitutive and induced defense mechanisms as Aristolochiaceae and basal angiosperms.

This research aims to understand the specific defense mechanism of *A. contorta* and specific response to its specialist herbivore *S. montela*. Since reference genome of family Aristolochiaceae has not been annotated, *de novo* transcriptome analyses of *A. contorta* under control and simulated specific herbivory were conducted for assessment of the defense mechanism at various layer. Research goals of this research are followed:

- 1) Does *A. contorta* respond to the specific herbivory of the *S. montela* differently from the simple physical wounding?
- 2) How *A. contorta* prime the later herbivory in damaged and undamaged systemic tissue?
- 3) Does the biosynthesis of the specific secondary metabolite differ by herbivore elicitor?

4.2. Methods

4.2.1. Plant materials and treatment

Seeds from the *Aristolochia contorta* population (37°05'N 127°05'E) in Pyeongtaek, Gyeonggi-do, Republic of Korea were collected at late 2018. Collected seeds were chilled in the refrigerator. Seeds were sterilized by soaking in [5 % NaOCl solution + 0.1% Triton X-100] in five minutes and [70% ethanol] in one minutes. Washed seeds were germinated and grown in the growth chamber (SW-904C, Gaon Scientific, Seoul) at 28 °C, long-day conditions (16 h light / 8 h dark) about eight weeks from sowing day. Germinated seedlings were transferred at the small plastic pot (8 cm \varnothing \times 10 cm height) filled with mix of sand and topsoil (2:1 in v/v). Transferred seedlings in plastic pots were grown in the growth chamber at 28 °C, long-day conditions (16 h light / 8 h dark) about four weeks. I selected the total 27 seedlings with similar height and leaf number and randomly divided into three groups.

To conduct simulated herbivory, oral secretion (OS) of *Sericinus montela* was collected and pooled from third or fourth instar larvae of in-bred colony from the population in Pyeongtaek, Gyeonggi-do, Republic of Korea. Larvae of *S. montela* was carefully rubbed and regurgitant was collected using long micropipette tip (gel

loading tip) and stored at -20°C before treatment. Before treatment, OS was diluted in 1:10 with distilled water. For simulated herbivory (W+OS) and simple wounding (W+DW) treatment, four rows of holes were made using a pattern wheel at top fifth and sixth leaves as local leaf. 20 µl of 1:10 diluted OS and distilled water (DW) were added to W+OS and W+DW treatment, respectively. Added OS or DW were gently rubbed into wounds using gloved finger (Joo et al., 2018). All three treatments including control were conducted to nine individuals.

After treatment for four hours, I collected leaves from the three treatment groups (W+OS, W+DW, and control). The top fifth and sixth leaves were collected as local leaf, and the third and fourth leaves were collected as systemic leaf (Fig. 4-1). Collected leaves were immediately frozen in liquid nitrogen and stored in -80 °C deep freezer before RNA extraction.

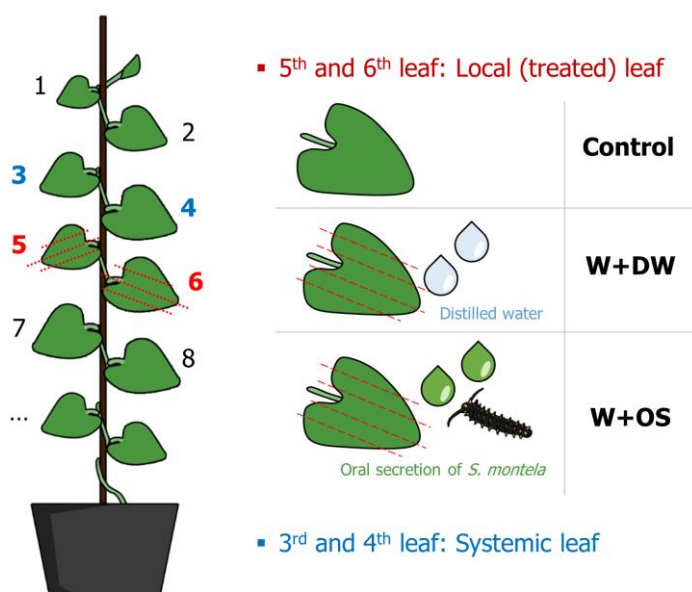


Fig. 4-1. Schematic diagram of artificial herbivory treatment.

4.2.2. mRNA library construction

After being fully ground, three local or systemic leaf samples of each treatment were pooled as one biological replicate (total $n = 3$ biological replicates for each treatment for mRNA library construction). Total RNA was isolated from pooled ground samples using TRIzol reagent. Concentration and purity of isolated RNA samples were checked using Nanodrop One^c (Thermo Fisher Scientific, Waltham, MA). Detailed experimental protocols were described in **Appendix A**.

The cDNA library construction and RNA-seq were performed by Macrogen (Seoul, Republic of Korea). TruSeq stranded mRNA library was constructed by Illumina HiSeq 2000 platform. Total 18 paired-end sequencing libraries with insert sizes about 101 bp were constructed, which resulted in a total of 1,374,735,810 reads. Sequenced data were produced in FASTQ format. Raw FASTQ transcriptome data has been deposited in the sequence reads archive (SRA), NCBI with accession number PRJNA665793.

4.2.3. *De novo* assembly and functional annotation

FastQC v0.11.7 software was used to quality assessment of the sequence reads (Andrew, 2010). Lower quality reads ($< Q30$) were filtered out and the remaining reads were trimmed using Trimmomatic 0.38 (Bolger et al., 2014). *De novo* assemblies were conducted from the clean reads using Trinity (Grabherr et al., 2011). Longest contigs were clustered as “unigenes (unique genes)” using CD-HIT-EST version 4.6 (Li and Godzik, 2006). Non-redundant unigenes, which have a minimum length of 200 bp, were used to be blasted against public databases, such as NCBI Nucleotide (NT), Kyoto Encyclopedia of Genes and Genomes (KEGG), Pfam, Gene Ontology (GO), NCBI non-redundant Protein (NR), Uniprot, and EggNOG.

4.2.4. Differentially expressed gene analysis

All differentially expressed gene (DEG) analysis and statistical analysis were performed using R version 4.0.2 (R Core Team, 2020). The DEGs between control and treatment (W+DW and W+OS) within local leaves or systemic leaves were identified with R package “DESeq” with $|\log_2(\text{fold change})| \geq 1$ and adjusted $p\text{-value} < 0.05$ as the threshold (Anders and Huber, 2010). Gene Ontology (GO) enrichment analysis of all DEGs was performed using R package “goseq” with Wallenius approximation with custom bias (contig length) data retrieved by R package “seqinr” (Charif and Lobry, 2007; Young et al., 2010). In similar, KEGG pathway enrichment analysis was also conducted based on adjusted $p\text{-value} < 0.05$ using R package “goseq”. For visualize the enriched GO term, REVIGO was used within the GO category “biological process” (Supek et al., 2011). Also, GO circle plots were made using R package “GOplot” (Walter et al., 2015).

4.2.5. Ordination of differentially expressed genes

Principal component analysis (PCA) of gene expression levels (FPKM value) was conducted and visualize by R package “ggplot2” (Wickham, 2016). For filter the most differentially expressed genes which contribute the ordination of samples in the plot, quadratic means of the eigenvalue of PC1 and PC2 were calculated. Clustering of the contigs and experimental conditions of some herbivore-related GO terms were conducted by R package “pheatmap” (Kolde and Kolde, 2015).

4.2.6. Validation of gene expression

For validate the gene expression from RNA-seq, quantitative real-time polymerase chain reaction (qRT-PCR) was used. From extracted mRNA of each samples which had been used in *de novo* transcriptome assembly, cDNAs were obtained using M-MLV reverse transcriptase (Promega, Madison, WI).

Reference genes (housekeeping genes) was filtered from the RNA-seq, which have normalized count (FPKM) > 10, length > 1,000 nt, and the lowest coefficient of variation (top 10% of SD/mean; Miao et al., 2015). Candidate reference genes and primers were validated by homogeneously amplified bands which were observed from the electrophoresis of PCR products. Finally, *AcACT101* (c81658_g1_i1) was selected and used as reference gene.

The qRT-PCR reaction was conducted using QuantStudio 6 (Applied Biosystems, Foster, CA) with KAPA SYBR FAST qPCR Master Mix (2X) (KAPA Biosystems, Wolburn, MA) in a reaction volume of 10 µl. The two-step thermal cycling profile employed was 15 sec at 95 °C for denaturation and 1 min at 60 °C for annealing and polymerization. The *AcACT101* (c81658_g1_i1) gene was included as internal control in the PCR reactions to normalize the variations in the amounts of primary cDNAs used. Relative expression level was calculated by *ddCt* method. Each sample was analyzed in three technical replicates for each gene. Primers of reference genes and selected DEGs were designed by Geneious Prime Version 2020.1.1. (<https://www.geneious.com>; Table 4-1).

Table 4-1. Used primers in qRT-PCR.

Contig	Annotation		Primer sequence(5'-->3')
c51887_g1_i1	<i>Ac4CL2</i>	F	AAGGCGAGGTGGAATGCTC
		R	TTTTCGCACCGGAAGCTTTG
c64106_g1_i1	<i>Ac6OMT</i>	F	TCTCCGGCAAGGACAAGAAC
		R	CGGCGTTGAAGAGCTTGTTT
c36845_g1_i1	<i>AcACS</i>	F	GCCGGGGTTATACAGATGGG
		R	AAAGGCCGTGGTAGTCTTGG
c81658_g1_i1	<i>AcACT101</i>	F	CCTCTCCGCCCTTTTCTCAG
		R	GAGCCCTTTCTCCTTCGCTT
c48813_g2_i1	<i>AcCht6</i>	F	GAGAGCAACACCCAGTACCC
		R	ACCATAGAGCCGCCTTGAAC
c64728_g1_i3	<i>AcCNMT</i>	F	ACCAAATCGTGCAGTTTGCC
		R	GCCTCATCCAGAGTTGTGCT
c106305_g1_i1	<i>AcCYP73A5</i>	F	CAGGGGGTTCGAGTTTGGATC
		R	TCCCTGCTTCGAATCCCCAC
c67503_g1_i1	<i>AcCYP76B1</i>	F	ACCCACCGATGATGAAGCAG
		R	GCCATTGCCCACTCTACTGT
c67391_g1_i6	<i>AcCYP76B6</i>	F	CGTGAAGTCTCCCGTTTCGAA
		R	ACAGTGTCCGCGATCGTATC
c50582_g1_i1	<i>AcCYP80B2</i>	F	CGTTCCTCACACTTTCGGGA
		R	TTCTCTCCCTCAAACCGGC
c55025_g1_i2	<i>AcCYP82C4</i>	F	CGAGCACCTGGGTTACAAC
		R	GCTCACCGTTTTCAACCCAC
c8034_g1_i1	<i>AcDODA</i>	F	GGAGAAAGTGCTGGTGACGA
		R	CGCCGGATACTTGAGCTGAT
c51752_g2_i1	<i>AcJMT</i>	F	GGAGACCTGGGTTGCTCTTC
		R	GGAGCGACTGTGAGATGGAG
c44532_g1_i1	<i>AcMYB34</i>	F	CACACAAACGCAGCACTACC
		R	CGGTCCCTTCTTCAAGCCAT
c91572_g1_i1	<i>AcNCS1</i>	F	ACTTGAGGTGATTGCGCAGA
		R	GGCTTCCAGACCAGAACCA
c63371_g1_i1	<i>AcNCS2</i>	F	CGGCCTCCATGATCAGATCC
		R	TTTCGAAGGACTGTTCCCCG
c64750_g2_i1	<i>AcNES1</i>	F	GGTCATGTGGCCAGTAGCTT
		R	TCGTCCCACCTGTAACTGC
c73635_g1_i1	<i>AcYLS9</i>	F	ATGCTCTTCCCGCTTTCAA
		R	GGGGTGAAGTGCTTGGTCTT
c60393_g2_i1	<i>AcPAL</i>	F	TCCGGAATCAGGTGGGAGAT
		R	CACCGCCTTTATGTTGTGCC
c64496_g1_i4	<i>AcPPO</i>	F	AAGACCACTCTTCGCACCTG
		R	TCTCACCAGACATTGCCCC
c61823_g1_i3	<i>AcSCPL18</i>	F	GATACGTGGGTGTGGGAGAC
		R	GACGGCAAGCTCCCATGTGA
c62822_g1_i2	<i>AcSSL10</i>	F	TATTTTGGCCTGCTCGTGGT
		R	CTCCACTGACGACCAAGGAC
c66825_g5_i1	<i>AcTyrDC2</i>	F	GCTCCATCCACAACCTTGGC
		R	CAAAGAAGGGGCCAGAGGAA
c74598_g1_i1	<i>AcTyrDC3</i>	F	CGATGAACTTCCGGGATCGT
		R	CACATCCTGTACTCCCTCGC

4.3. Results

4.3.1. Overview of the *A. contorta* transcriptome

The clean sequence reads were assembled into 169,133 contigs by Trinity. The longest and non-redundant contigs were filtered, total 92,323 unigenes were followed. Average length of unigenes and N50 length were 860.2 bp and 1,579 bp, respectively. Total annotated ratio of unigenes was 39.21% (36,202 unigenes). Annotated ration of gene ontology (GO) database and KEGG database (KO_EUK) were 30.58% and 37.31%, respectively (Table 4-2). Number of open reading frames (ORFs) was predicted about 21,866 by TransDecoder program (<http://transdecoder.sourceforge.net/>). Contigs that have more than one read count value was zero were excluded in the analysis. Therefore, total 26,611 unigenes were used for further statistical analysis.

Table 4-2. Summary of annotations of the *Aristolochia contorta* transcriptome.

Annotation database	Number of annotated unigenes	Percentage of all-unigenes (%)
Nr	34,207	37.05
Nt	22,371	24.23
UniProt	24,760	26.82
KEGG	20,948	22.69
EggNOG	31,110	33.70
GO	28,231	30.58
Total number of all-unigenes	92,323	-

4.3.2. Gene expression among experimental conditions

Principal component analysis (PCA) on the expression level of differentially expressed contigs showed that damaged local leaf (both W+DW and W+OS) was ordinated as distinctive group from other experimental conditions (Fig. 4-2). Under control (non-damaged) condition, local leaf and systemic leaf showed different aspects on the 2-D plot of PCA. Systemic leaf under damaged signal (both W+DW and W+OS) partially overlapped to the control condition. Proportion of variance of principal component 1 (PC1) and PC2 were 23.0% and 19.3%, respectively. After PC3, proportion of variance decreased under 10%.

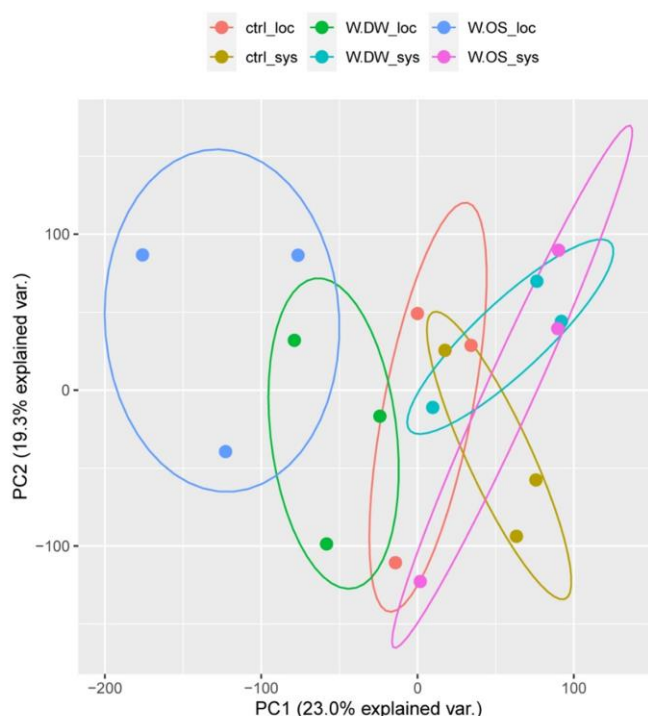


Fig. 4-2. Principal component analysis (PCA) on the expression level (FPKM values) of each contigs. Ellipses indicate the confidential interval of ± 1 SD for each treatment.

Contigs that have the significance to the PCA ordination were filtered by the square mean of the eigenvalues of PC1 and PC2 (Table 4-3). The most significant contig was predicted as serine/arginine repetitive matrix protein. Other significant contigs were predicted to have the DNA, RNA, and chromatin binding activity, such as small nuclear ribonucleoprotein, acetyltransferase, and sister-chromatid cohesion protein. Enzymes on the intercellular transport, such as the exportin-4, *AP5*-complex subunit zeta-1, and *SAC3* family protein A were predicted to contribute the ordination of transcriptome of the damaged leaves. Four of twenty most-significant contigs were predicted as pentatricopeptide repeat-containing protein. However, three of twenty most-significant contigs could not be annotated by public database.

Total 3,177 contigs were filtered as differentially expressed genes (DEGs) at least the one of the four comparisons; 1) Control vs. W+DW in local leaf; 2) Control vs. W+OS in local leaf; 3) Control vs. W+DW in systemic leaf; 4) Control vs. W+OS in systemic leaf (Fig. 4-3a). In local leaf, total 837 contigs (451 up- and 386 down-regulated) and 2,391 contigs (1,307 up- and 1,084 down-regulated) were differentially expressed under W+DW and W+OS treatment, respectively. In systemic leaf, total 367 contigs (207 up- and 160 down-regulated) and 256 contigs (169 up- and 87 down-regulated) were differentially expressed under W+DW and W+OS treatment, respectively (Fig. 4-3b). Over half of the total DEGs (1,875 contigs) differentially expressed only in local leaf under W+OS treatment. Eleven contigs differentially expressed among all comparisons.

Table 4-3. Contigs which showed the higher eigenvalues on principal component analysis of FPKM values. PC = principal component.

Contig	Gene annotation	PC1 eigenvalue	PC2 eigenvalue
c58190_g1_i8	serine/arginine repetitive matrix protein 2-like	0.0030	-0.0132
c64492_g1_i6	exportin-4	0.0015	-0.0134
c57629_g3_i1	(unannotated)	-0.0009	-0.0134
c7383_g1_i1	U11/U12 small nuclear ribonucleoprotein 31 kDa protein	0.0032	-0.0131
c58736_g2_i4	uncharacterized protein LOC110113897	-0.0008	-0.0134
c60736_g1_i3	N-terminal acetyltransferase B complex auxiliary subunit NAA25 isoform X1	0.0018	-0.0133
c64075_g3_i4	pentatricopeptide repeat-containing protein At1g06710, mitochondrial	-0.0034	-0.0130
c64824_g1_i4	putative pentatricopeptide repeat-containing protein At5g06400, mitochondrial	-0.0022	-0.0132
c55510_g1_i1	ubinuclein-1-like	-0.0026	-0.0131
c65717_g2_i6	AP-5 complex subunit zeta-1	-0.0011	-0.0133
c49191_g1_i1	sister-chromatid cohesion protein 3	0.0020	-0.0132
c54944_g1_i2	SAC3 family protein A	-0.0005	-0.0134
c59106_g2_i2	putative pentatricopeptide repeat-containing protein At1g13630 isoform X1	0.0025	-0.0131
c59271_g1_i1	pentatricopeptide repeat-containing protein At1g11710, mitochondrial	-0.0053	-0.0122
c66382_g1_i8	extracellular ribonuclease-like	0.0073	-0.0112
c67264_g2_i13	structural maintenance of chromosomes protein 6B-like	0.0013	-0.0132
c66125_g8_i3	GTPase Der	-0.0003	-0.0133
c37173_g1_i2	plasma membrane ATPase 4	-0.0054	-0.0121
c40047_g1_i3	E3 ubiquitin-protein ligase BRE1-like 2	-0.0046	-0.0125
c59545_g1_i5	uncharacterized LOC104606611	0.0019	-0.0131

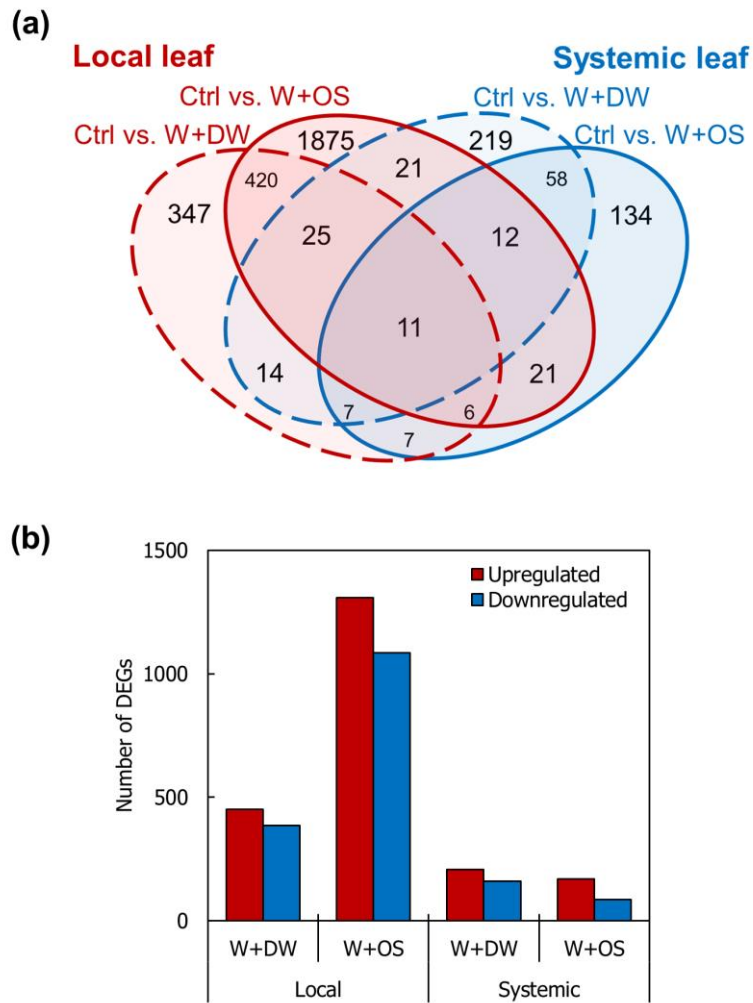


Fig. 4-3. The number of DEGs in three comparison groups. **(a)** Venn diagram of all DEGs (all up- and down-); **(b)** the number of up- and downregulated DEGs (compared to the control) of local and systemic leaf. Ctrl. = control; W+DW = wounded with distilled water; W+OS = wounded with oral secretion of *S. montela*.

4.3.3. Gene Ontology enrichment analysis

Gene Ontology (GO) enrichment analysis was conducted on the 3,177 DEGs, and 6,318 GO terms were annotated. In biological process category, GO term "amino acid transmembrane transport", "catabolic process", "methylation", "circadian rhythm", "metabolic process", "nitrogen compound metabolic process", "chaperone-mediated protein folding", "hydrogen peroxide catabolic process", "cytokinin biosynthetic process", and "response to chitin" were significantly enriched in local leaf under W+DW treatment (Fig. 4-4a, Appendix B). In local leaf under W+OS treatment, biological process GO term "oligopeptide transport", "chaperone mediated protein folding requiring cofactor", "immune system process", "protein-chromopore linkage", "metabolic process", "photosynthesis", "catabolic process", "cell communication", "primary metabolic process", "photosynthesis, light harvesting in photosystem I", "lignin biosynthetic process", and "response to wounding" were significantly enriched in local leaf under W+OS treatment (Fig. 4-4b).

In systemic leaf, biological process GO term "oligopeptide transport", "circadian rhythm", "developmental process", "nitrogen compound metabolic process", "metabolic process", "glycogen biosynthetic process", "gibberellic acid homeostasis", and "defense response to fungus" were significantly enriched under W+DW treatment (Fig. 4-4c). Biological process GO term, such as "metabolic process", "cell proliferation", "cell wall organization or biogenesis", "golgi organization", "carbohydrate metabolic process", "protein acetylation", "secondary metabolite biosynthetic process", and "defense response to other organism" were significantly enriched in systemic leaf under W+OS treatment (Fig. 4-4d).

(a) Local leaf, Ctrl vs. W+DW

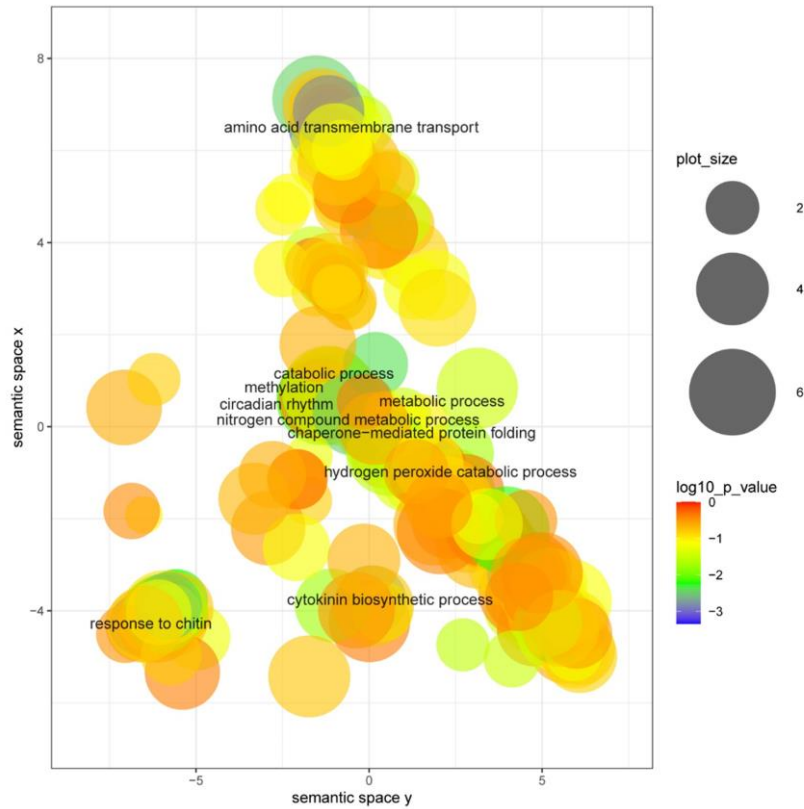


Fig. 4-4. The result of Gene Ontology (GO) analysis by REVIGO (biological process). **(a)** Control versus W+DW local leaf; **(b)** Control versus W+OS local leaf; **(c)** Control versus W+DW systemic leaf; **(d)** Control versus W+OS systemic leaf. The \log_{10} values of the p -value for each cluster were represented based on the color gradation. The bubble size indicates the frequency of the GO term in the underlying GO database (bubbles of more general terms are larger).

(b) Local leaf, Ctrl vs. W+OS

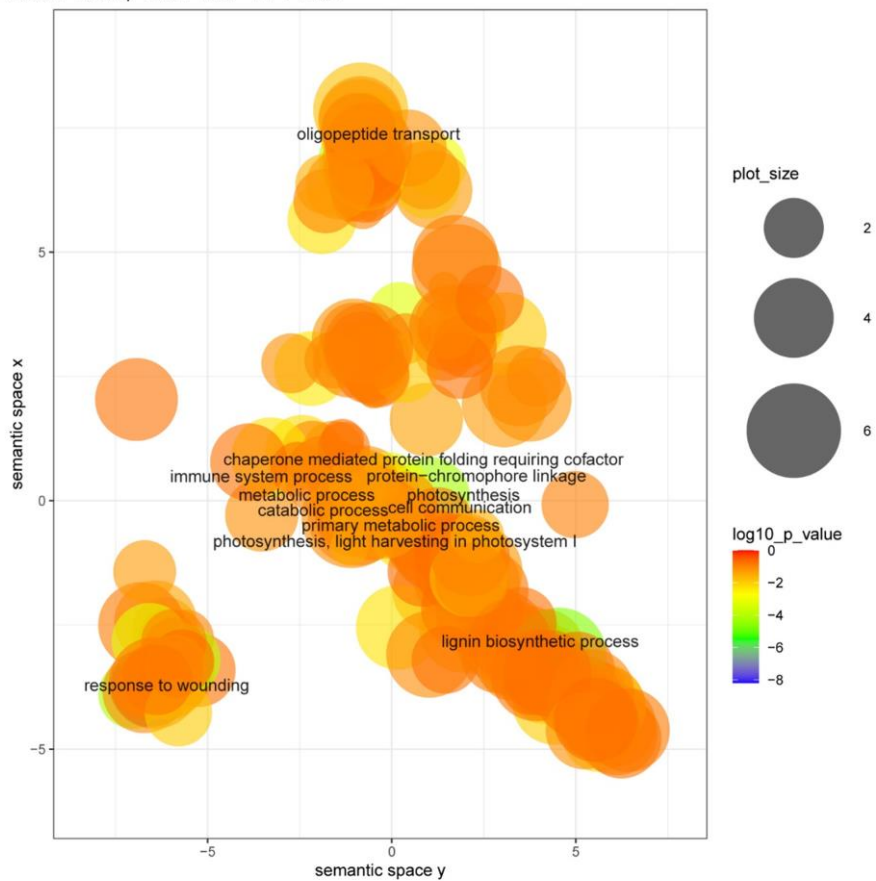


Fig. 4-4. (continued)

(c) Systemic leaf, Ctrl vs. W+DW

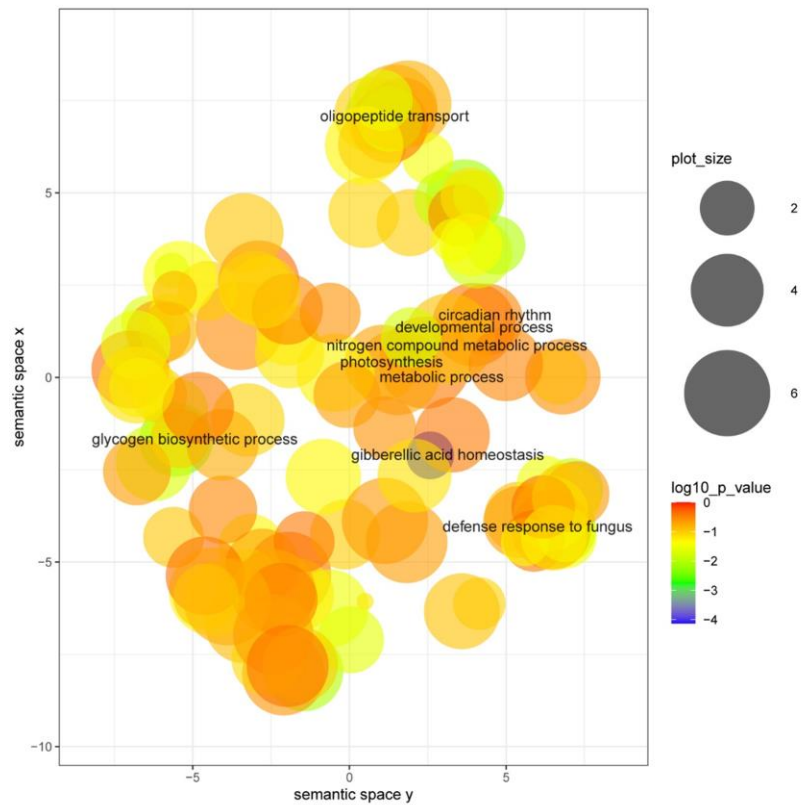


Fig. 4-4. (continued)

(d) Systemic leaf, Ctrl vs. W+OS

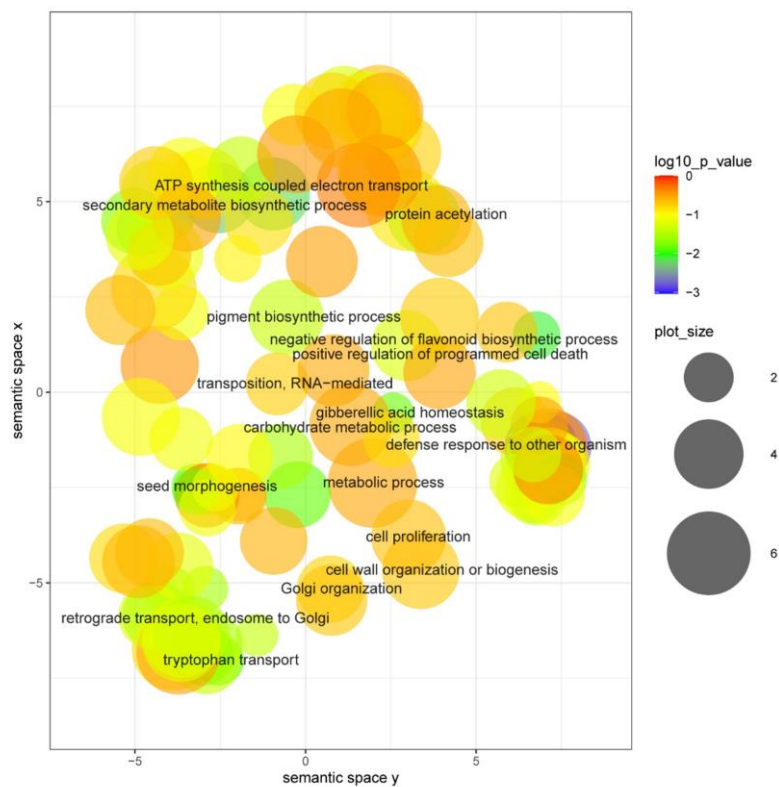
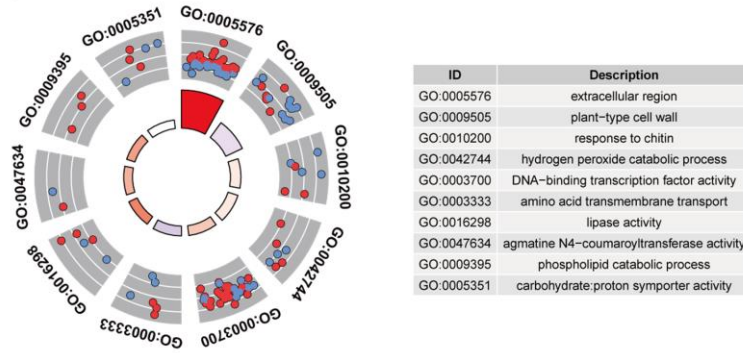


Fig. 4-4. (continued)

The most-enriched 10 GO terms were visualized by GO circle plot under four comparisons (Fig. 4-5). In local leaf under W+DW treatment, GO terms, such as “extracellular region”, “DNA-binding transcription factor activity”, “plant-type cell wall”, “response to chitin”, “hydrogen oxide catabolic process”, and “amino acid transmembrane transport” were the most enriched (Fig. 4-5a). The GO term, such as “response to wounding”, “extracellular region”, “plasma membrane”, “DNA-binding transcription activity”, “plant-type cell wall”, and “lignin biosynthetic process” were the most enriched in local leaf under W+OS treatment (Fig. 4-5b).

In systemic leaf under W+DW treatment, GO term, such as “integral component of membrane” and “sequence-specific DNA binding” were most enriched (Fig. 4-5c). The GO term, such as “iron ion binding”, “oxidoreductase activity”, “copper ion binding”, and “secondary metabolic process” were most enriched under W+OS treatment in systemic leaf (Fig. 4-5d).

(a) Local leaf, Ctrl vs. W+DW



(b) Local leaf, Ctrl vs. W+OS

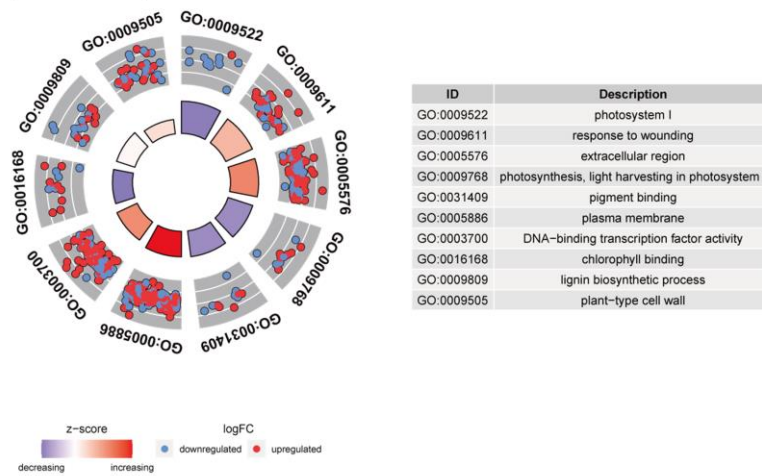
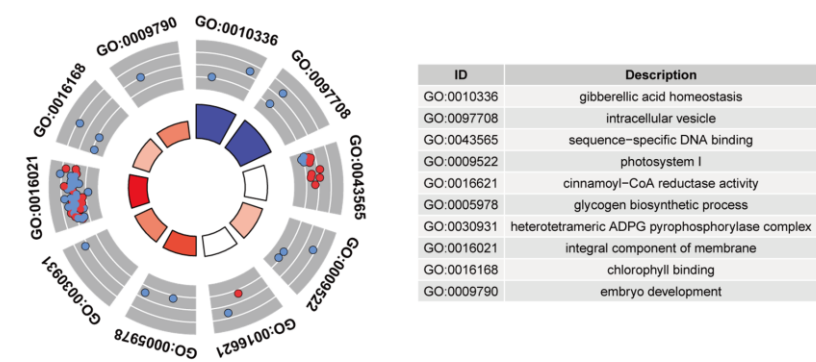


Fig. 4-5. GO circle plot displaying gene annotation enrichment analysis. **(a)** most-enriched DEGs in W+DW (versus control), local leaf; **(b)** most-enriched DEGs in W+OS (versus control), local leaf; **(c)** most-enriched DEGs in W+DW (versus control), systemic leaf; **(d)** most-enriched DEGs in W+OS (versus control), systemic leaf; Radar chart shows the distribution of individual terms in the annotation categories. The fold changes (FC) of gene expression values ($\log_2\text{FC}$) were derived from three biological replications corresponding to each sample. The outer to inner layers of gray circles indicate the relative fold change of gene expression (from higher to lower). The height of the inner rectangle represents the p -value of the GO term. The rectangles were colored with the red gradient according to the z -score ($p < 0.05$, FDR adjusted $p < 0.05$). $Z\text{-score} = (\text{upregulated} - \text{downregulated}) / \sqrt{\text{upregulated} + \text{downregulated}}$

(c) Systemic leaf, Ctrl vs. W+DW



(d) Systemic leaf, Ctrl vs. W+OS

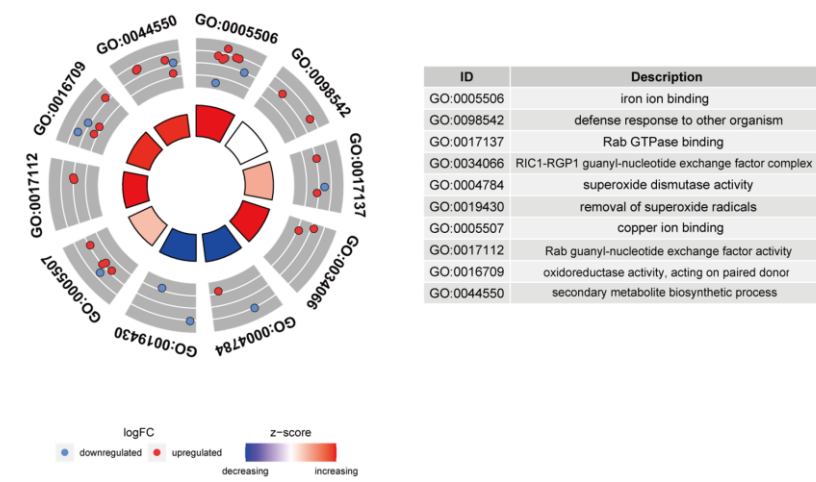


Fig. 4-5. (continued)

4.3.4. Kyoto Encyclopedia of Genes and Genomes (KEGG) pathway enrichment analysis

As a result of KEGG pathway enrichment analysis, 48, 35, 31, and 37 pathways were significantly enriched in control vs. W+DW in local leaf, control vs. W+OS in local leaf, control vs. W+DW in systemic leaf, and control vs. W+OS in systemic leaf, respectively. In local leaf, KO (KEGG orthology) terms such as “peroxidase”, “phospholipase C”, “transcription factor *MYB*”, “nuclear transcription factor Y, alpha”, “alpha-galactosidase”, “pyrimidine/purine-5’-nucleotide nucleosidase”, “4-coumarate--CoA ligase” were significantly enriched (Fig. 4-6a). Under control vs. W+OS in local leaf, pathway “transcription factor *MYB*”, “peroxidase”, “auxin-responsive protein *IAA*”, “glutathione S-transferase”, “aquaporin *TIP*”, and “cinnamyl-alcohol dehydrogenase” were significantly enriched (Fig. 4-6b).

In systemic leaf, overall gene ratio (ratio between number of differentially genes in the category and the number of total genes in the category) was low. Under control vs. W+DW in systemic leaf, pathway “light-harvesting complex II chlorophyll a/b binding protein 1” and “glutathione S-transferase” were significantly enriched (Fig. 4-6c). There was only one category (*RAB6A-GEF* complex partner protein 1) significantly enriched with more than one differentially expressed gene in systemic leaf, under control vs. W+OS treatment (Fig. 4-6d).

(a) Local leaf, Ctrl vs. W+DW



Fig. 4-6. Top 20 enriched KEGG pathways among the annotated DEGs across four comparisons. **(a)** Control versus W+DW local leaf; **(b)** Control versus W+OS local leaf; **(c)** Control versus W+DW systemic leaf; **(d)** Control versus W+OS systemic leaf.; The y-axis on the left represents KEGG pathways, and the x-axis indicates the enrichment factor.

(b) Local leaf, Ctrl vs. W+OS



Fig. 4-6. (continued)

(c) Systemic leaf, Ctrl vs. W+DW



Fig. 4-6. (continued)

(d) Systemic leaf, Ctrl vs. W+OS

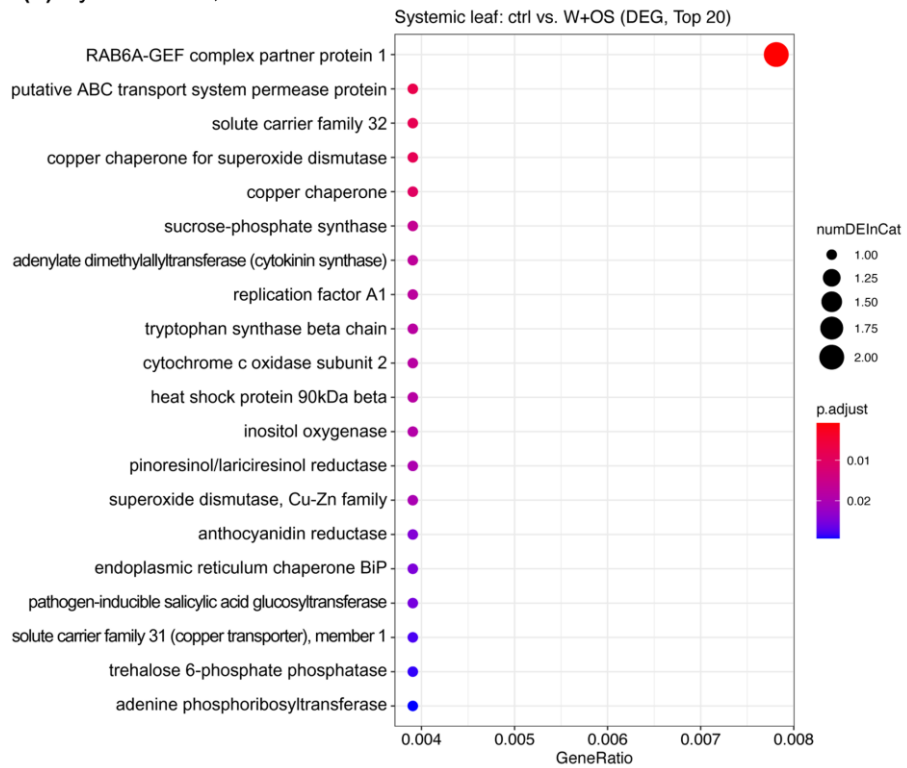


Fig. 4-6. (continued)

4.3.5. Difference in the expression profile on the herbivory defense

In GO term “defense response (GO:0006952)”, damaged local leaves (both W+DW and W+OS) showed differed gene expression pattern in the heatmap (Fig. 4-7a). Some contigs expressed differently under W+DW and W+OS treatment in local leaf, respectively. Local leaf with W+OS treatment showed distinctive expression pattern in GO term “response to wounding (GO:0009611)” to the other experimental condition (Fig. 4-7b). Local leaf with W+OS treatment also showed distinctive expression pattern in GO term “secondary metabolite biosynthesis process (GO:0044550)” relative to the other experimental condition (Fig. 4-7c). On the other hand, gene expression pattern of the local leaf with W+DW treatment showed the similar gene expression pattern to the control treatment in GO term “secondary metabolite biosynthesis process”.

Specific secondary metabolite biosynthesis seemed to be induced in systemic leaf, rather than the local leaf (Fig. 4-7d, e). In GO term "alkaloid biosynthetic process (GO:0009821)", gene expression of wounded local leaves (both W+DW and W+OS) seemed to be downregulated (Fig. 4-7d). In GO term “tyrosine decarboxylase activity (GO:0004837)”, gene expression level of systemic leaves under W+DW condition were higher than other experimental conditions (Fig. 4-7e). Contig c32998_g1_i1 (probable aromatic-L-amino-acid decarboxylase-like) showed the higher gene expression level under W+OS in local leaf, but average gene expression level was too low (FPKM = 2.19 ± 2.13).

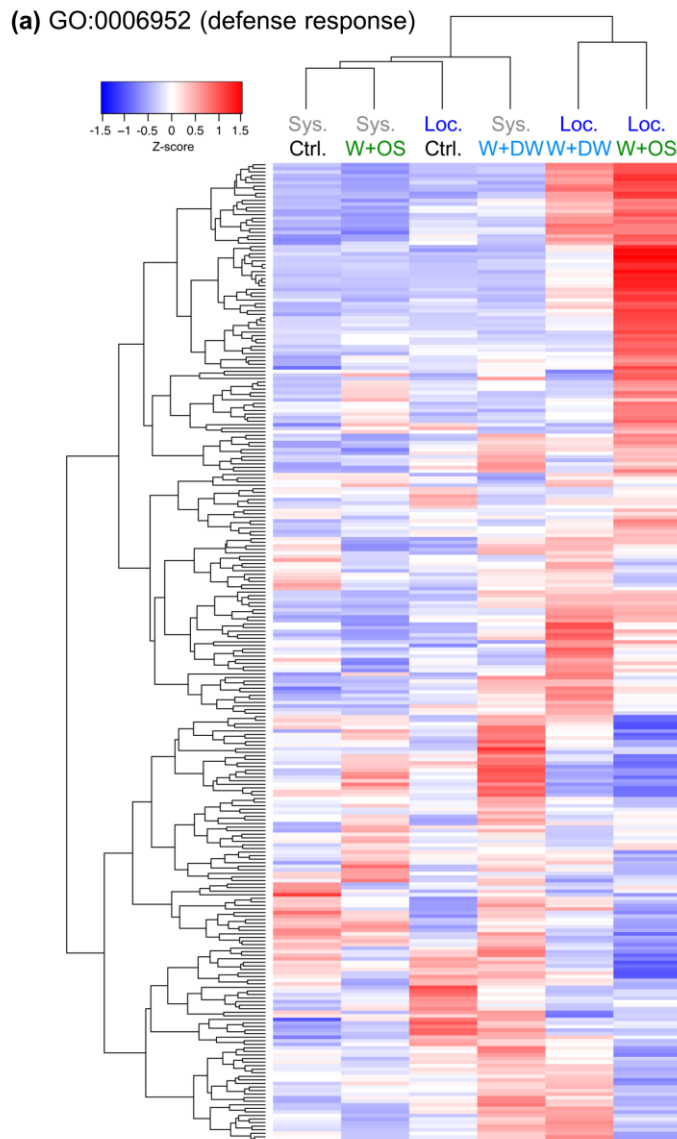


Fig. 4-7. Expression profile heatmap and clustering in some herbivory and specific secondary metabolite related GO annotations under various treatments. Color represents the Z-score of the average expression level. **(a)** GO:0006952 (defense response); **(b)** GO:0009611 (response to wounding); **(c)** GO:0044550 (secondary metabolite biosynthesis process); **(d)** GO:0009821 (alkaloid biosynthetic process); **(e)** GO:0004837 (tyrosine decarboxylase activity). Loc. = local leaf; Sys. = systemic leaf; Ctrl. = control; W+DW = wounded with distilled water; W+OS = wounded with oral secretion of *S. montela*.

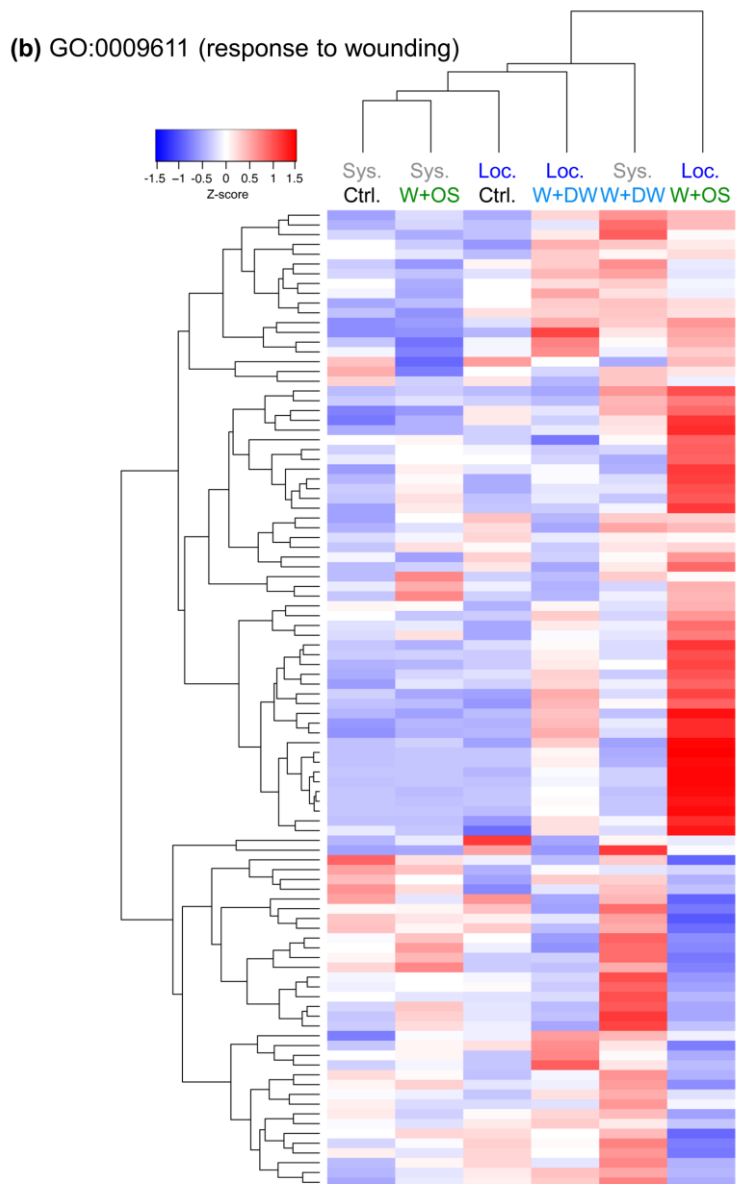


Fig. 4-7. (continued)

(c) GO:0044550 (secondary metabolite biosynthesis process)

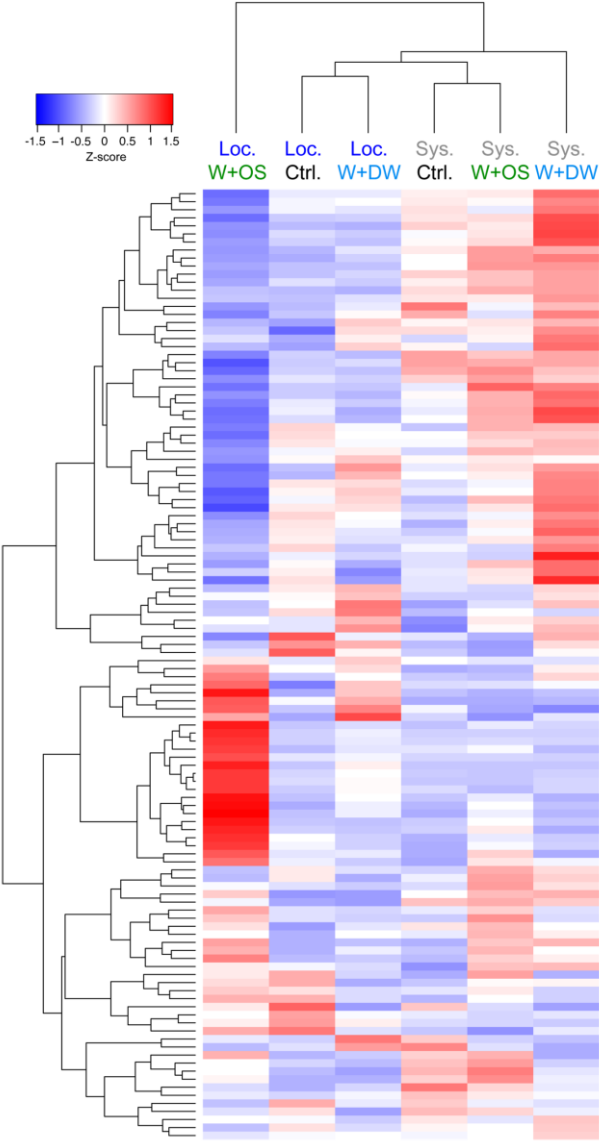
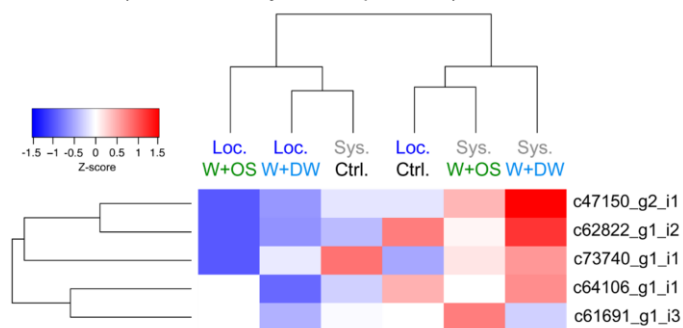


Fig. 4-7. (continued)

(d) GO:0009821 (alkaloid biosynthetic process)



(e) GO:0004837 (tyrosine decarboxylase activity)

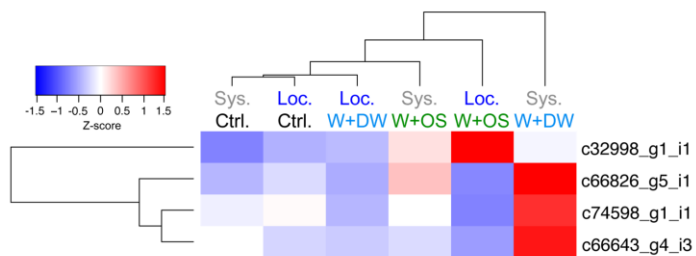


Fig. 4-7. (continued)

In GO term “defense response (GO:0006952)”, contigs which are classified into transcription factors, protein kinases, and other defense-related proteins were differentially expressed in damaged local leaf (Table 4-4). Overall fold change in local leaf was higher in W+OS rather than W+DW. Homologs to transcription factor *MYB* family, *WRKY* family, and ethylene-responsive transcription factor were highly expressed under W+OS treatment in local leaf. Signaling cascade seemed to be activated in the wounded local leaf by probable kinase activity of serine/threonine-protein kinase, protein kinase 2B, *APK1A*, *MLO6-like*, and diacylglycerol kinase-2-like. Reactive oxygen species (ROS) signal could be propagated by probable respiratory burst oxidase homolog protein E by wounding. Also, some probable anti-infection genes (detoxification of the pathogen xenobiotics) seemed to be induced, such as *YLS9-like*, polygalacturonase inhibitor precursor, chitinase 6, and *RG43*. Expression of homologs of cysteine proteinase inhibitor B-like and *BOI*-related E3 ubiquitin protein ligase 3 were induced, which are predicted to protein degradation. Defense-related secondary metabolite biosynthesis were also predicted to be induced by homologs of phenylalanine ammonia-lyase-like protein and S-norcochlorogenic acid synthase 2.

Table 4-4. Differentially expressed genes (DEGs) in the cluster of upregulated genes under artificial herbivory of local leaf in defense response (GO:0006952). Fold change refers the log₂ ratio of read count between treatment and control.

contig	annotation	Fold change			
		Local leaf		Systemic leaf	
		W+DW	W+OS	W+DW	W+OS
c44532_g1_i1	transcription factor MYB34-like	2.36	4.68	-0.46	-0.68
c44532_g2_i1	transcription factor MYB102-like	1.88	4.24	-0.69	-1.12
c32901_g1_i1	polygalacturonase inhibitor precursor	2.20	4.19	-0.47	-1.27
c61545_g1_i2	probable WRKY transcription factor 72	1.52	4.06	-0.80	0.29
c73635_g1_i1	protein YLS9-like	2.09	3.98	0.52	1.15
c60619_g2_i1	pop:7497006 uncharacterized protein LOC7497006	2.65	3.46	-0.38	-0.37
c52838_g1_i1	G-type lectin S-receptor-like serine/threonine-protein kinase At1g11330	2.73	3.15	-1.28	-1.18
c55200_g1_i2	respiratory burst oxidase homolog protein E	-0.58	2.98	0.38	1.43
c61943_g1_i3	LRR receptor-like serine/threonine-protein kinase GSO1	1.24	2.67	-0.68	0.36
c62243_g1_i1	atr:18448760 uncharacterized protein LOC18448760	1.00	2.64	-1.15	0.03
c51310_g1_i2	NEP1-interacting protein 1-like	0.40	2.57	-0.99	-0.85
c48813_g2_i1	chitinase 6	0.80	2.49	-0.13	0.04
c89919_g1_i1	cysteine proteinase inhibitor B-like	1.60	2.12	-0.07	-0.23
c30136_g1_i1	probable BOI-related E3 ubiquitin-protein ligase 3	0.90	2.05	-0.57	0.22
c7247_g1_i1	putative disease resistance protein RGA3	1.38	1.99	0.24	-0.40
c56519_g1_i1	protein kinase 2B, chloroplastic-like	0.85	1.98	-0.53	-0.27
c57727_g1_i1	protein POLYCHOME	0.72	1.92	-0.30	0.83
c63371_g1_i1	S-norococlaurine synthase 2	0.81	1.76	0.01	0.45
c63500_g1_i2	protein LURP-one-related 8-like	1.01	1.74	-0.03	0.13
c67475_g6_i2	putative disease resistance protein RGA3	1.04	1.67	-0.23	-0.10
c55594_g1_i1	ethylene-responsive transcription factor 12-like	0.70	1.37	-0.62	-0.40
c52484_g1_i4	protein kinase APK1A, chloroplastic	0.87	1.35	-0.27	-0.43
c67050_g9_i1	protein kinase 2B, chloroplastic	0.61	1.26	-0.13	-0.06
c36501_g1_i1	defensin Ec-AMP-D2	0.32	1.16	-0.65	0.08
c67776_g1_i1	MLO-like protein 6	0.26	1.15	0.18	0.35
c27587_g1_i2	phenylalanine ammonia-lyase-like	-0.97	1.08	-0.21	0.13
c60090_g1_i1	diacylglycerol kinase 2-like	0.26	1.02	-0.07	0.26

Some contigs of GO term “defense response (GO:0006952)” were upregulated only in systemic leaf (Table 4-5). Signaling cascade in systemic leaf seemed to be induced by probable kinase activity of serine/threonine-protein kinase, leucine-rich repeat receptor-like protein kinase, and histidine kinase. Homologs of disease resistance protein *RPS2* also induced by systemic response. Jasmonic acid and abscisic acid related signaling pathway seemed to be induced by induction of *TIFY 3A-like*, *C2-DOMAIN ABA-RELATED 7-like*. Expression of homolog of S-norococlaurine synthase 2-like was also induced in systemic response. In addition, RNA silencing could be induced by expression of putative nuclear RNA export factor *SDE5*. Homolog of trihelix transcription factor *ASR3-like* was also induced in the systemic response.

Table 4-5. Upregulated genes ($\log_2\text{fc}>0.5$) in the cluster of upregulated group under artificial herbivory of systemic leaf in defense response (GO:0006952). Fold change refers the \log_2 ratio of read count between treatment and control condition.

contig	annotation	Fold change			
		Local leaf		Systemic leaf	
		W+DW	W+OS	W+DW	W+OS
c59369_g2_i1	lja:Lj3g3v3639520.1 Lj3g3v3639520.1; -	-1.18	-0.52	0.97	1.68
c65198_g1_i1	bvg:104906854 uncharacterized LOC104906854	0.40	-0.32	0.89	1.59
c67514_g2_i1	G-type lectin S-receptor-like serine/threonine-protein kinase At1g11330	1.18	1.39	1.42	1.49
c50330_g1_i2	probable leucine-rich repeat receptor-like protein kinase At1g35710	0.26	0.09	0.40	1.23
c31725_g1_i2	leucine-rich repeat receptor-like serine/threonine/tyrosine-protein kinase SOBIR1	-0.84	0.19	0.29	0.96
c66429_g17_i1	peq:110035602 uncharacterized protein LOC110035602	-1.06	-1.62	0.81	0.93
c31887_g1_i1	disease resistance protein RPS2-like	-0.72	-0.53	0.91	0.92
c47247_g1_i1	protein TIFY 3A-like	-0.80	0.20	0.45	0.87
c55249_g2_i1	histidine kinase 5	-0.19	-0.93	0.46	0.78
c65621_g10_i1	nnu:104598203 uncharacterized LOC104598203	0.00	-0.25	0.65	0.77
c67611_g1_i3	probable disease resistance protein At1g12280	0.15	-0.01	0.27	0.62
c63321_g1_i1	trihelix transcription factor ASR3-like	-0.60	-0.49	0.63	0.61
c54257_g1_i3	protein C2-DOMAIN ABA-RELATED 7- like	-0.24	0.29	0.24	0.57
c65967_g1_i1	disease resistance protein RPS2-like	-0.58	-0.35	0.16	0.54
c52989_g2_i1	S-noroclaurine synthase 2-like	-0.29	-0.22	0.32	0.53
c65918_g7_i1	putative disease resistance protein RGA1	-0.05	0.62	-0.02	0.53
c55298_g2_i2	receptor-like serine/threonine-protein kinase SD1-8	-0.63	0.24	-0.51	0.51
c62246_g3_i4	putative nuclear RNA export factor SDE5	-0.84	-1.13	0.51	0.51

In GO term “response to wounding (GO:0009611)”, induced pattern was mainly shown in the local leaf, especially under W+OS treatment (Table 4-6). Further gene expression seemed to be induced by some putative transcription factor, such as *MYB34-like*, *MYB102-like*, *WRKY40*, ethylene-responsive transcription factor (*ERF*) *RAP2-4*, and *NAC*-domain-containing protein 2. Signaling by kinase also seemed to be induced by receptor like protein kinase S.2, probable protein phosphatase 2C 25, phytohemokine receptor 1, and diacylglycerol kinase 2-like. Jasmonic acid signaling and biosynthesis seemed to be induced from homologs of 4-coumarate--CoA ligase-like 6, jasmonate O-methyltransferase-like, *TIFY 9-like*, and 3-ketoacyl-CoA thiolase. Ethylene mediated signaling also seemed to be induced by 1-aminocyclopropane-1-carboxylate synthase, as well as *ERF*. Some secondary metabolite biosynthesis which are known to be induced by wounding seemed to be induced, such as phenylalanine ammonia-lyase-like, aromatic-L-amino-acid decarboxylase-like, and (S)-coclaurine N-methyltransferase. Expression of homologs of subtilisin inhibitor *CLSI-I-like* and E3 ubiquitin-protein ligase *RMA1H1-like* were also induced, which are predicted to protein degradation.

Table 4-6. Differentially expressed genes (DEGs) in the cluster of upregulated genes under artificial herbivory of local leaf in response to wounding (GO:0009611). Fold change refers the log₂ ratio of read count between treatment and control condition.

contig	annotation	Fold change			
		Local leaf		Systemic leaf	
		W+DW	W+OS	W+DW	W+OS
c44532_g1_i1	transcription factor MYB34-like	2.36	4.68	-0.46	-0.68
c44532_g2_i1	transcription factor MYB102-like	1.88	4.24	-0.69	-1.12
c51752_g2_i1	jasmonate O-methyltransferase-like	2.38	3.73	-1.30	0.37
c53985_g3_i1	protein TIFY 9-like	1.13	3.49	0.20	0.23
c60393_g2_i1	phenylalanine ammonia-lyase-like	1.16	3.09	-0.45	1.87
c62243_g1_i1	atr:18448760 uncharacterized protein LOC18448760	1.00	2.64	-1.15	0.03
c48813_g2_i1	chitinase 6	0.80	2.49	-0.13	0.04
c65641_g1_i2	jasmonate O-methyltransferase	0.66	2.40	0.01	0.90
c32998_g1_i1	aromatic-L-amino-acid decarboxylase-like	0.18	2.36	1.11	2.03
c50058_g1_i3	CBS domain-containing protein CBSX5	1.04	2.25	1.30	0.24
c46629_g1_i2	probable WRKY transcription factor 40	0.68	2.22	-0.01	0.10
c61168_g3_i1	receptor like protein kinase S.2	0.63	2.18	0.07	0.86
c44663_g1_i1	3-ketoacyl-CoA thiolase 2, peroxisomal	0.55	1.81	-0.47	0.04
c66475_g2_i3	jasmonate O-methyltransferase-like	0.56	1.80	-0.11	0.66
c36209_g1_i1	subtilisin inhibitor CLSI-I-like	0.20	1.75	0.28	2.03
c51887_g1_i1	4-coumarate--CoA ligase 2	0.95	1.68	0.36	0.13
c61770_g1_i1	E3 ubiquitin-protein ligase RMA1H1-like	0.65	1.61	-0.20	-0.11
c50980_g1_i1	rboh, rbohD; respiratory burst oxidase homolog protein C-like	-0.26	1.54	0.91	0.34
c61168_g5_i1	receptor like protein kinase S.2-like	0.50	1.52	-0.16	0.12
c62879_g1_i1	phytosulfokine receptor 2	0.71	1.43	-0.15	-0.16
c40698_g1_i1	probable protein phosphatase 2C 25	0.09	1.33	-0.11	-0.15
c46235_g1_i2	high-affinity nitrate transporter 3.1	0.55	1.26	0.49	0.74
c64728_g1_i3	(S)-coclaurine N-methyltransferase	-0.57	1.14	0.45	1.59
c36845_g1_i1	1-aminocyclopropane-1-carboxylate synthase	-0.71	1.13	-0.41	0.36
c27587_g1_i2	phenylalanine ammonia-lyase-like	-0.97	1.08	-0.21	0.13
c21129_g1_i1	NAC domain-containing protein 2	-0.06	1.08	0.24	0.08
c66565_g6_i1	ABC transporter G family member 11	0.32	1.03	-0.56	-0.37
c60090_g1_i1	diacylglycerol kinase 2-like	0.26	1.02	-0.07	0.26
c63538_g2_i2	ethylene-responsive transcription factor RAP2-4	0.39	1.01	0.07	0.19

In local leaf, several contigs of GO term “secondary metabolite biosynthesis process (GO:0044550)” were highly expressed under W+OS treatment rather than other treatments (Table 4-7). Biosynthesis of alkaloid compounds also seemed to be induced by expression of homologs of (S)-N-methylcoclaurine 3'-hydroxylase isozyme 2 (isoquinoline alkaloid reticuline biosynthesis) and tryptamine 5-hydroxylase-like (serotonine).

Biosynthesis of phenolic compounds including flavonoid and phenylpropanoids group seemed to be induced by the induced gene expression of homologs of secondary metabolite biosynthesis enzymes. Induced expression of homologs of cytochrome P450 82C4 (*CYP82C4*; xanthotoxin 5-hydroxylase), trans-cinnamate 4-monooxygenase (*CYP73A5*), and cytochrome P450 71A1 (possible trans-cinnamic acid 4-hydrolase) were involved in phenylpropanoids biosynthesis. Induced gene expression of homologs of flavonoid 3'-monooxygenase (bitter-masking flavonoid biosynthesis) and isoflavone 2'-hydroxylase-like (pterocarpin phytoalexins) seemed to be contribute the biosynthesis of flavonoids. Terpenoid biosynthesis seemed to be induced by expression of geraniol 8-hydroxylase-like. In addition, detoxification of xenobiotic compounds from specialist herbivore seemed to be induced by expression of 7-ethoxycoumarin O-deethylase, FAD-dependent urate hydroxylase, and premnaspirodien oxygenase-like and cytochrome P450 77A2 (*CYP77A2*; wax biosynthesis).

Table 4-7. Differentially expressed genes (DEGs) in the cluster of upregulated genes under artificial herbivory (W+OS) of local leaf in secondary metabolite biosynthesis process (GO:0044550). Fold change refers the log₂ ratio of read count between treatment and control condition.

contig	annotation	Fold change			
		Local leaf		Systemic leaf	
		W+DW	W+OS	W+DW	W+OS
c55025_g1_i2	cytochrome P450 82C4	5.44	7.61	-0.53	-0.17
c67391_g1_i6	geraniol 8-hydroxylase-like	2.34	5.67	-0.04	-0.08
c67587_g2_i1	flavonoid 3'-monooxygenase	1.94	5.26	-0.21	0.63
c55715_g2_i1	geraniol 8-hydroxylase	1.27	3.65	0.43	-0.67
c67100_g3_i1	cytochrome P450 76AD1	0.69	3.58	-0.46	0.45
c55715_g1_i3	geraniol 8-hydroxylase-like	1.14	3.45	0.81	-0.93
c106305_g1_i1	trans-cinnamate 4-monooxygenase	2.14	3.45	-0.22	-0.25
c48129_g1_i1	cytochrome P450 71A1	0.99	2.76	-0.98	0.65
c20619_g1_i1	CYP71BE5; premnaspirodien oxygenase-like	0.90	2.73	-0.38	-0.79
c53523_g2_i1	cytochrome P450 71A1-like isoform X1	0.90	2.67	-0.09	1.02
c67503_g1_i1	7-ethoxycoumarin O-deethylase	-0.39	2.46	-0.56	0.77
c53523_g1_i1	cytochrome P450 71A9-like	0.64	2.44	-0.08	1.12
c67132_g3_i3	flavonoid 3'-monooxygenase-like	0.06	2.14	0.03	0.55
c67435_g2_i1	isoflavone 2'-hydroxylase-like	1.47	2.03	-2.43	-1.11
c48443_g1_i1	tryptamine 5-hydroxylase-like	0.36	1.88	-0.77	0.31
c48151_g1_i2	hbr:110642661 uncharacterized protein LOC110642661	-0.85	1.82	0.94	1.89
c66806_g4_i1	pvu:PHAVU_009G061600g hypothetical protein	0.80	1.79	0.23	-0.49
c52675_g1_i1	cytochrome P450 77A2	1.74	1.73	-0.08	-0.73
c48151_g2_i1	FAD-dependent urate hydroxylase	-1.08	1.72	0.49	1.34
c67384_g1_i1	geraniol 8-hydroxylase-like	0.38	1.60	0.62	-0.07
c63956_g1_i3	flavonoid 3'-monooxygenase-like	-0.37	1.49	-0.81	0.59
c50582_g1_i1	probable (S)-N-methylcoclaurine 3'- hydroxylase isozyme 2	0.45	0.96	-0.14	0.13

Some contigs of GO term “secondary metabolite biosynthesis process (GO:0044550)” were highly expressed in damaged (both W+OS and W+DW) systemic leaf (Table 4-8). Flavonoid 6-hydroxylase (cytochrome P450 71D9) seemed to be induced in systemic response to artificial herbivory. Expression of probable phenylalanine N-monooxygenase was also induced in systemic leaf. Similar to the local leaf, gene expression of 7-ethoxycoumarin O-deethylase and FAD-dependent urate hydroxylase were induced, which could detoxify some xenobiotic compounds. Biosynthesis of gibberellin and abscisic acid seemed to be induced by the expression of ent-kaurene oxidase 2-like and zeaxantin epoxidase, respectively.

Some contigs, which have been predicted to function of possible specific secondary metabolite biosynthesis, were not differentially expressed in local leaf (Table 3-9). Expression of benzyl alcohol O-benzoyltransferase and *STRICTOSIDINE SYNTHASE-LIKE* 10-like were induced in wounded systemic leaf. Expression of (RS)-norcoclaurine 6-O-methyltransferase homologs seemed not to be induced by damage, both in local and systemic response (Table 4-9a). Expression of tyrosine/DOPA decarboxylases seemed to be induced by W+DW and/or W+OS in systemic leaf (Table 4-9b).

Table 4-8. Upregulated genes ($\log_2fc > 0.5$) in the cluster of upregulated group under artificial herbivory of systemic leaf in secondary metabolite biosynthesis process (GO:0044550). Fold change refers the \log_2 ratio of read count between treatment and control condition.

contig	annotation	Fold change			
		Local leaf		Systemic leaf	
		W+DW	W+OS	W+DW	W+OS
c65465_g3_i1	atr:110008273 uncharacterized protein LOC110008273	0.22	-2.04	1.12	1.01
c57168_g3_i2	cytochrome P450 71D9	0.37	0.16	0.72	0.96
c67046_g18_i1	nnu:104598203 uncharacterized LOC104598203	-0.17	-0.66	0.50	0.91
c57168_g1_i2	cytochrome P450 71D9	-0.35	-0.95	0.45	0.72
c67308_g3_i1	oeu:111412753 uncharacterized protein LOC111412753	0.09	-0.52	0.43	0.68
c55026_g1_i1	FAD-dependent urate hydroxylase	-0.74	-0.61	0.62	0.67
c7380_g1_i1	lycopene epsilon cyclase, chloroplastic isoform X1	-0.68	-0.93	0.63	0.64
c64861_g1_i3	atr:110008273 uncharacterized protein LOC110008273	0.34	0.15	0.49	0.62
c56544_g4_i1	cytochrome P450 71A1-like	-0.41	-0.41	0.38	0.60
c30013_g1_i1	phenylalanine N-monooxygenase	-0.47	-2.07	1.27	0.56
c14756_g1_i2	7-ethoxycoumarin O-deethylase-like	0.22	-0.48	-0.02	0.56
c51033_g1_i1	ent-kaurene oxidase 2-like	-0.61	-1.00	0.68	0.55
c66585_g4_i2	jre:108985366 uncharacterized protein LOC108985366	-0.21	-0.31	0.65	0.55
c65580_g2_i2	lang:109359653 uncharacterized LOC109359653	-0.42	-0.56	0.52	0.53
c54482_g1_i3	zeaxanthin epoxidase, chloroplastic	-0.44	-0.62	0.42	0.52
c66732_g1_i2	bvg:109135776 uncharacterized LOC109135776	0.41	-0.16	0.73	0.52
c62809_g2_i2	ent-kaurene oxidase, chloroplastic-like	-0.57	-1.11	1.23	0.52

Table 4-9. Fold changes of contigs which are involved in **(a)** alkaloid biosynthetic process (GO:0009821) and **(b)** tyrosine decarboxylase activity (GO:0004837). Fold change refers the log2 ratio of read count between treatment and control condition.

(a) GO:0009821 (alkaloid biosynthetic process)

contig	annotation	Fold change			
		Local leaf		Systemic leaf	
		W+DW	W+OS	W+DW	W+OS
c47150_g2_i1	benzyl alcohol O-benzoyltransferase	-1.17	-1.64	1.01	0.67
c62822_g1_i2	protein STRICTOSIDINE SYNTHASE-LIKE 10-like	-1.14	-1.23	0.70	0.47
c73740_g1_i1	(RS)-norcoclaurine 6-O-methyltransferase-like	0.18	-0.46	-0.19	-0.23
c64106_g1_i1	(RS)-norcoclaurine 6-O-methyltransferase-like	-1.33	-0.20	0.40	0.38
c61691_g1_i3	(RS)-norcoclaurine 6-O-methyltransferase (EC:2.1.1.128)	-0.47	0.04	-0.36	0.44

(b) GO:0004837 (tyrosine decarboxylase activity)

contig	annotation	Fold change			
		Local leaf		Systemic leaf	
		W+DW	W+OS	W+DW	W+OS
c32998_g1_i1	aromatic-L-amino-acid decarboxylase-like	0.18	2.36	1.11	2.03
c66826_g5_i1	tyrosine/DOPA decarboxylase 1-like	-0.70	-0.73	1.53	1.14
c74598_g1_i1	tyrosine/DOPA decarboxylase 2-like	-0.63	-0.60	0.50	0.15
c66643_g4_i3	tyrosine decarboxylase 1	-0.23	-0.06	0.26	0.04

4.3.6. Validation of gene expression by qRT-PCR

Validation qRT-PCR of some differentially expressed genes in three major GO term under artificial herbivory (defense response, response to wounding, and secondary metabolite biosynthesis process), contigs in alkaloid biosynthetic process, tyrosine decarboxylase activity, and additional general response to herbivory (polyphenol oxidase) were conducted. In “defense response” (GO:0006952), homologs of chitinase 6 (c48813_g2_i1; hereafter *AcCht6*), transcription factor *MYB34*-like (c44532_g1_i1; hereafter *AcMYB34*), S-norcoclaurine synthase 2 (c63371_g1_i1; hereafter *AcNCS2*), and protein *YLS9*-like (c73635_g1_i1; hereafter *AcYLS9*) were strongly induced in local leaf, especially under W+OS treatment (Fig. 4-8). Expression level of S-norcoclaurine synthase 1 (c91572_g1_i1; hereafter *AcNCS1*) was induced by both W+DW and W+OS, in both local and systemic leaf.

In “response to wounding (GO:0009611)”, gene expression of 4-coumarate--CoA ligase 2 (c51887_g1_i1; hereafter *Ac4CL2*), 1-aminocyclopropane-1-carboxylate synthase (c36645_g1_i1; hereafter *AcACS*), (S)-coclaurine N-methyltransferase (c64728_g1_i3; hereafter *AcCNMT*), jasmonate O-methyltransferase-like (c51572_g2_i1; hereafter *AcJMT*), and phenylalanine ammonia-lyase-like (c60393_g2_i1; hereafter *AcPAL*) were induced under W+OS treatment in local leaf (Fig. 4-9)

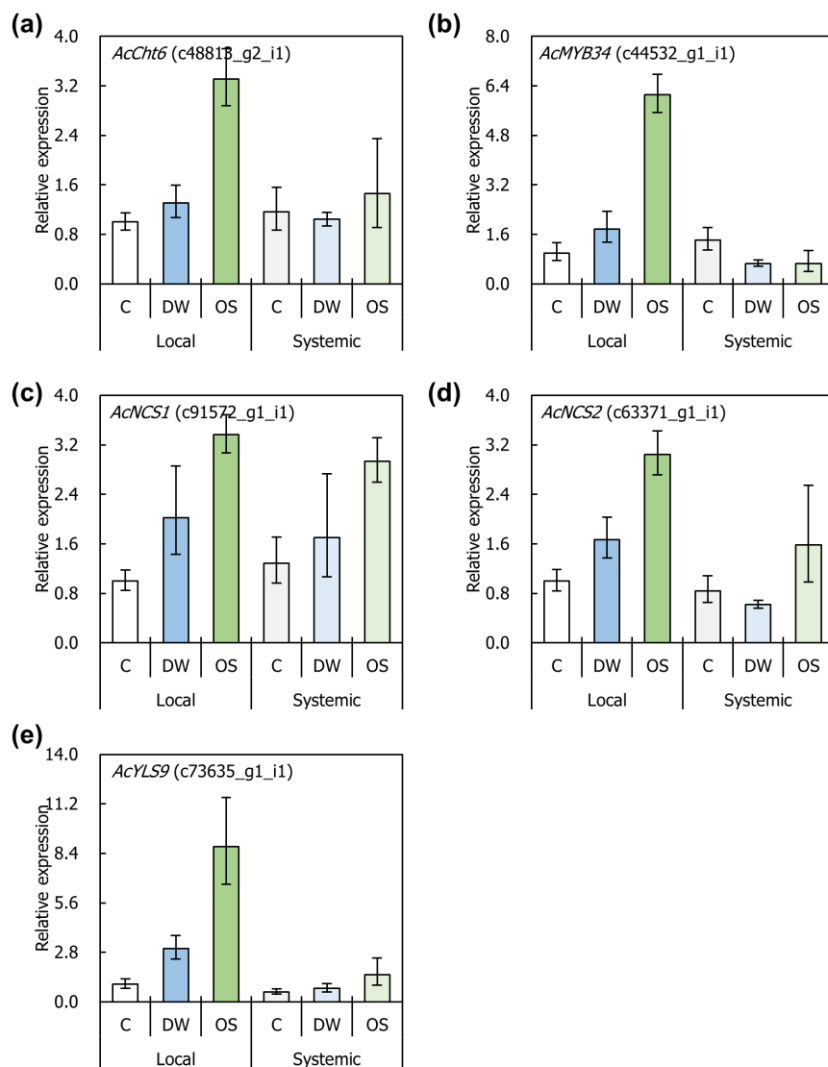


Fig. 4-8. The result of qRT-PCR for selected genes in GO term "defense response" (GO:0006952). **(a)** c48813_g2_i1 (*AcCht6*); **(b)** c44532_g1_i1 (*AcMYB34*); **(c)** c91572_g1_i1 (*AcNCSI*); **(d)** c63371_g1_i1 (*AcNCS2*); **(e)** c73635_g1_i1 (*AcYLS9*). C = control; DW = wounding with distilled water; OS = wounding with oral secretion of *S. montela*.

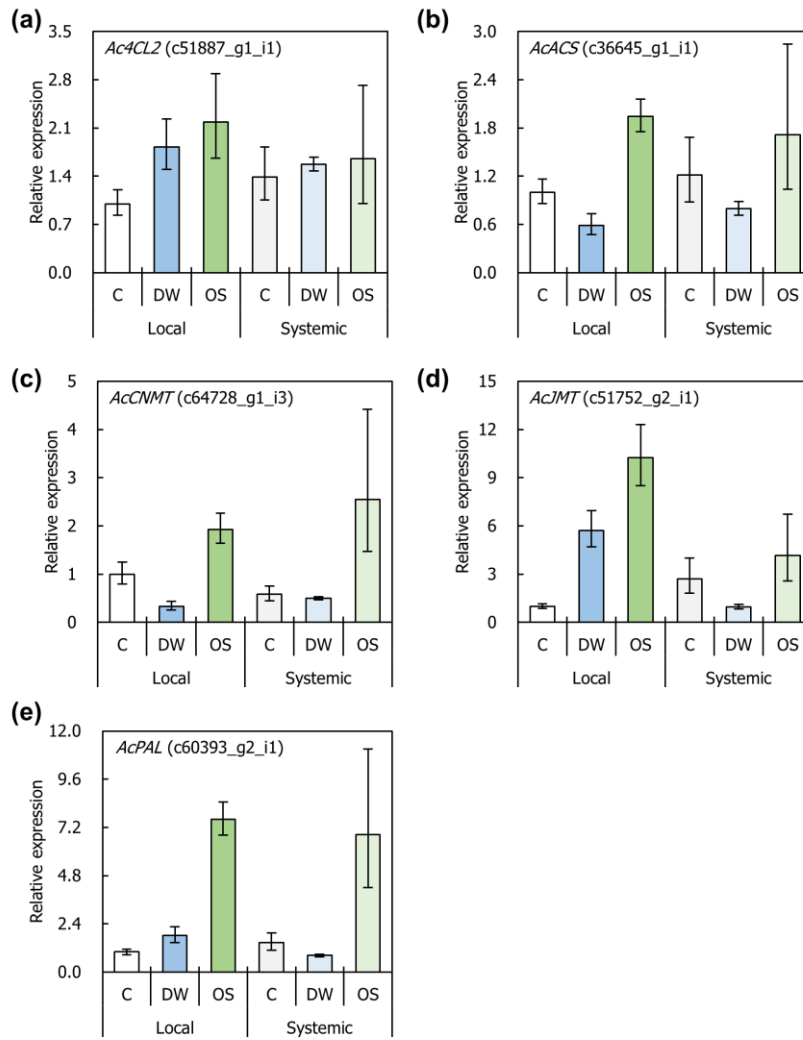


Fig. 4-9. The result of qRT-PCR for selected genes in GO term “response to wounding” (GO:0009611). **(a)** c51887_g1_i1 (*Ac4CL2*); **(b)** c36845_g1_i1 (*AcACS*); **(c)** c64728_g1_i3 (*AcCNMT*); **(d)** c51752_g2_i1 (*AcJMT*); **(e)** c60393_g2_i1 (*AcPAL*). C = control; DW = wounding with distilled water; OS = wounding with oral secretion of *S. montela*.

In “secondary metabolite biosynthesis process (GO:0044550)”, gene expression of trans-cinnamate 4-monooxygenase (c106305_g1_i1; hereafter *AcCYP73A5*), 7-ethoxycoumarin O-deethylase (c67503_g1_i1; hereafter *AcCYP76B1*), geraniol 8-dehydroxylase-like (c67391_g1_i1; hereafter *AcCYP76B6*), cytochrome P450 82C4 (c55025_g1_i2; hereafter *AcCYP82C4*), (3S)-linalool/(E)-nerolidol/(E,E)-geranyl linalool synthase (c64750_g2_i1; hereafter *AcNES*), and serine carboxypeptidase-like 18 (c61823_g1_i3; hereafter *AcSCPL8*) were highly induced under damaged local leaves, especially under W+OS treatment (Fig. 4-10). On the other hand, induction of gene expression of artificial herbivory treatment was relatively lower in probable (S)-N-methylcoclaurine 3'-hydroxylase isozyme 2 (c50582_g1_i1; hereafter *AcCYP80B2*).

Gene expression level was not significantly induced by both W+DW and W+OS treatment in "alkaloid biosynthetic process (GO:0009821)" and "tyrosine decarboxylase activity (GO:0004837)" (Fig. 4-11a-d). Expression level of polyphenol oxidase (c64496_g1_i4; hereafter *AcPPO*) was increased under W+OS treatment in local leaf as general response to herbivory (Fig. 4-11f).

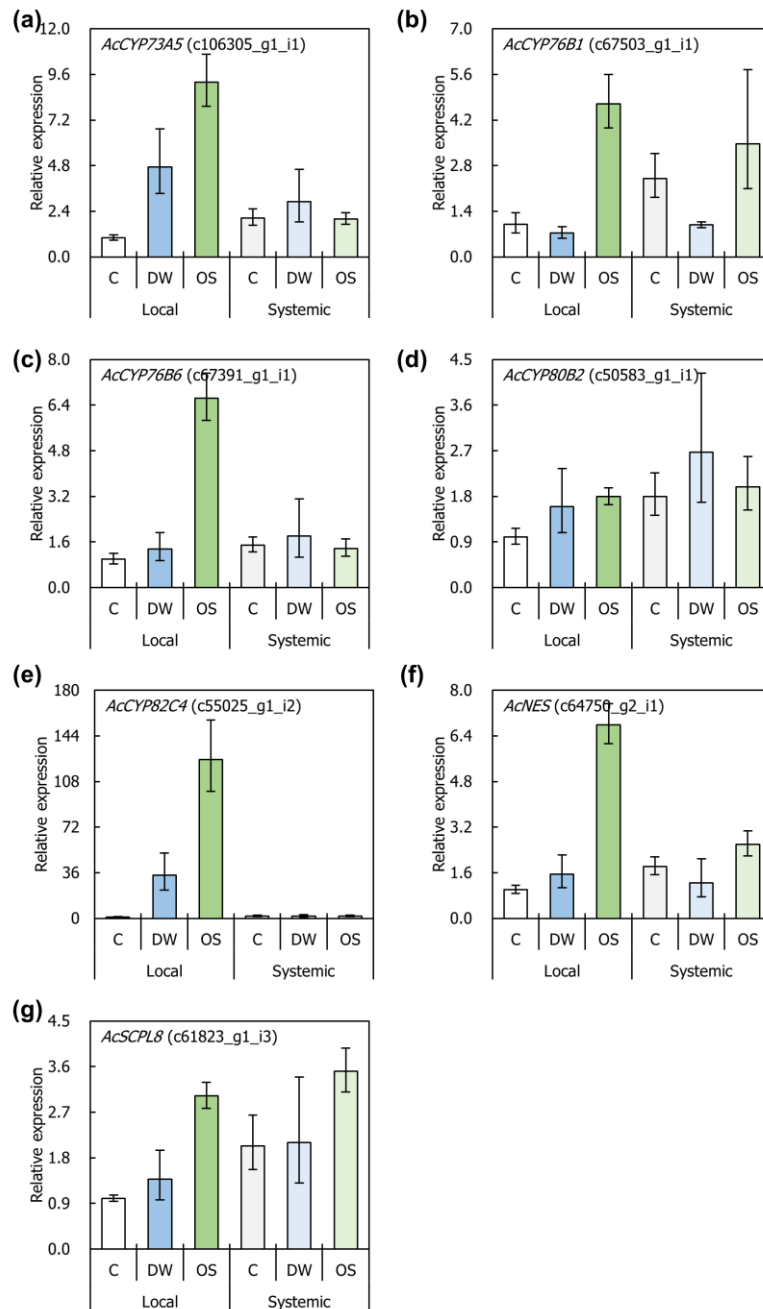


Fig. 4-10. The result of qRT-PCR for selected genes in GO term “secondary metabolite biosynthesis process” (GO:0044550). **(a)** c106305_g1_i1 (*AcCYP73A5*); **(b)** c67503_g1_i1 (*AcCYP76B1*); **(c)** c67391_g1_i1 (*AcCYP76B6*); **(d)** c50583_g1_i1 (*AcCYP80B2*); **(e)** c55025_g1_i2 (*AcCYP82C4*); **(f)** c64750_g2_i1 (*AcNES*); **(g)** c61823_g1_i3 (*AcSCPL8*). C = control; DW = wounding with distilled water; OS = wounding with oral secretion of *S. montela*.

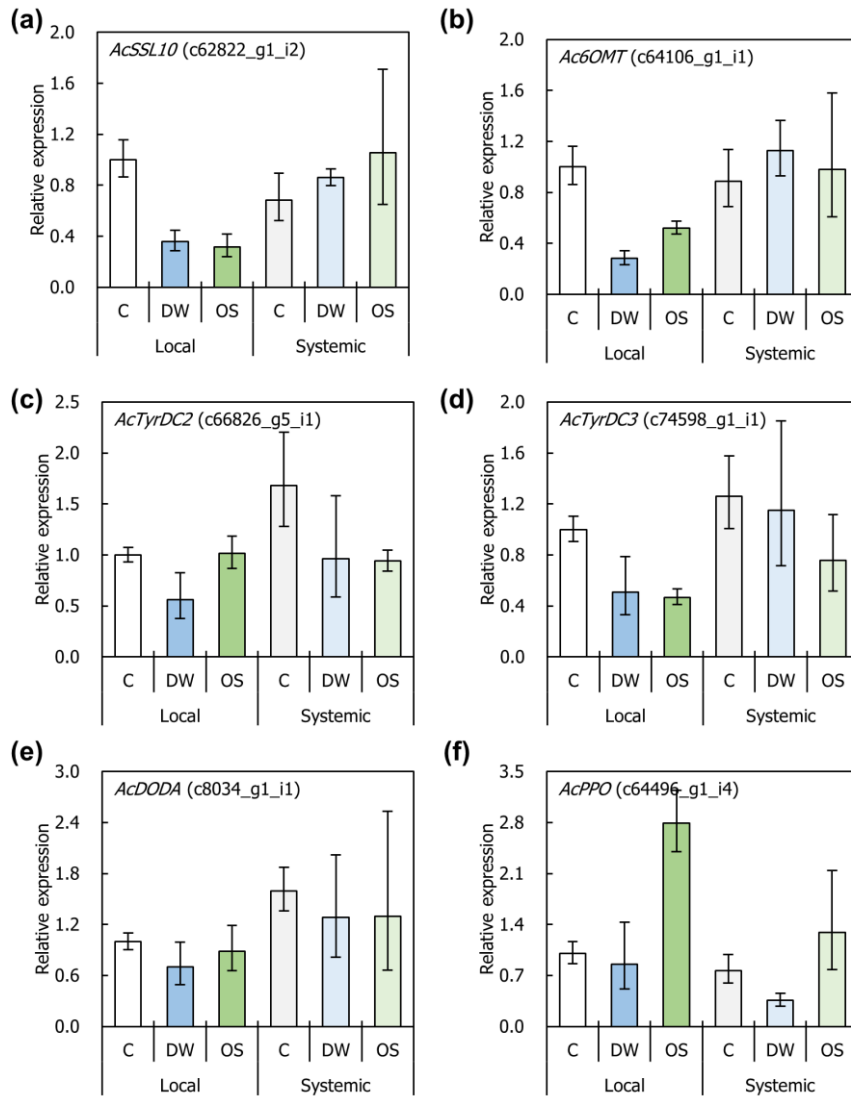


Fig. 4-11. The result of qRT-PCR for selected genes in GO term “alkaloid biosynthetic process” (a, b; GO:0009821), GO term “tyrosine decarboxylase activity” (c, d; GO:0004837), DOPA monooxygenase activity (e; GO:0036263), and DOPA dioxygenase activity (f; GO:0046556). (a) c62822_g1_i2 (*AcSSL10*); (b) c64106_g1_i1 (*Ac6OMT*); (c) c66826_g5_i1 (*AcTyrDC2*); (d) c74598_g1_i1 (*AcTyrDC3*); (e) c8034_g1_i1 (*AcDODA*); (f) c64496_g1_i4 (*AcPPO*). C = control; DW = wounding with distilled water; OS = wounding with oral secretion of *S. montela*.

4.4. Discussion

4.4.1. Response to the special herbivory in the wounded leaf

Insect elicitor could enhance the additional “induced” response rather than the simple wounding (Wu and Baldwin, 2010). However, elicitors also could suppress the gene expression of host plant (Consales et al., 2012). In the present study, most of the DEGs were differentially expressed under W+OS treatment in local leaf exclusively (Fig. 4-3a). *Aristolochia contorta* seemed to respond to elicitor of the oral secretion more rather than the simple wounding, which implies the specific perception of the signal of specialist herbivore. This point could be further confirmed by comparison of the difference in transcriptome response between the generalist and specialist (Reymond et al., 2004). However, feeding *Aristolochia* leaves to generalist lepidopteran larvae causes high lethality, which makes it harder to collect oral secretion of generalist species which fed on the *A. contorta* (Sikkink et al., 2020). Therefore, in the present study, response to specific herbivore of *A. contorta* has been discussed with comparison of the gene expression of W+OS treatment to control treatment.

Both treatments W+DW and W+OS enriched the GO terms, such as “catabolic process”, “metabolic process”, and “chaperone-mediated protein folding” (Fig. 4-4). These are the fundamental response to the wounding or herbivory, even in the abiotic stress (Kant et al., 2015). The most enriched GO terms were similar between W+OS and W+DW treatment (Fig. 4-5). Cellular component “plant-type cell wall” or “extracellular region” or some cell-wall component related terms (e.g. “agmatine N4-coumaroyltransferase activity” and “lignin biosynthetic process”) were highly enriched under both conditions, which could be considered as the

enhancement of secondary cell wall against further herbivory (Gaquerel et al., 2014). On the other hand, some photosynthesis-related terms were seemed to be downregulated by the W+OS treatment (Fig. 4-5b), which are known to be indirectly suppressed in defense (Nabity et al., 2009).

Enriched KEGG ontology terms reveals that expression level of peroxidase, glutathione S-transferase, *MYB* transcription factor, xyloglucan:xyloglucosyl transferase, and EREBP-like factors were highly enriched under both W+OS and W+DW treatment (Fig. 4-4). Under herbivory, ROS signal by superoxide is induced by jasmonic acid, which induces late defense-related genes (peroxidase and glutathione S-transferase; Gatehouse, 2002). Ethylene signaling pathway-related gene expression was also induced in damaged leaf (e.g. EREBP-like factor). Reactive oxygen species and ethylene related signals could be propagated into the other undamaged tissue systemically (Gatehouse, 2002). Thus, regardless of the elicitor, signals of the damage seemed to propagate systemically.

Both GO enrichment analysis and KEGG Orthology enrichment analysis revealed that biosynthesis of the extracellular molecules such as lignin and xyloglucan in damaged leaves. Increase of these compounds leads to increase in the carbon:nitrogen ratio, which causes the decrease of the food quality to the herbivore (Xie et al., 2018). This could contribute to the intake behavior of the both generalist and specialist herbivore.

Some putative defense-related unigenes showed the higher expression level under application of oral secretion of *S. montela* rather than the simple wounding (Figs. 4-8~4-11). Some transcription factors (e.g. *WRKY* transcription factor) or DNA-binding compounds were upregulated under W+OS treatment, rather than W+DW treatment, which implies that “induced” response might be stronger under

simulated herbivory rather than simple leaf damage (Phukan et al., 2016). Simulated herbivory also induced the gene expression of homologs of enzymes which inhibits the phytophagous insects (e.g. polygalacturonase inhibitor precursor, chitinase, and some proteinase inhibitor). Therefore, induced response to the herbivore elicitor seemed to be also present in *A. contorta*, as well as the well-known response of the Solanaceae and Brassicaceae from the previous study (Bonaventure et al., 2011).

Some volatile phytohormones such as methyl jasmonic acid (MeJA) and ethylene (e.g. homologs of jasmonate O-methyltransferase and 1-aminocyclopropane-1-carboxylate synthase) were also expected to be synthesized more under W+OS treatment, similar to the KEGG Orthology enrichment analysis (Table 4-6). In addition, biosynthesis of secondary metabolite (e.g. geraniol 8-hydroxylase, flavonoid 3'-monooxygenase, and cytochrome P450 71A1) seemed to be more induced under W+OS treatment rather than simple wounding (Fig. 4-10). Not only the toxic compounds, flavor also seemed to differ under W+OS treatment. Geraniol-derived monoterpenols could attract the predators and/or parasites (Ilc et al., 2016). Tri-trophic interactions by volatile compounds seemed to be strengthened under the herbivory of specialist, rather than the simple wounding (Wu and Baldwin, 2010).

In case of *N. attenuata*, most of the commonly upregulated genes by herbivory showed the more induced pattern under the chewing herbivory of specialist rather than the other herbivores (Voelckel and Baldwin, 2008). Some homologous genes (e.g. cinnamic acid 4-hydrolase, *PPO*, and 4-Coumarate-CoA ligase) showed the similar pattern in *A. contorta*, which showed the highly induced pattern under W+OS rather than W+DW. In microarray study of Reymond et al. (2004), function of genes in *Arabidopsis thaliana* induced by its specialist herbivore *Pieris rapae* were classified as follows: defense protein, indole glucosinolate

metabolism, phenolic metabolism, oxypilin metabolism (probable jasmonic acid biosynthesis), metabolite/hormone biosynthesis, detoxification/redox processes, abiotic stress, reallocation of resources, signal transduction, and transcription factors. Except glucosinolate metabolism, which are mainly expressed in Brassicaceae family, functions of enriched contigs of *A. contorta* were similar to *A. thaliana*. On the other hand, enriched “defense protein” genes *A. thaliana* (e.g. lectin, Cys proteinase, β -1,3-glucanase, and β -glucosidase) were different from *A. contorta* (Reymond et al., 2004). This result could imply that most of the defense mechanism against herbivory is also conserved in the *A. contorta*.

4.4.2. Systemic response against special herbivory

Secondary metabolite biosynthesis of systemic leaves is known as partially similar to the response of the damaged leaves (Gatehouse, 2002). Gene Ontology enrichment analysis and KEGG orthology enrichment analysis showed that the expression level of defense-related terms such as GO term “defense response to fungus” and “nitrogen compound metabolic process” were differed in systemic leaf under artificial herbivory. However, most-enriched terms of systemic leaves were not similar to the local damaged leaves (Fig. 4-5). Also, number of DEGs were low and both enriched GO and KEGG orthology terms had the low enriched gene ratio.

Some systemin-related genes or volatiles which are involved in the systemic transmission of the herbivore signals were upregulated under W+OS treatment rather than the W+DW treatment. Some of defense response genes (e.g. *AcNCSI*, *AcPAL*, and *AcSCPL8*) are upregulated in both local and systemic leaf under W+OS treatment, rather than W+DW treatment (Figs. 4-8~4-11). Further systemic defense response could occur in a delayed manner (Gatehouse, 2002). Up-

regulation of some transcription factors and kinases could support this prediction (Table 4-5). Systemic response might express within signaling cascades different from local damaged leaves, even it produces a same final product (Wu and Baldwin, 2010). To clarify the priming of the systemic leaves, time-course gene expression should be studied regarding the delay of the systemic response.

4.4.3. Defense of the *Aristolochia contorta* against its specific herbivore

In general, polyphenol oxidase (*PPO*) and proteinase inhibitors (*PIs*) are known as the herbivore resistance components (Constabel et al., 2000; Gatehouse, 2002). Homologs of polyphenol oxidase *AcPPO* (c64496_g1_i4) was upregulated under W+OS treatment rather than the W+DW treatment (Fig. 4-11f). Induced expression level of polyphenol oxidase differs among the herbivore species (Bosch et al., 2014). In tomato, specialist herbivore could suppress the expression of *PPO* (Bosch et al., 2014). Expression levels of some proteinase inhibitors were also upregulated under W+OS treatment rather than the W+DW treatment (Table 4-8). In addition, other genes which are involved in general response such as chitinase, *MYB* transcription factors, and jasmonate O-methyltransferase were up-regulated under W+OS treatments.

Tyrosine-derived alkaloids are commonly known to be synthesized in limited clades (Khan et al., 2013). The biosynthetic pathway and the intermediate compounds have been assessed for pharmacological use, while the enzymes which involves in the biosynthetic pathway are not clear (Attaluri et al., 2014). On the other hand, highly induced gene expression of *AcNCS* (S-norcochlorine synthase) could be followed by isoquinoline alkaloids biosynthesis such as magnoflorine (Fig. 4-8; Canedo-Téxon et al., 2019). Therefore, some tyrosine-derived isoquinoline alkaloids

seemed to be induced under herbivory. In case of *A. thaliana*, some glucosinolate biosynthesis-related gene expressions were induced by specific herbivory of *P. rapae*, which are classified as family Brassicaceae specific-secondary metabolite group (Reymond et al., 2004).

However, most of the specific defense mechanisms are known to role as “constitutive” defense mechanism (Gatehouse, 2002). Regardless of its toxicity, which secondary metabolites are “inducible” or “constitutive” seemed to be different from each final product. Aristolochic acid, which is known as the specific compound in the family Aristolochiaceae, is classified as the member of isoquinoline alkaloids or aporphine alkaloids (Shamma and Guinaudeau, 1985). Specific secondary metabolite aristolochic acid in *Asarum* species is cumulated constitutively both in roots and leaves (Wang et al., 2018). In similar, aristolochic acids are cumulated at diverse tissues in *Aristolochia* species (Heinrich et al., 2009). Previous study revealed that the expression level of tyrosine decarboxylases (*TyrDCs*) is correlated to the aristolochic acid contents, whereas the other genes which are involved in the aristolochic acid biosynthesis are unclear (Wang et al., 2018). From the expression levels of *TyrDCs* under simulated herbivory, biosynthesis of the aristolochic acids seemed to be “constitutive” process rather than “induced” response in the present study (Fig. 4-11). In the other study, quantification of some tyrosine-derived alkaloids revealed that some specific secondary metabolites including aristolochic acids were not significantly induced by wounding with specific herbivore elicitor in *A. controta* (Fig. 4-12; Park, 2020). This results are similar to the previous study on the *Nicotiana* species wounded with the caterpillar regurgitants, which showed that the herbivore elicitor did not induce the biosynthesis of specific alkaloid nicotine (McCloud and Baldwin, 1997). Although aristolochic acids are fatal to the generalist

herbivores, some *Aristolochia*-eating specialist herbivore has detoxification enzyme activity (Nishida, 1994). Thus, the role of aristolochic acids might be “constitutive” defense against the generalist herbivore rather than “induced” defense response.

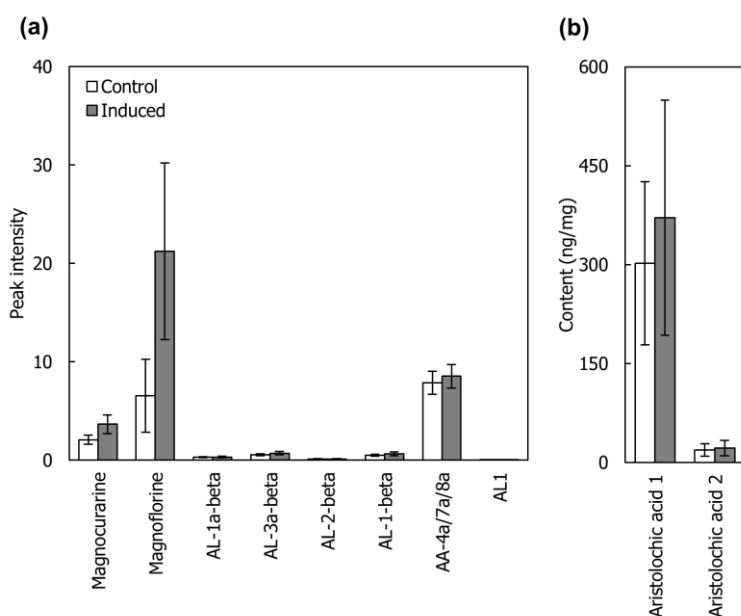


Fig. 4-12. Secondary metabolite content in control (undamaged) and induced (wounded and rubbed with the oral secretion of *S. montela* and sampled after 48 hours) in greenhouse experiment. All metabolites did not show the statistical significance in *t*-test ($p \geq 0.05$) (Park, 2021).

In summary, defense response of *A. contorta* to specialist herbivore could be inferred from the transcriptome under artificial herbivory treatment. Major responses are similar to the other eudicot species. For example, signaling pathway by ROS, MeJA, and ethylene seemed to be induced. Also, further gene expression was expected to be regulated by the induction of transcription factor *MYBs* and *WRKYs*. There were various genes which are involved in the affect the insect metabolism such as chitinase, *PIs*, and some xenobiotic compound detoxifying genes. Lignin biosynthesis also seemed to be induced from the expression of some phenylpropanoid biosynthesis-related genes.

Biosynthesis of some distinctive secondary metabolites seemed to be induced by herbivory. While family Aristolochiaceae-specific secondary metabolites such as aristolochic acid seemed not to be induced by herbivory, some alkaloid compounds such as reticuline (from *AcCYP80B2* and *AcNCSs*) seemed to be synthesized after herbivory, which could be the precursor of morphine or magnoflorine (Canedo-Téxon et al., 2019). Biosynthesis of these inducible secondary metabolites could induce the prevention of generalist herbivore, rather than specialist herbivore. Simulated herbivory seemed to be able to induce the biosynthesis of phenolic compounds such as the bitter-taste by flavonoid biosynthetic pathway and the other phenylpropanoids metabolism. Also, volatile sesquiterpene compounds such as geraniol-derived (e.g. loganin; Battersby et al., 1970) and nerolidol-derived (from *AcNES*; Schnee et al., 2002) compounds could be involved in the induction the tri-trophic interaction. For assess the defensive effect of induced secondary metabolites, validation by the secondary metabolite biosynthesis which are predicted to be induced by transcriptome analysis should be conducted.

4.5. Conclusion

Under the simulate herbivory of specialist herbivore *S. montela*, elicitor seemed to induce gene expression of defense response and secondary metabolite biosynthesis of *A. contorta* leaves rather than the simple wounding (Fig. 4-13). This results suggest the defense mechanism against specialist herbivore of basal angiosperms was mostly similar to the previous studied eudicots. Systemic response against herbivory also occurred partially compared to the local damaged leaf. Biosynthesis of some volatile compounds and alkaloids were predicted to be induced under herbivory, which could prevent the generalist herbivores. However, specific secondary metabolite biosynthesis of *Aristolochia* such as aristolochic acids seemed to did not induced by both simple wounding and specific herbivory, which implies that specific secondary metabolite in *A. contorta* might be involved in the constitutive defense. For more understanding the relationship between *A. contorta* and *S. montela*, multi-layer approach should be further conducted such as deep sequencing and quantification of the secondary metabolite content.

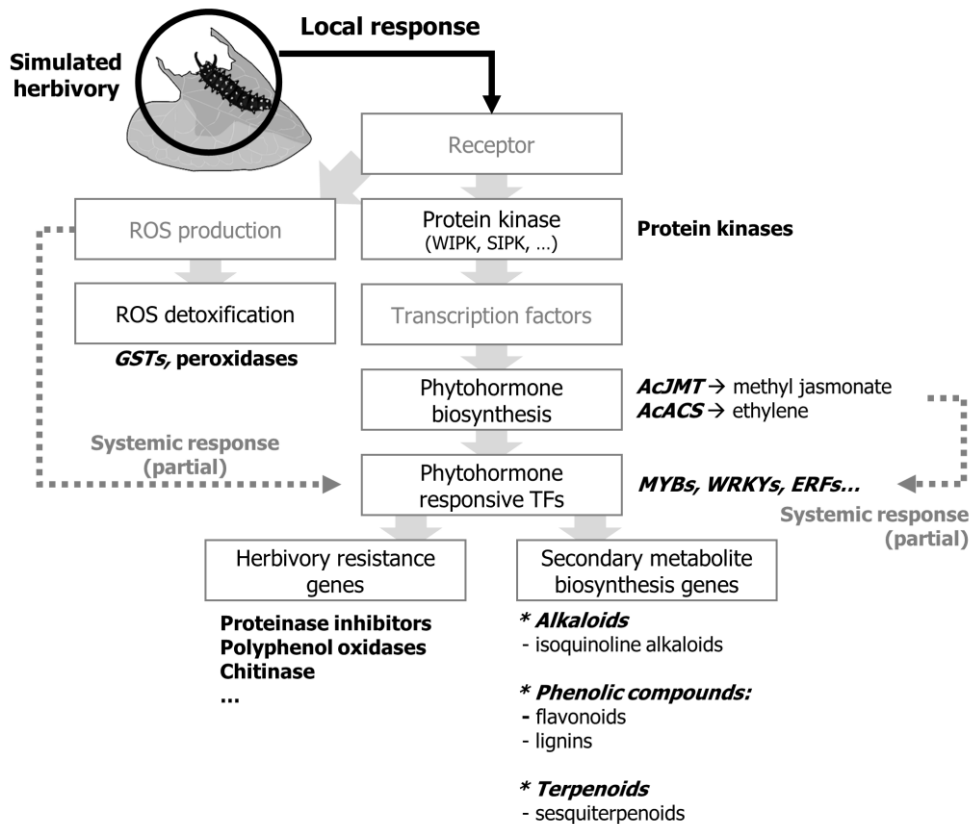


Fig. 4-13. Summary of the transcriptomic change of *A. contorta* under artificial herbivory of *S. montela*.

Chapter 5. General conclusion

I studied on the response of *A. contorta* to herbivory in ecological and molecular biological perspective from field and laboratory experiment. Populations of *A. contorta* showed the relatively lower intra-population genetic diversity, which seemed to be caused by high proportion of clonal propagation. In field experiment on growth response to leaf damage, most of the growth characteristics of *A. contorta* showed the compensatory growth by leaf damage. High light availability induced the higher phenotypic plasticity under leaf damage. Therefore, *A. contorta* seemed to be able to inhabit with the moderate herbivory stress. Transcriptomic response of *A. contorta* under simulated herbivory revealed that *A. contorta* respond to the herbivory in various ways rather than the simple wounding as well as the other eudicot species. Some secondary metabolites including alkaloids were predicted to be induced by herbivory, which could affect the generalist herbivores rather than the specialist herbivores. However, specific secondary metabolites of *Aristolochia* seemed not to be induced by herbivory stress. From my study, *A. contorta* seemed to be able to co-exist with the specialist herbivore *S. montela* under the herbivory stress by the compensatory growth and defense mechanism (Fig. 5-1). Results from this study could contribute to the integrative understanding of plant response to herbivory as well as the conservation of plant-herbivore interaction.

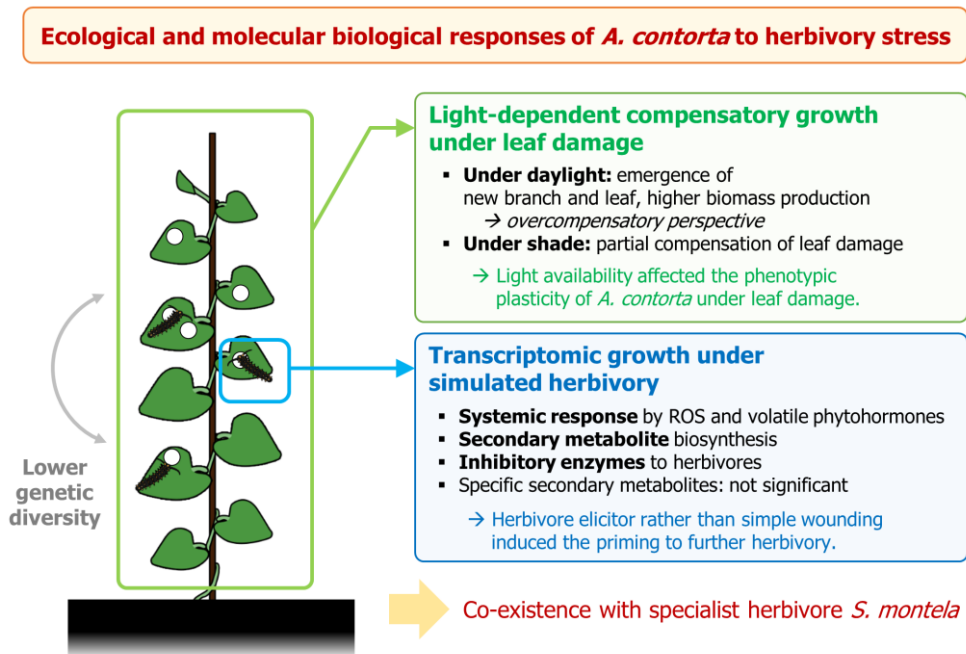


Fig. 5-1. Summary of the response of *A. contorta* to the herbivory stress.

References

- Aarssen, L. W. 1995. Hypothesis for the evolution of apical dominance in plants: implications for the interpretation of overcompensation. *Oikos* **74**(1), 149-156.
- Ågren, G. I. 1985. Limits to plant production. *J. Theoret. Biol.* **113**(1), 89-92.
- Ali, J. G. & Agrawal, A. A. 2012. Specialist versus generalist insect herbivores and plant defense. *Trends Plant Sci.* **17**(6), 293-302.
- Anders, S. & Huber, W. 2010. Differential expression analysis for sequence count data. *Genome Biol.* **11**, R106.
- Andrews, S. 2010. FastQC: a quality control tool for high throughput sequence data.
- Attaluri, S., Iden, C. R., Bonala, R. R. & Johnson, F. 2014. Total synthesis of the aristolochic acids, their major metabolites, and related compounds. *Chem. Res. Toxicol.* **27**, 1236-1242.
- Ballina-Gómez, H. S., Iriarte-Vivar, S., Orellana, R. & Santiago, L. S. 2010. Compensatory growth responses to defoliation and light availability in two native Mexican woody plant species. *J. Trop. Ecol.* **26**(2), 163-171.
- Barton, K. E. 2008 Phenotypic plasticity in seedling defense strategies. *Oikos* **117**, 917-925.
- Battersby, A. R., Brown, S. H., & Payne, T. G. 1970. Biosynthesis of loganin and the indole alkaloids from hydroxygeraniol–hydroxyneryl. *J. Chem. Soc. D Chem. Comm.* **13**, 827-828.
- Bazzaz, F. A., Chiariello, N. R., Coley, P. D. & Pitelka, L. F. 1987. Allocating resources to reproduction and defense. *Bioscience* **37**(1), 58-67.
- Bernays, E. A. 1989. Host range in phytophagous insects: the potential role of generalist predators. *Evol. Ecol.* **3**, 299-311.
- Bliss, B. J., Wanke, S., Barakat, A., Ayyampalayam, S., Wickett, N., Wall, P. K., Jiao, Y., Landherr, L., Ralph, P. E., Hu, Y., Neinhuis, C., Leebens-Mack, J., Arumuganathan, K., Clifton, S. W., Maximova, S. N., Ma, H. & dePamphilis, C. W. 2013. Characterization of the basal angiosperm *Aristolochia fimbriata*: a potential experimental system for genetic studies. *BMC Plant Biol.* **13**, 13.
- Bolger, A. M., Lohse, M. & Usadel, B. 2014. Trimmomatic: a flexible trimmer for Illumina sequence data. *Bioinformatics* **30**(15), 2114-2120.

- Bonaventure, G., VanDoorn, A. and Baldwin, I. T. 2011. Herbivore-associated elicitors: FAC signaling and metabolism. *Trends Plant Sci.* **16**, 6.
- Bosch, M., Berger, S., Schaller, A. & Stinzi, A. 2014. Jasmonate-dependent induction of polyphenol oxidase activity in tomato foliage is important for defense against *Spodoptera exigua* but not against *Manduca sexta*. *BMC Plant Biol.* **14**, 257.
- Canedo-Téxon, A., Ramón-Farías, F., Monribot-Villanueva, J. L., Villafán, E., Alonso-Sánchez, A., Pérez-Torres, C. A., Ángeles, G., Guerrero-Analco, J. A. & Ibarra-Laclette, E. 2019. Novel findings to the biosynthetic pathway of magnoflorine and taspine through transcriptomic and metabolomic analysis of *Croton draco* (Euphorbiaceae). *BMC Plant Biol.* **19**, 560.
- Charif, D. & Lobry, J. R. 2007. SeqinR 1.0-2: a contributed package to the R project for statistical computing devoted to biological sequences retrieval and analysis. In *Structural Approaches to Sequence Evolution*, 207-232. Springer, Berlin, Heidelberg.
- Consales, F., Schweizer, F., Erb, M., Gouhier-Darimont, C., Bodenhausen, N., Bruessow, F., Shbhy, I. & Reymond, P. 2012. Insect oral secretions suppress wound-induced responses in *Arabidopsis*. *J. Exp. Bot.* **63(2)**, 727-737.
- Constabel, C. P., Yip, L., Patton, J. J. & Christoper, M. E. 2000. Polyphenol oxidase from hybrid Poplar cloning and expression in response to wounding and herbivory. *Plant Physiol.* **124**, 285-295.
- Cranshaw, W. S. & Radcliffe, E. B. 1980. Effect of defoliation on yield of potatoes. *J. Econ. Entomol.* **73(1)**, 131-134.
- Crawley, M. J. 1989. Insect herbivores and plant population dynamics. *Ann. Rev. Entomol.* **34**, 531-564.
- de Castro, E. C. P., Zagrobelny, M., Cardoso, M. Z. & Bak, S. 2018. The arms race between heliconiine butterflies and *Passiflora* plants – new insights on an ancient subject. *Biol. Rev.* **93**, 555-573.
- DeWalt, S. J., Schnitzer, S. A. & Denslow, J. S. 2000. Density and diversity of lianas along a chronosequence in a central Panamanian lowland forest. *J. Trop. Ecol.* **16**, 1-9.
- Edger, P. P., Heidel-Fischer, H. M., Bekaert, M., Rota, J., Glöckner, G., Platts, A. E., Heckel, D. G., Der, J. P., Wafula, E. K., Tang, M., Hofberger, J. A.,

- Smithson, A., Hall, J. C., Blanchette, M., Bureau, T. E., Wright, S. I., dePamphilis, C. W., Schranz, M. E., Barker, M. S., Conant, G. C., Wahlberg, N., Vogel, H., Pires, J. C. & Wheat, C.W. 2015. The butterfly plant arms-race escalated by gene and genome duplications. *Proc. Nat. Acad. Sci. USA* **112**, 8362-8366.
- Ehrlich, P. R. & Raven, P. H. 1964. Butterflies and plants: a study in coevolution. *Evolution* **18**, 586–608.
- Endara, M-J., Coley, P. D., Ghabash, G., Nicholls, J. A., Dexter, K. G., Donoso, D. A., Stone, G. N., Pennington, R. T. & Kursar, T. A. 2017. Coevolutionary arms race versus host defense chase in a tropical herbivore–plant system. *Proc. Nat. Acad. Sci. USA* **114(36)**, E7499-E7505.
- Field, C. & Mooney, H.A. 1983. Leaf age and seasonal effects on light, water, and nitrogen use efficiency in a California shrub. *Oecologia* **56**, 348–355.
- Frost, C. J., Appel, H. M., Carlson, J. E., de Moraes, C. M., Mescher, C. & Schultz, J. C. 2007. Within-plant signalling via volatiles overcomes vascular constraints on systemic signalling and primes responses against herbivores. *Ecol. Lett.* **10**, 490-498.
- Gaquerel, E., Gulati, J. & Baldwin, I. T. 2014. Revealing insect herbivory-induced phenolamide metabolism: from single genes to metabolic network plasticity analysis. *Plant J.* **79**, 679-692.
- Gatehouse, J. A. 2002. Plant resistance towards insect herbivores: a dynamic interaction. *New Phytol.* **156**, 145-169.
- GBIF Secretariat. 2019. *Aristolochia contorta* Bunge. In: GBIF Backbone Taxonomy. Checklist dataset <https://doi.org/10.15468/39omei> accessed 2020-10-11.
- Gianoli, E., Molina-Montenegro, M. A. & Becerra, J. 2007. Interactive effects of leaf damage, light intensity and support availability on chemical defenses and morphology of a twining vine. *J. Chem. Ecol.* **33**, 95-103.
- Gloss, A. D., Dittrich, A. C. N., Goldman-Huertas, B. & Whiteman, N. K. 2013. Maintenance of genetic diversity through plant–herbivore interactions. *Curr. Opin. Plant Biol.* **16(4)**, 443-450.
- Grabherr, M. G., Haas, B. J., Yassour, M., Levin, J. Z., Thompson, D. A., Amit, I., Adiconis, X., Fan, L., Raychowdhury, R., Zeng, Q., Chen, Z., Mauceli, E.,

- Hacohen, N., Gnirke, A., Rhind, N., di Palma, F., ZBirren, B. W., Nusbaum, C., Lindblad-Toh, K., Friedman, N. & Rgev, A. 2011. Trinity: reconstructing a full-length transcriptome without a genome from RNA-Seq data. *Nature Biotechnol.* **29**(7), 644.
- Hegarty, E. E. 1989. Canopy dynamics of lianes and trees in subtropical rainforest. *Aust. J. Ecol.* **14**(4), 559-560.
- Heinrich, M., Chan, J., Wanke, S., Neinhuis, C. & Simmonds, M. S. J. 2009. Local uses of *Aristolochia* species and content of nephrotoxic aristolochic acid 1 and 2: A global assessment based on bibliographic sources. *J. Ethnopharmacol.* **125**, 108-144.
- Hong, S. -J., Kim, S. Y., Ravazanaadii N., Han, K., Kim, S. -H. & Kim, N. J. 2014. Temperature-dependent development of the swallowtail butterfly, *Sericinus montela* Gray. *Int. J. Indust. Entomol.* **29**(2), 153-161.
- Hough-Goldstein, J. & LaCross, S. J. 2012. Interactive effects of light environment and herbivory on growth and productivity of an invasive annual vine, *Persicaria perfoliata*. *Arthropod-Plant Inte.* **6**, 103-112.
- Ilc, T., Parage, C., Boachon, B., Navrot, N. & Werck-Reichart, D. 2016. Monoterpenol oxidative metabolism: role in plant adaptation and potential applications. *Front. Plant Sci.* **7**, 509.
- Jander, G. 2014. Revisiting plant-herbivore co-evolution in the molecular biology era. *Ann. Plant Rev.* **47**, 361-384.
- Järemo, J., Nilsson, P. & Tuomi, J. 1996. Plant compensatory growth: herbivory or competition?. *Oikos* **77**(2), 238-247.
- Joo, Y., Schuman, M. C., Goldberg, J. K., Kim, S. -G., Yon, F., Brütting, C. & Baldwin, I. T. 2018. Herbivore-induced volatile blends with both “fast” and “slow” components provide robust indirect defence in nature. *Func. Ecol.* **32**, 136-149.
- Kant, M. R., Jonckheere, W., Knecht, B., Lemos, F., Liu, J., Schimmel, B. C. J., Villarroel, C. A., Ataide, L. M. S., Dermauw, W., Glas, M., Janssen, A., van Leeuwen, T., Schuurink, R. C., Sabelis, M.W. & Egas, M. 2015. Mechanisms and ecological consequences of plant defence induction and suppression in herbivore communities. *Annu. Bot.* **115**(7), 1015-1051.
- Kergoat, G. J., Meseguer, A. S. & Jousset, E. 2016. Evolution of plant-insect

- interactions: Insights from macroevolutionary approaches in plants and herbivorous insects. *Adv. Bot. Res.* **81**, 25-53.
- Khan, F., Qidwai, T., Shukla, R.K. & Gupta, V. 2013. Alkaloids derived from tyrosine: modified benzyltetrahydroisoquinoline alkaloids. In: Ramawat. K. and Mérillon, J. M. (eds.) *Natural Products*. Springer, Berlin, Heidelberg.
- Kim, D. S. & Kwon, Y. J. 2010. Metapopulation dynamics of the oriental long-tailed swallow *Sericinus montela* (Lepidoptera: papilionidae) in Korea. *Kor. J. Appl. Entomol.* **49**(4), 289-297.
- Kolde, R. & Kolde, M. R. 2015. Package ‘pheatmap’. *R Package* **1**(7), 790.
- Koo, A. J. K. & Howe, G. A. 2009. The wound hormone jasmonate. *Phytochemistry* **70**, 1571-1580.
- Kotowska, A. M., Cahill Jr, J. F., & Keddie, B. A. 2010. Plant genetic diversity yields increased plant productivity and herbivore performance. *J. Ecol.* **98**(1), 237-245.
- Lentz, K. A. & Cipollini Jr., D. F. 1998. Effect of light and simulated herbivory on growth of endangered northeastern bulrush, *Scirpus ancistrochaetus* Schuyler. *Plant Ecol.* **139**, 125-131.
- Lesica, P. & Allendorf, F. W. 1999. Ecological genetics and the restoration of plant communities: mix or match? *Restor. Ecol.* **7**(1), 42-50.
- Li, W. & Godzik, A. 2006. CD-HIT: a fast program for clustering and comparing large sets of protein or nucleotide sequences. *Bioinformatics* **22**(13), 1658-1659.
- McCloud, E. S. & Baldwin, I. T. 1997. Herbivory and caterpillar regurgitants amplify the wound-induced increases in jasmonic acid but not nicotine in *Nicotiana sylvestris*. *Planta* **203**, 430-435.
- McNaughton, S. J. 1979. Grazing as an optimization process: grass-ungulate relationships in the Serengeti. *Am. Nat.* **113**, 691-703.
- Mendiburu, F. D. 2015. Package ‘agricolae’. <https://cran.r-project.org/web/packages/agricolae/> (Accessed 14th October 2020).
- Miao, Z., Xu, W., Li, D., Hu, X., Liu, J., Zhang, R., Tong, Z., Dong, J., Su, Z., Zhang, L., Sun, M., Lin, W., Du, Z., Hu, S. & Wang, T. 2015. De novo transcriptome analysis of *Medicago falcata* reveals novel insights about

- the mechanisms underlying abiotic stress-responsive pathway. *BMC Genomics* **16**, 818.
- Miller, J. S. 1987. Host-plant relationships in the Papilionidae (Lepidoptera): parallel cladogenesis or colonization? *Cladistics* **3(2)**, 105-120.
- Min, S. J., Kim, H. -T. & Kim, J. G. 2012. Assessment of genetic diversity of *Typha angustifolia* in the development of cattail stands. *J. Ecol. Field Biol.* **35(1)**, 27-34.
- Nabity, P. D., Zavala, J. A. & DeLucia E. H. 2009. Indirect suppression of photosynthesis on individual leaves by arthropod herbivory. *Annu. Bot.* **103(4)**, 655-663.
- Naiman, R. J., Bechtold, J. S., Drake, D. C., Latterell, J. J., O'Keefe, T. C., & Balian, E. V. 2005. Origins, patterns, and importance of heterogeneity in riparian systems. *In: Ecosystem Function in Heterogeneous Landscapes*, Lovett, G. M., Turner, M. G. & Weather, K. C. (eds.), Springer, New York, NY.
- Nakonechnaya, O. V., Kholina, A. B., Koren, O. G. & Zhuravlev, Y. N. 2012. Genetic diversity of a rare species *Aristolochia contorta* Bunge (Aristolochiaceae) in Primorsky Krai. *Russian J. Genet.* **48(2)**, 152-162.
- Nallu, S., Hill, J. A., Don, K., Sahagun, C., Zhang, W., Meslin, C., Snell-Rood, E., Clark, N. L., Morehouse, N. I., Bergelson, J., Wheat, C. W. & Kronforst, M. R. 2018. The molecular genetic basis of herbivory between butterflies and their host plants. *Nat. Ecol. Evol.* **2**, 1418-1427.
- Nam, B. E., Nam, J. M. & Kim, J. G. 2016. Effects of habitat differences on the genetic diversity of *Persicaria thunbergii*. *J. Ecol. Environ.* **40**, 11.
- Nei, M. 1973. Analysis of gene diversity in subdivided populations. *Proc. Nat. Acad. Sci. USA* **70**, 3321-3323.
- Nishida, R. 1994. Sequestration of plant secondary compounds by butterflies and moths. *Chemoecology* **5**, 127-138.
- Nishida, R. & Fukami, H. 1989. Ecological adaptation of an Aristolochiaceae-feeding swallowtail butterfly, *Atrophaneura alcinous*, to aristolochic acids. *J. Chem. Ecol.* **15**, 2549-2562.
- Ogran, A., Faigenboim, A. & Barazani, O. 2019. Transcriptome responses to different herbivores reveal differences in defense strategies between populations of *Eruca sativa*. *BMC Genomics* **20**, 843.

- Oksanen, J., Blanchet, F. G., Kindt, R., Legendre, P., Minchin, P. R., O'Hara, R. B., Simpson, G. L., Solymos, P., Stevens, M. H. H. & Wagner, H. 2013. Package 'vegan'.
- Park, H. J. 2020. *Effects of Environmental Factors on Growth and Defenses of Host plant, Aristolochia contorta, and consequences of its specialist herbivore, Sericinus montela*. Doctoral Dissertation, Seoul National University, Seoul, Republic of Korea. (in progress)
- Park, H. & Kim, J. G. 2020. Temporal and spatial variations of vegetation in a riparian zone of South Korea. *J. Ecol. Environ.* **44**, 9.
- Park, S. H., Nam, B. E. & Kim, J. G. 2019. Shade and physical support are necessary for conserving the *Aristolochia contorta* population. *Ecol. Eng.* **135**, 108-115.
- Petschenka, G. & Agrawal, A. A. 2016. How herbivores coopt plant defenses: natural selection, specialization, and sequestration *Curr. Opin. Insect Sci.* **14**, 17-24.
- Phukan, U. J., Jeena, G. S. & Shukla, R. K. 2016. WRKY transcription factors_ molecular regulation and stress responses in plants. *Front. Plant Sci.* **7**, 760.
- Priestap, H. A., Velandia, A. E., Johnson, J. V. & Barbieri, M. A. 2012. Secondary metabolite uptake by the *Aristolochia*-feeding papilionoid butterfly *Battus polydamas*. *Biochem. Syst. Ecol.* **40**, 126-137.
- R Core Team. 2020. R: A Language and Environment for Statistical Computing. R Foundation for Statistical Computing, Vienna, Austria. <https://www.R-project.org>.
- Rausher, M. D., Iwao, K., Simms, E. L., Ohsaki, N. & Hall, D. 1993. Induced resistance in *Ipomoea purpurea*. *Ecology* **74**, 20-29.
- Reymond, P., Bodenhausen, N., van Poecke, R. M. P., Krishnamurthy, V., Dicke, M. & Farmer, E. E. 2004. A conserved transcript pattern in response to a specialist and a generalist herbivore. *Plant Cell* **16**, 3132-3147.
- Schierenbeck, K. A., Mack, R. N. & Sharitz, R. R. 1994. Effects of herbivory on growth and biomass allocation in native and introduced species of *Lonicera*. *Ecology* **75**, 1661-1672.
- Schnee, C., Köllner, T. G., Gershenzon, J. & Degenhardt, J. 2002. The maize gene terpene synthase 1 encodes a sesquiterpene synthase catalyzing the

- formation of (E)- β -farnesene,(E)-nerolidol, and (E, E)-farnesol after herbivore damage. *Plant Physiol.* **130(4)**, 2049-2060.
- Schlichting, C. D. 1986. The evolution of phenotypic plasticity in plants. *Ann. Rev. Ecol. Syst.* **17(1)**, 667-693.
- Schuman, M. C., Allmann, S. & Baldwin, I. T. 2015. Plant defense phenotypes determine the consequences of volatile emission for individuals and neighbors. *eLife* **4**, 1-43.
- Schuuman, M. C. & Baldwin, I. T. 2016. The layers of plant responses to insect herbivores. *Annu. Rev. Entomol.* **61**, 373-394.
- Shamma, M. & Guinaudeau, H. 1984. Aporphinoid alkaloids. *Nat. Prod. Rep.* **1(2)**, 201-207.
- Sikkink, K., Hostager, R., Kobiela, M. E., Fremling, N., Johnston, K., Zambre, A. & Snell-Rood, E. C. 2020. Tolerance of novel toxins through generalized mechanisms: simulating gradual host shifts of butterflies. *Am. Nat.* **195**, 485-503.
- Soykan, C. U., Brand, L. A., Ries, L., Stromberg, J. C., Hass, C., Simmons Jr., D. A., Patterson, W. J. D. & Sabo, J. L. 2012. Multitaxonomic diversity patterns along a desert riparian-upland gradient. *PLoS ONE* **7(1)**, e28235.
- Strauss, S.Y. & Agrawal, A.A. 1999. The ecology and evolution of plant tolerance to herbivory. *Trends Ecol. Evol.* **14**, 179-185.
- Supek, F., Bošnjak, M., Škunca, N. & Šmuc, T. 2011. REVIGO summarizes and visualizes long lists of gene ontology terms. *PLoS ONE* **6(7)**, e21800.
- Trumble, J. T., Kolodny-Hirsch, D. M. & Ting, I. P. 1993. Plant compensation for arthropod herbivory. *Annu. Rev. Entomol.* **38**, 93–119.
- Valladares, F., Sanchez-Gomez, D. & Zavala, M.A. 2006. Quantitative estimation of phenotypic plasticity: bridging the gap between the evolutionary concept and its ecological applications. *J. Ecol.* **94**, 1103–1116.
- Vidon, P. G. F. & Hill, A. R. 2004. Landscape controls on the hydrology of stream riparian zones. *J. Hydrol.* **292**, 210-228.
- Voelckel, C. & Baldwin, I. T. 2004. Herbivore-induced plant vaccination. Part II. Array-studies reveal the transience of herbivore-specific transcriptional imprints and a distinct imprint from stress combinations. *Plant J.* **38**, 650-663.

- Voronkova, N. M., Kholina, A. B., Koldaeva, M. N., Nakonechnaya, O. V. & Nechaev, V. A. 2018. Morphophysiological dormancy, germination, and cryopreservation in *Aristolochia contorta* seeds. *Plant Ecol. Evol.* **151(1)**, 77-86.
- Walther, W., Sanchez-Cabo, F. & Ricote, M. 2015. GOplot: an R package for visually combining expression data with functional analysis. *Bioinformatics* **31(17)**, 2912-2914.
- Wang, X., Hui, F., Yang, Y. & Yang, S. 2018. Deep sequencing and transcriptome analysis to identify genes related to biosynthesis of aristolochic acid in *Asarum heterotropoides*. *Sci. Rep.* **8**, 17850.
- Wickham, H. 2016. *ggplot2: Elegant Graphics for Data Analysis*. Springer-Verlag, New York.
- Williams, J. G. K., Kubelik, A. R., Livak, K. J., Rafalski, J. A. & Tingey, S. V. 1990. DNA polymorphisms amplified by arbitrary primers are useful as genetic markers. *Nucleic Acids Res.* **18**, 6531-6535.
- Wimp, G. M., Young, W. P., Woolbright, S. A., Martinsen, G. D., Keim, P. & Whitham, T. G. 2004. Conserving plant genetic diversity for dependent animal communities, *Ecol. Lett.* **7**, 776-780.
- Wu, J. & Baldwin, I. T. 2010. New insights into plant responses to the attack from insect herbivores. *Annu. Rev. Genet.* **44**, 1-24.
- Xie, M., Zhang, J., Tschaplinski, T. J., Tuskan, G. A., Chen, J. -G. & Muchero, W. 2018. Regulation of lignin biosynthesis and its role in growth-defense tradeoffs. *Front. Plant Sci.* **9**, 1427.
- Yeh, F. C. & Boyle, T. J. B. 1997. Population genetic analysis of codominant and dominant markers and quantitative traits. *Belgian J. Bot.* **129**, 157-163.
- Young, M. D., Wakefield, M. J., Smyth, G. K. & Oshlack, A. 2010. Gene ontology analysis for RNA-seq: accounting for selection bias. *Genome Biol.* **11**, R14.
- Zhou, J., Chen, X., Cui, Y., Sun, W., Li, Y., Wang, Y., Song, J. & Yao, H. 2017. Molecular structure and phylogenetic analyses of complete chloroplast genomes of two *Aristolochia* medicinal species. *Int. J. Mol. Sci.* **18**, 1839.
- Züst, T. & Agrawal, A. A. 2017. Trade-offs between plant growth and defense against insect herbivory: an emerging mechanistic synthesis. *Ann. Rev. Plant Biol.* **68(1)**, 513-534.

Abstract in Korean

귀방울덩굴(*Aristolochia contorta*)은 귀방울덩굴과(*Aristolochiaceae*)에 속하는 덩굴성 초본식물로, 귀방울덩굴과 특유의 이차 대사산물을 생산한다. 또한 귀방울덩굴은 꼬리명주나비(*Sericanus montela*)의 유일한 기주식물이다. 귀방울덩굴과 꼬리명주나비의 상호작용에 관한 이해는 두 종의 공존의 지속가능성을 이해하는 데 있어 반드시 필요하다. 본 연구에서는 초식에 대한 귀방울덩굴의 반응을 파악하기 위하여 초식 스트레스 조건에서 귀방울덩굴의 반응에 관한 생태학, 분자생물학적 현상에 관하여 알아보았다.

첫째로, 장기적인 귀방울덩굴 개체군의 지속 가능성을 파악하기 위하여 개체군의 유전적 다양성을 조사하였다. 귀방울덩굴 생육이 활발한 것으로 알려진 국내의 네 개체군에서 잎을 채집하여 유전체 DNA를 추출하여 분석에 사용하였다. 개체군 내 유전적 다양성과 개체군간 유전적 다양성은 5개 무작위 프라이머를 이용한 RAPD (randomly amplified polymorphic DNA) 방법을 사용하여 분석하였다. 수변 경계종임을 고려했을 때, 다른 습지식물들에 비하여 유전적 다양성이 상대적으로 낮은 것으로 나타났다 ($h: 0.0607 \sim 0.1401$; $I: 0.0819 \sim 0.1759$). 또한 지리적 거리와 무관하게 개체군 GP는 다른 개체군들로부터 유전적 거리가 큰 것으로 나타났다. 이러한 결과는 귀방울덩굴의 파편화된 서식지 범위와 낮은 유성생식 비율에 기인한 것으로 보인다.

둘째로, 초식 스트레스에 의한 귀방울덩굴의 표현형적 가소성을 알아보려고 메조코즘 실험을 수행하였다. 두 가지 빛 가용성 조건(일광 조건 및 그늘 조건) 하에서 생육 중인 일년생 개체의 어린 잎 혹은 성숙 잎을 손상시킨 후 생육 반응을 조사하였다. 상대광도는 대부분의 형태적 특성에 영향을 미쳤다. 잎 손상은 새로운 가지와 잎의 생성을 유도하는 효과를 보였다. 또한 잎 손상이 일어난 개체에서 생물량 또한 높은 것으로 나타났다. 이러한 잎 손상에 따른 보상 생장은 성숙 잎보다 어린 잎을 손상시켰을 때 더 크게 나타났다. 또한 표현형적 가소성의 경우 일광 조건에서 더 큰 것으로 나타났다. 이러한 결과는 적절한 빛이 주어졌을 때 귀방울덩굴은 적정 수준의 초식 스트레스 하에서도 활발한 생장을 보

일 수 있음을 시사한다.

마지막으로 쥐방울덩굴의 전사체의 *de novo assembly*를 수행하여 초식 스트레스 하에서 유전자 발현 양상 변화를 파악하고자 하였다. 대조군, 단순 잎 손상(W+DW), 손상 부위에 꼬리명주나비 유충 구강 분비물을 처리한 모의 초식(W+OS) 세 처리 조건에서 쥐방울덩굴 잎의 전사체 변화를 비교하였으며, 전신 반응(systemic response) 또한 비교하였다. 총 3,177개 DEG (differentially expressed genes) 중 절반 이상인 1,875개 DEG가 W+OS 처리가 가해진 조건에서만 다르게 발현되는 contig들에 해당하였다. 세포벽 혹은 리그닌 생합성 관련 term들의 발현 양상으로 미루어 보아, 두 처리조건 모두에서 세포벽 보강이 유도됨을 유추할 수 있었다. 또한 두 처리조건에서 모두 활성산소종(reactive oxygen species), 에틸렌, 자스몬산 등과 관련된 신호전달 경로를 활성화시키는 것으로 추정되었다. W+OS 조건에서 일반적인 초식 반응에 관여하는 것으로 알려진 polyphenol oxidase, chitinase, MYB transcription factors, jasmonate O-methyltransferase 등의 발현량이 증가하는 것으로 나타났다. 알칼로이드계 물질을 포함한 일부 이차 대사산물들의 합성량이 초식에 의해 유도되는 것으로 보였으나, 아리스톨로크산과 같은 *Aristolochia*속 특이적인 이차 대사산물 발현과 관련된 유전자 발현은 유도되지 않는 것으로 나타났다. 이러한 결과로부터 기저 속씨식물에서 특이적 초식동물에 대한 방어기작은 일반적인 방어기작을 증가시키는 방향으로 유도되는 것으로 유추하였다.

본 연구로부터, 쥐방울덩굴은 특이적 초식동물인 꼬리명주나비의 초식에 대한 보상 성장과 방어 기작을 통해 공존할 수 있음을 알 수 있었다. 이러한 연구 결과는 식물-곤충 상호작용 관점에서의 보전과 관련된 기초적인 자료를 제공함과 더불어 초식에 대한 식물의 반응에 대한 다각적 이해에 기여할 수 있을 것이다.

학번: 2013-23382

주요어: 꼬리명주나비, 보상성장, 유전적 다양성, 이차 대사산물, 전사체, 쥐방울덩굴, 특이적 초식동물

Appendix A. Detailed methods for RNA extraction of *Aristolochia contorta*

Tissues of *Aristolochia contorta* were sampled and immediately frozen within the aluminum foil pouch using liquid nitrogen. Frozen samples were transferred to the 2.0 ml tube and ground into frozen powder using chilled pellet pestle under liquid nitrogen. For each sample, 50 ~ 100 mg of grounded *A. contorta* sample was transferred to autoclaved 2.0 ml tube under liquid nitrogen to keep the low temperature. Tubes were moved to room temperature and 1.0 ml of TRIzol reagent (Ambion, Thermo Fisher, Waltham, MA) was added to each tube. Grounded frozen samples and added TRIzol reagent were homogenized using chilled pellet pestle. Homogenized samples were incubated in 10 min and centrifuged at 4°C, 13,000 g in 15 min.

Supernatant (about 1.0 ml) was transferred to new 1.5 ml tube and 0.25 ml of chloroform solution was added. Supernatant and chloroform solution was mixed by hand shaking in 15 sec. Mixed solution was incubated at room temperature in 2 ~ 3 min and centrifuged at 4°C, 13,000 g in 15 min. Clear supernatant (0.4 ml) was transferred to new 1.5 ml tube. Isopropanol (0.2 ml) and high salt (0.2 ml; mixture of 23.5 g of trisodium citrate and 24 ml of 5 M NaCl solution were added by distilled water to make 100 ml of total volume and autoclaved before use) solution were added to the transferred supernatant. Mixture was incubated under room temperature in 15 min and centrifuged at 4°C, 12,000 g in 10 min.

Supernatant was discarded and pellet was washed by 1 ml of 75% ethanol and centrifuged at 4°C, 7,500 g in 5 min. Wash by 75% ethanol was repeated two times. Moisture of pellet was eliminated by micropipette and dry in clean bench

about 10 min. Deionized water (40 ul) was added to the dried pellet and incubated under 65°C heating block in 10 min. Concentration and purity were measured using Nanodrop ONE[®] (Thermo Fisher, Waltham, MA). Average quantity and quality of extracted RNA samples were differed by its tissue (**Table A-1**).

For synthesis of cDNA, 1 ug of aliquot RNA samples was mixed to 1 ul of OligodT (10 pmol/ul) and total volume was adjusted to 12.5 ul in total volume. Mixture was incubated under 90°C heating block in 1 min and immediately transferred in ice. Additional mixture of 2 ul of dNTP (10 pmol/ul), 4 ul of M-MLV RT 5x buffer, and 0.5 ul of M-MLV reverse transcriptase (Promega, Madison, WI) was added the cooled sample. Reverse transcription reaction was conducted under 42°C in 1 hour. After the reverse transcription reaction, 60 ul of distilled was added. Products were validated by PCR reaction by *AcACT101* primer (645F: 5'-AGCCGTGCTTTCTCTATATG-3'; 1156R: 5'-CAGGGAACATAGTTGAACCA-3') using gel electrophoresis. Validated cDNA samples used to qRT-PCR.

Table A-1. Average (\pm SD) quantity and quality of extracted RNA of *A. contorta* by modified TRIzol method.

Tissue	RNA (ng/ul)	A ₂₆₀ /A ₂₈₀	A ₂₆₀ /A ₂₃₀	A ₂₆₀	A ₂₈₀
Leaf	476.5 \pm 197.8	2.13 \pm 0.03	2.29 \pm 0.19	11.91 \pm 4.95	5.60 \pm 2.34
Shoot	455.8 \pm 124.3	2.12 \pm 0.03	2.09 \pm 0.53	11.40 \pm 3.11	5.37 \pm 1.50
Root	319.8 \pm 199.4	2.11 \pm 0.05	1.67 \pm 0.42	8.00 \pm 4.99	3.83 \pm 2.55

Appendix B. GO (gene ontology) barplot of enriched contigs under wounding or artificial herbivory treatment in *Aristolochia contorta*

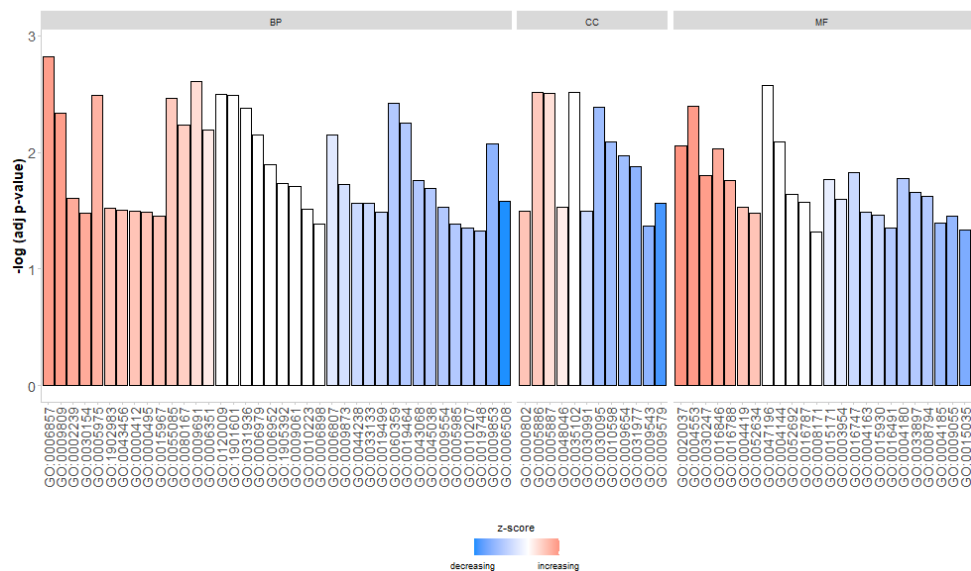


Fig. B-1. GO barplot displaying gene annotation enrichment analysis of DEGs in W+DW versus control, local leaf of *A. contorta*. Enriched GO terms were filtered by adjusted p -value (< 0.05) and `reduced_overlap()` function of R package “GOplot”.

Table B-1. List and enrichment score of enriched GO terms in the GO barplot (**Fig. B-1**) of in W+DW versus control, local leaf of *A. contorta*.

Ontology	Category	term	p-value	# of DEGs
Biological Process	GO:0006857	oligopeptide transport	0.00152	6
	GO:0009809	lignin biosynthetic process	0.00460	6
	GO:0002239	response to oomycetes	0.02505	2
	GO:0030154	cell differentiation	0.03336	8
	GO:0005975	carbohydrate metabolic process	0.00326	15
	GO:1902983	DNA strand elongation involved in mitotic DNA replication	0.03027	1
	GO:0043456	regulation of pentose-phosphate shunt	0.03156	1
	GO:0000412	histone peptidyl-prolyl isomerization	0.03204	1
	GO:0000495	box H/ACA snoRNA 3'-end processing	0.03238	1
	GO:0015967	diadenosine tetraphosphate catabolic process	0.03508	1
	GO:0055085	transmembrane transport	0.00346	11
	GO:0080167	response to karrikin	0.00580	6
	GO:0009691	cytokinin biosynthetic process	0.00248	3
	GO:0006351	transcription, DNA-templated	0.00641	36
	GO:0120009	intermembrane lipid transfer	0.00316	2
	GO:1901601	strigolactone biosynthetic process	0.00326	2
	GO:0031936	negative regulation of chromatin silencing	0.00421	2
	GO:0006979	response to oxidative stress	0.00713	10
	GO:0006952	defense response	0.01282	16
	GO:1905392	plant organ morphogenesis	0.01838	2
	GO:0009061	anaerobic respiration	0.01964	2
	GO:0010223	secondary shoot formation	0.03092	2
	GO:0006898	receptor-mediated endocytosis	0.04144	2
	GO:0006807	nitrogen compound metabolic process	0.00710	3
	GO:0009873	ethylene-activated signaling pathway	0.01874	6
	GO:0044238	primary metabolic process	0.02713	1
	GO:0033133	positive regulation of glucokinase activity	0.02724	1
	GO:0019499	cyanide metabolic process	0.03270	1
	GO:0060359	response to ammonium ion	0.00377	2
	GO:0019464	glycine decarboxylation via glycine cleavage system	0.00557	2
	GO:0043068	positive regulation of programmed cell death	0.01753	2
	GO:0045038	protein import into chloroplast thylakoid membrane	0.02030	2
	GO:0009554	megasporogenesis	0.02965	2

Table B-1. (continued)

Ontology	Category	term	p-value	# of DEGs
Biological Process	GO:0005985	sucrose metabolic process	0.04123	2
	GO:0010207	photosystem II assembly	0.04479	2
	GO:0019748	secondary metabolic process	0.04744	2
	GO:0009853	photorespiration	0.00845	4
	GO:0006508	proteolysis	0.02656	13
Cellular Component	GO:0000802	transverse filament	0.03195	1
	GO:0005886	plasma membrane	0.00307	76
	GO:0005887	integral component of plasma membrane	0.00311	14
	GO:0048046	apoplast	0.02968	11
	GO:0035102	PRC1 complex	0.00308	2
	GO:0030991	intraciliary transport particle A	0.03216	1
	GO:0030095	chloroplast photosystem II	0.00408	3
	GO:0010598	NAD(P)H dehydrogenase complex (plastoquinone)	0.00817	3
	GO:0009654	photosystem II oxygen evolving complex	0.01081	3
	GO:0031977	thylakoid lumen	0.01318	4
	GO:0009543	chloroplast thylakoid lumen	0.04253	4
	GO:0009579	thylakoid	0.02752	8
Molecular Function	GO:0020037	heme binding	0.00884	15
	GO:0004553	hydrolase activity, hydrolyzing O-glycosyl compounds	0.00403	9
	GO:0030247	polysaccharide binding	0.01570	6
	GO:0016846	carbon-sulfur lyase activity	0.00925	2
	GO:0016788	hydrolase activity, acting on ester bonds	0.01749	5
	GO:0004419	hydroxymethylglutaryl-CoA lyase activity	0.02981	1
	GO:0052634	C-19 gibberellin 2-beta-dioxygenase activity	0.03306	1
	GO:0047196	long-chain-alcohol O-fatty-acyltransferase activity	0.00269	2
	GO:0004144	diacylglycerol O-acyltransferase activity	0.00817	2
	GO:0052692	raffinose alpha-galactosidase activity	0.02289	2
	GO:0016787	hydrolase activity	0.02676	16
	GO:0008171	O-methyltransferase activity	0.04853	2
	GO:0015171	amino acid transmembrane transporter activity	0.01726	5
	GO:0003954	NADH dehydrogenase activity	0.02533	3
	GO:0016747	transferase activity, transferring acyl groups other than amino-acyl groups	0.01501	4
	GO:0004163	diphosphomevalonate decarboxylase activity	0.03294	1
	GO:0015930	glutamate synthase activity	0.03428	1

Table B-1. (continued)

Ontology	Category	term	<i>p</i>-value	# of DEGs
	GO:0016491	oxidoreductase activity	0.04498	13
	GO:0004180	carboxypeptidase activity	0.01662	2
	GO:0033897	ribonuclease T2 activity	0.02203	2
	GO:0008794	arsenate reductase (glutaredoxin) activity	0.02366	2
	GO:0004185	serine-type carboxypeptidase activity	0.04046	3
	GO:0009055	electron transfer activity	0.03502	7
	GO:0015035	protein disulfide oxidoreductase activity	0.04613	5

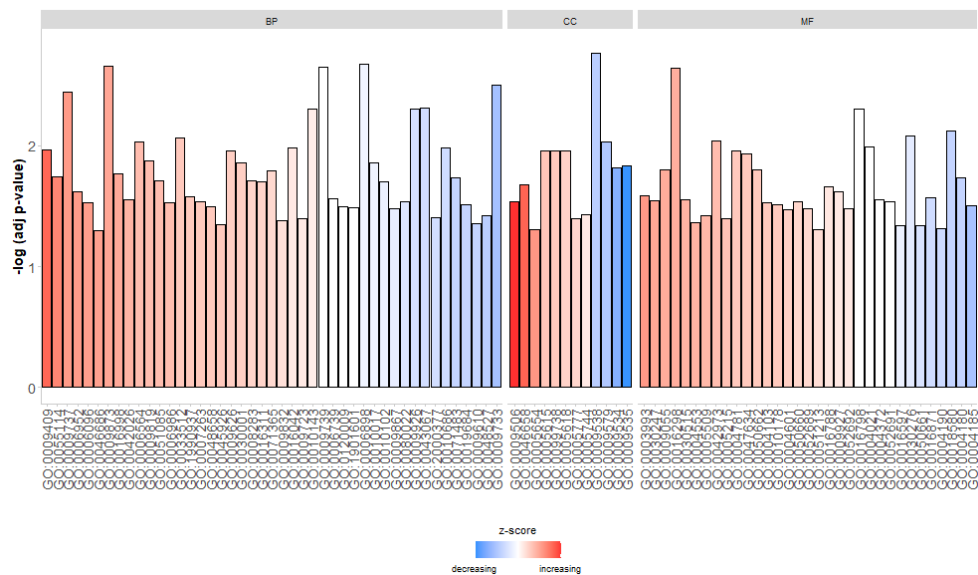


Fig. B-2. GO barplot displaying gene annotation enrichment analysis of DEGs in W+OS versus control, local leaf of *A. contorta*. Enriched GO terms were filtered by adjusted p -value (< 0.05) and `reduced_overlap()` function of R package “GOplot”.

Table B-2. List and enrichment score of enriched GO terms in the GO barplot (**Fig. B-2**) of in W+OS versus control, local leaf of *A. contorta*.

Ontology	Category	term	p-value	# of DEGs
Biological Process	GO:0009409	response to cold	0.01083	25
	GO:0055114	oxidation-reduction process	0.01798	65
	GO:0009737	response to abscisic acid	0.00356	33
	GO:0006952	defense response	0.02417	38
	GO:0006096	glycolytic process	0.02965	10
	GO:0046686	response to cadmium ion	0.04995	24
	GO:0009873	ethylene-activated signaling pathway	0.00217	15
	GO:0016998	cell wall macromolecule catabolic process	0.01701	5
	GO:0042026	protein refolding	0.02809	4
	GO:0006564	L-serine biosynthetic process	0.00929	3
	GO:0009819	drought recovery	0.01339	3
	GO:0051085	chaperone cofactor-dependent protein refolding	0.01930	3
	GO:0006986	response to unfolded protein	0.02962	3
	GO:0033512	L-lysine catabolic process to acetyl-CoA via saccharopine	0.00854	2
	GO:1990937	xylan acetylation	0.02646	2
	GO:0007263	nitric oxide mediated signal transduction	0.02907	2
	GO:0048658	anther wall tapetum development	0.03198	2
	GO:0045926	negative regulation of growth	0.04497	2
	GO:0009626	plant-type hypersensitive response	0.01109	10
	GO:0030001	metal ion transport	0.01379	10
	GO:0008283	cell population proliferation	0.01963	7
	GO:0016311	dephosphorylation	0.01993	7
	GO:0071365	cellular response to auxin stimulus	0.01617	4
	GO:0009832	plant-type cell wall biogenesis	0.04187	6
	GO:0016042	lipid catabolic process	0.01034	12
	GO:0009723	response to ethylene	0.04015	12
	GO:0010143	cutin biosynthetic process	0.00492	5
	GO:0009739	response to gibberellin	0.00223	10
	GO:0006739	NADP metabolic process	0.02723	2
	GO:0120009	intermembrane lipid transfer	0.03169	2
	GO:1901601	strigolactone biosynthetic process	0.03227	2
	GO:0006898	receptor-mediated endocytosis	0.00211	5
	GO:0010017	red or far-red light signaling pathway	0.01380	5

Table B-2. (continued)

Ontology	Category	term	p-value	# of DEGs
Biological Process	GO:0010102	lateral root morphogenesis	0.01997	3
	GO:0009867	jasmonic acid mediated signaling pathway	0.03334	8
	GO:0080022	primary root development	0.02898	4
	GO:0009926	auxin polar transport	0.00494	10
	GO:0043067	regulation of programmed cell death	0.00481	5
	GO:2000377	regulation of reactive oxygen species metabolic process	0.03964	5
	GO:0010686	tetracyclic triterpenoid biosynthetic process	0.01047	2
	GO:0071483	cellular response to blue light	0.01847	3
	GO:0019684	photosynthesis, light reaction	0.03086	3
	GO:0009610	response to symbiotic fungus	0.04402	3
	GO:0048527	lateral root development	0.03776	4
	GO:0009733	response to auxin	0.00312	22
Cellular Component	GO:0009506	plasmodesma	0.02878	61
	GO:0046658	anchored component of plasma membrane	0.02093	15
	GO:0005654	nucleoplasm	0.04955	11
	GO:0005615	extracellular space	0.01101	11
	GO:0099738	cell cortex region	0.01107	2
	GO:0005618	cell wall	0.01101	35
	GO:0005777	peroxisome	0.03994	21
	GO:0005744	TIM23 mitochondrial import inner membrane translocase complex	0.03753	3
	GO:0009538	photosystem I reaction center	0.00170	4
	GO:0009579	thylakoid	0.00919	20
	GO:0009534	chloroplast thylakoid	0.01510	18
	GO:0009535	chloroplast thylakoid membrane	0.01452	38
Molecular Function	GO:0003993	acid phosphatase activity	0.02575	7
	GO:0030247	polysaccharide binding	0.02829	12
	GO:0009055	electron transfer activity	0.01577	17
	GO:0016298	lipase activity	0.00227	8
	GO:0030515	snoRNA binding	0.02812	4
	GO:0004553	hydrolase activity, hydrolyzing O-glycosyl compounds	0.04304	16
	GO:0005509	calcium ion binding	0.03825	23
	GO:0042973	glucan endo-1,3-beta-D-glucosidase activity	0.00905	3
	GO:0005215	transporter activity	0.04022	19
	GO:0004781	sulfate adenylyltransferase (ATP) activity	0.01095	2

Table B-2. (continued)

Ontology	Category	term	p-value	# of DEGs
Molecular Function	GO:0047634	agmatine N4-coumaroyltransferase activity	0.01158	2
	GO:0050662	coenzyme binding	0.01574	8
	GO:0004103	choline kinase activity	0.02937	2
	GO:0010178	IAA-amino acid conjugate hydrolase activity	0.03048	2
	GO:0004601	peroxidase activity	0.03391	10
	GO:0050660	flavin adenine dinucleotide binding	0.02881	14
	GO:0052689	carboxylic ester hydrolase activity	0.03319	9
	GO:0051213	dioxygenase activity	0.04939	11
	GO:0016788	hydrolase activity, acting on ester bonds	0.02192	10
	GO:0009927	histidine phosphotransfer kinase activity	0.02392	3
	GO:0052692	raffinose alpha-galactosidase activity	0.03324	3
	GO:0016798	hydrolase activity, acting on glycosyl bonds	0.00491	8
	GO:0004021	L-alanine:2-oxoglutarate aminotransferase activity	0.01029	2
	GO:0004372	glycine hydroxymethyltransferase activity	0.02804	2
	GO:0052691	UDP-arabinopyranose mutase activity	0.02880	2
	GO:0016597	amino acid binding	0.04584	3
	GO:0030276	clathrin binding	0.00825	6
	GO:0050661	NADP binding	0.04589	7
	GO:0016871	cycloartenol synthase activity	0.02675	2
	GO:0004190	aspartic-type endopeptidase activity	0.04878	11
	GO:0018580	nitronate monooxygenase activity	0.00759	3
	GO:0004180	carboxypeptidase activity	0.01825	3
	GO:0004185	serine-type carboxypeptidase activity	0.03155	6

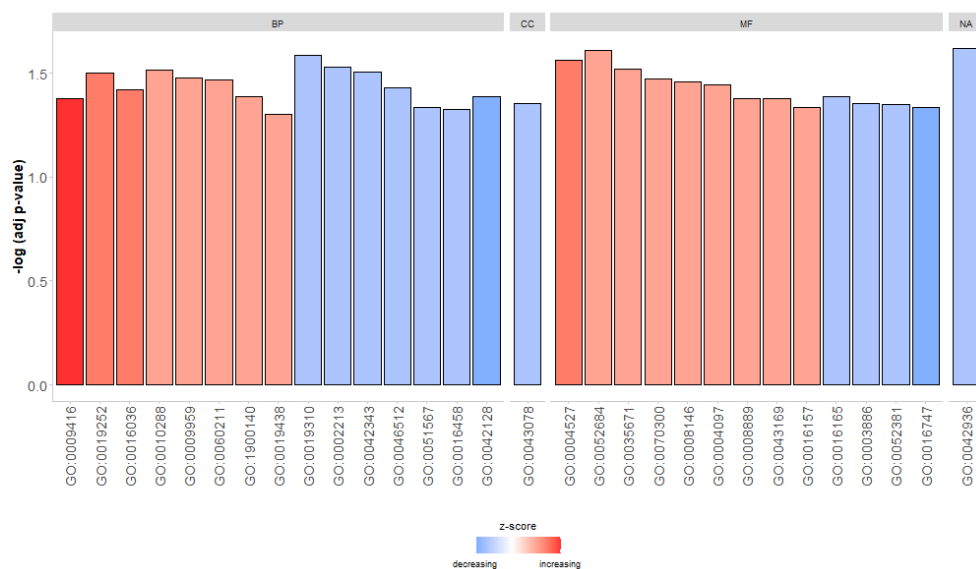


Fig. B-3. GO barplot displaying gene annotation enrichment analysis of DEGs in W+DW versus control, systemic leaf of *A. contorta*. Enriched GO terms were filtered by adjusted *p*-value (< 0.05) and `reduced_overlap()` function of R package “GOplot”.

Table B-3. List and enrichment score of enriched GO terms in the GO barplot (**Fig. B-1**) of in W+DW versus control, systemic leaf of *A. contorta*.

Ontology	Category	term	p-value	# of DEGs
Biological Process	GO:0009416	response to light stimulus	0.04197	4
	GO:0019252	starch biosynthetic process	0.03143	2
	GO:0016036	cellular response to phosphate starvation	0.03780	2
	GO:0010288	response to lead ion	0.03048	1
	GO:0009959	negative gravitropism	0.03349	1
	GO:0060211	regulation of nuclear-transcribed mRNA poly(A) tail shortening	0.03398	1
	GO:1900140	regulation of seedling development	0.04103	1
	GO:0019438	aromatic compound biosynthetic process	0.04978	1
	GO:0019310	inositol catabolic process	0.02606	1
	GO:0002213	defense response to insect	0.02949	1
	GO:0042343	indole glucosinolate metabolic process	0.03116	1
	GO:0046512	sphingosine biosynthetic process	0.03704	1
	GO:0051567	histone H3-K9 methylation	0.04643	1
	GO:0016458	gene silencing	0.04704	1
	GO:0042128	nitrate assimilation	0.04105	2
Cellular Component	GO:0043078	polar nucleus	0.04408	1
Molecular Function	GO:0004527	exonuclease activity	0.02750	2
	GO:0052684	L-serine hydro-lyase (adding indole, L-tryptophan-forming) activity	0.02469	1
	GO:0035671	enone reductase activity	0.03035	1
	GO:0070300	phosphatidic acid binding	0.03370	1
	GO:0008146	sulfotransferase activity	0.03467	1
	GO:0004097	catechol oxidase activity	0.03609	1
	GO:0008889	glycerophosphodiester phosphodiesterase activity	0.04192	1
	GO:0043169	cation binding	0.04197	1
	GO:0016157	sucrose synthase activity	0.04611	1
	GO:0016165	linoleate 13S-lipoxygenase activity	0.04087	1
	GO:0003886	DNA (cytosine-5-)-methyltransferase activity	0.04440	1
	GO:0052381	tRNA dimethylallyltransferase activity	0.04472	1
	GO:0016747	transferase activity, transferring acyl groups other than amino-acyl groups	0.04641	2

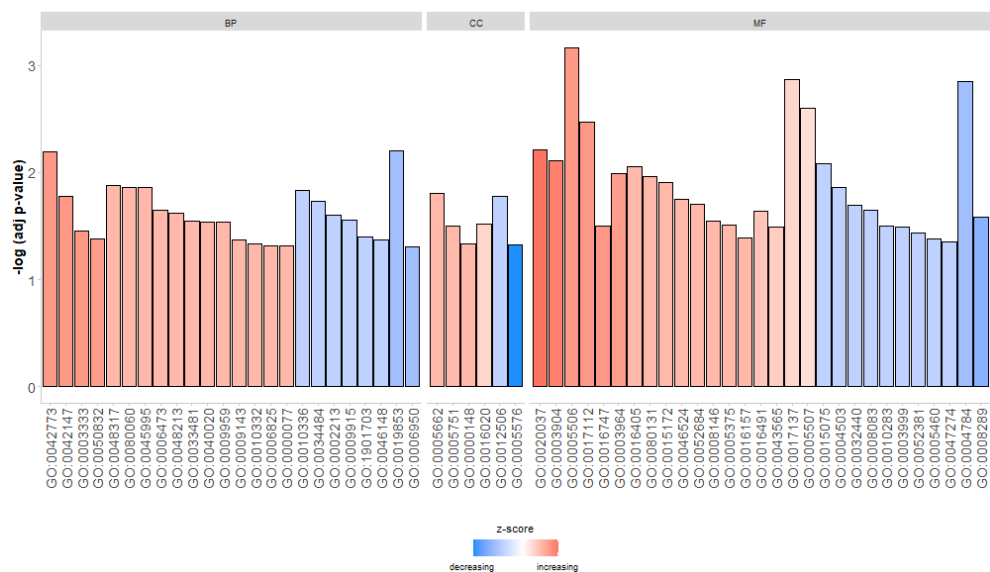


Fig. B-4. GO barplot displaying gene annotation enrichment analysis of DEGs in W+OS versus control, systemic leaf of *A. contorta*. Enriched GO terms were filtered by adjusted p -value (< 0.05) and `reduced_overlap()` function of R package “GOplot”.

Table B-4. List and enrichment score of enriched GO terms in the GO barplot (**Fig. B-4**) of in W+OS versus control, systemic leaf of *A. contorta*.

Ontology	Category	term	p-value	# of DEGs
Biological Process	GO:0042773	ATP synthesis coupled electron transport	0.00643	2
	GO:0042147	retrograde transport, endosome to Golgi	0.01663	2
	GO:0003333	amino acid transmembrane transport	0.03501	2
	GO:0050832	defense response to fungus	0.04145	5
	GO:0048317	seed morphogenesis	0.01311	1
	GO:0080060	integument development	0.01363	1
	GO:0045995	regulation of embryonic development	0.01384	1
	GO:0006473	protein acetylation	0.02258	1
	GO:0048213	Golgi vesicle prefusion complex stabilization	0.02390	1
	GO:0033481	galacturonate biosynthetic process	0.02821	1
	GO:0040020	regulation of meiotic nuclear division	0.02885	1
	GO:0009959	negative gravitropism	0.02899	1
	GO:0009143	nucleoside triphosphate catabolic process	0.04220	1
	GO:0010332	response to gamma radiation	0.04635	1
	GO:0006825	copper ion transport	0.04848	1
	GO:0000077	DNA damage checkpoint	0.04873	1
	GO:0010336	gibberellic acid homeostasis	0.01483	1
	GO:0034484	raffinose catabolic process	0.01873	1
	GO:0002213	defense response to insect	0.02485	1
	GO:0009915	phloem sucrose loading	0.02772	1
	GO:1901703	protein localization involved in auxin polar transport	0.04006	1
	GO:0046148	pigment biosynthetic process	0.04231	1
	GO:0019853	L-ascorbic acid biosynthetic process	0.00625	2
	GO:0006950	response to stress	0.04907	2
Cellular Component	GO:0005662	DNA replication factor A complex	0.01564	1
	GO:0005751	mitochondrial respiratory chain complex IV	0.03161	1
	GO:0000148	1,3-beta-D-glucan synthase complex	0.04592	1
	GO:0016020	membrane	0.03032	12
	GO:0012506	vesicle membrane	0.01684	1
	GO:0005576	extracellular region	0.04725	10

Table B-4. (continued)

Ontology	Category	term	p-value	# of DEGs
Molecular Function	GO:0020037	heme binding	0.00608	7
	GO:0003904	deoxyribodipyrimidine photo-lyase activity	0.00782	3
	GO:0005506	iron ion binding	0.00069	8
	GO:0017112	Rab guanyl-nucleotide exchange factor activity	0.00337	2
	GO:0016747	transferase activity, transferring acyl groups other than amino-acyl groups	0.03176	2
	GO:0003964	RNA-directed DNA polymerase activity	0.01032	5
	GO:0016405	CoA-ligase activity	0.00886	1
	GO:0080131	hydroxyjasmonate sulfotransferase activity	0.01086	1
	GO:0015172	acidic amino acid transmembrane transporter activity	0.01232	1
	GO:0046524	sucrose-phosphate synthase activity	0.01780	1
	GO:0052684	L-serine hydro-lyase (adding indole, L-tryptophan-forming) activity	0.01985	1
	GO:0008146	sulfotransferase activity	0.02836	1
	GO:0005375	copper ion transmembrane transporter activity	0.03081	1
	GO:0016157	sucrose synthase activity	0.04088	1
	GO:0016491	oxidoreductase activity	0.02277	6
	GO:0043565	sequence-specific DNA binding	0.03245	8
	GO:0017137	Rab GTPase binding	0.00135	3
	GO:0005507	copper ion binding	0.00251	5
	GO:0015075	ion transmembrane transporter activity	0.00833	1
	GO:0004503	monophenol monooxygenase activity	0.01365	1
	GO:0032440	2-alkenal reductase [NAD(P)+] activity	0.02002	1
	GO:0008083	growth factor activity	0.02254	1
	GO:0010283	pinorelinol reductase activity	0.03193	1
	GO:0003999	adenine phosphoribosyltransferase activity	0.03236	1
	GO:0052381	tRNA dimethylallyltransferase activity	0.03695	1
	GO:0005460	UDP-glucose transmembrane transporter activity	0.04155	1
	GO:0047274	galactinol-sucrose galactosyltransferase activity	0.04458	1
	GO:0004784	superoxide dismutase activity	0.00142	2
	GO:0008289	lipid binding	0.02589	3